Elucidating circadian light entrainment and plasticity in the SCN at the molecular and network levels

By

Suil Kim

Dissertation

Submitted to the Faculty of the

Graduate School of Vanderbilt University

in partial fulfillment of the requirements

for the degree of

DOCTOR OF PHILOSOPHY

in

Neuroscience

March 31, 2022

Nashville, Tennessee

Approved:

Danny G. Winder, Ph.D., Chair

Ronald B. Emeson, Ph.D.

Carl H. Johnson, Ph.D.

Douglas G. McMahon, Ph.D.

DEDICATION

타지에서 항상 신경써주는 부모님과 동생, 그리고 곁에서 언제나 버팀목이 되어주는 사랑스러운 아내 다미에게 이 박사 학위 논문을 바칩니다.

ACKNOWLEDGEMENTS

I would like to first thank the Vanderbilt University Interdisciplinary Graduate Program for allowing me to pursue my PhD in the US and assisting administrative procedures and career development. Also, I cannot forget to acknowledge the Vanderbilt International Scholarship Program which had financially supported two years of stipend for me and other international PhD students in the biomedical sciences. It also greatly helped me to settle in a foreign country in many aspects including getting my social security card and staying connected to other international students. The Neuroscience Program offered me a great opportunity to learn different aspects of neuroscience through rigorous academic coursework and great seminars.

Next, I would like to express my deepest gratitude to my PhD advisor and mentor Doug McMahon. When I came to Vanderbilt, I knew nothing about circadian rhythms. Rotating in his lab intrigued me into studying this fascinating field. Doug is the one I can always go to and ask for scientific advice. He has been incredibly supportive of my research and me growing as an independent scientist. Thanks for everything!

I want to thank my committee members Danny Winder, Ron Emeson, and Carl Johnson for helpful discussions and constructive comments. I am also thankful to Carl for hosting the Clock Journal Club and creating an environment that encourages critical appraisal of articles. I would also like to thank past and current members of the McMahon lab — David Sprinzen, Michael Tackenberg, Lili Xu, Justin Siemann, Manuel Giannoni-Guzman, Olivia Cox, and Patricia McCleskey — for their training and/or support throughout this journey. Particularly, I am very grateful to David for being extremely generous to spend his time in helping me get my ex vivo entrainment project off the ground.

I must thank all my friends I have met in graduate school for making my time in Nashville more enjoyable and memorable. Particularly, I feel extremely lucky to have best friends in my IGP cohort: Lorena Harvey, Rachana Nitin, Sai Aung Soe Lin, Ying Ji, and Cara Schornak. We share many good memories, and I am looking forward to many more years of friendship.

Lastly, I am extremely grateful to my family for all the love and support throughout one of the toughest times in my life. I will always thank my parents, Hwang-nyun Kim and Buock Kwon, for their sacrifices and giving me opportunities to live the life I have. I am also thankful to my sister Sohee Kim for being my constant companion in every moment. Finally, I would like to thank my best treasure and wife Dami Ko for her endless love and unwavering trust. Without her, I have not done this. Our recently born dearest son, Yujune Kim, has brought me a lot of happiness during dissertation writing.

TABLE OF CONTENTS

Page

DEDICATION iii

ACKNOWLEDGEMENTS iv

LIST OF TABLES vii

LIST OF FIGURES viii

CHAPTER I. Introduction 1

1.1 Circadian rhythms and light entrainment 1

1.2 The molecular and cellular architecture of the SCN 9

1.3 After-effects of light exposure on circadian rhythms 24

CHAPTER II. Light sets the brain's daily clock by regional quickening and slowing of the molecular clockworks at dawn and dusk 33

2.1 Abstract 33

2.2 Introduction 35

2.3 Results 37

2.4 Discussion 69

2.5 Materials and methods 76

CHAPTER III. DNA methylation is a widespread mechanism of light-induced period plasticity of circadian behavior and SCN rhythms 83

3.1 Abstract 83

3.2 Introduction 84

3.3 Results 85

3.4 Discussion 96

3.5 Materials and methods 98

CHAPTER IV. Conclusions and future directions 103

REFERENCES 110

LIST OF TABLES

Table Page

1.1 Effects of knocking out TTFL genes in mice 14

1.2 Key resources table 77

LIST OF FIGURES

Figure Page

1.1. Phase resetting of circadian rhythms to light exposure 3

1.2 Entrainment of circadian rhythms to discrete light pulses.....6

1.3 Transcription-translation feedback loops for mammalian circadian clockworks 11

1.4 The SCN neural network 16

1.5 Molecular pathways underlying light-induced resetting of the SCN clock.....21

2.1 Graphical abstract 34

2.2 Long-term optogenetic stimulation system for circadian entrainment ex vivo 39

2.3 Improved PER2::LUC rhythmicity in SCN slice explanted from young mice to culture medium containing stabilized glutamine 40

2.4 Diagram of an integrated system for long-term luminescence recording and optogenetic stimulation.....42

2.5 ChrimsonR-driven optogenetic stimulation alters the waveform of SCN PER2 rhythm to reset the SCN clock.....43

2.6 Optogenetic cycles entrain PER2::LUC rhythms in the SCN by triggering daily waveform changes that match the SCN clock to the cycle period.....47

2.7 PER2::LUC rhythms in SCN slices entrain to optogenetic T-cycles 49

2.8 Quantification of period during entrainment and period changes following entrainment using Lomb-Scargle periodogram.....50

2.9 Acrophase fitting of PER2::LUC bioluminescence actograms from Figure 2.5 51

2.10 SCN entrain to optogenetic simulation of dawn and dusk via differential PER2::LUC rhythm waveform changes.....54

2.11 Acrophase fitting of PER2::LUC bioluminescence actograms from Figure 2.10. 56
2.12 Quantification of period during entrainment and period changes following entrainment using Lomb-Scargle periodogram.....56
2.13 Phase jump in circadian behavior during long skeleton photoperiod entrainment.....58
2.14 Gradual shifts from equinox to long optogenetic skeleton photoperiods reveal SCN PER2::LUC rhythms stably entrained to long skeleton photoperiods.....60
2.15 Regional distribution of circadian phase and period in the SCN, and heterogeneity of the phase and the period responses in the SCN to Optogenetic Light Pulses.....64
2.16 ChrimsonR-tdT fluorescence levels in different phase shift clusters in the Figure 2.15C for CT14 and CT21 stimulation.....68
3.1 DNA methylation mediates after-effects on circadian period following long photoperiod entrainment 86
3.2 DNA methylation mediates after-effects on circadian period of locomotor behavioral rhythms without affecting acute phase delays 90
3.3 DNA methylation mediates VIP-induced after-effects on the ex vivo SCN rhythm period without affecting acute phase delays 92
3.4 DNA methylation is critical for after-effects on the ex vivo SCN rhythm period following acute optogenetic stimulation of SCN neurons..... 95

CHAPTER I

Introduction

1.1 Circadian rhythms and light entrainment

Let there be Sunlight. It is the most important source of energy for organisms on Earth and creates 24-hour day-night cycles and seasons. Most, if not all, life on Earth spanning from bacteria to humans have accordingly evolved internal timing mechanisms generating endogenous rhythms in physiology and behavior with a period of approximately 24 hours[1]. These rhythms are termed circadian rhythms. One of the most prominent and classic examples of circadian rhythms is rodent locomotor activity. Mice show nocturnal patterns of locomotor behavior with a period of ~ 23.7 hours in constant darkness with no external timing cues such as light[2].

Circadian rhythms have three main fundamental properties[3]. First and foremost, circadian rhythms persist with a period close to 24 hours in constant environmental conditions without external timing cues. Such a period is termed a free-running period (FRP). Secondly, circadian rhythms can be reset by an environmental cue, and match its period to that of an environmental cycle. Such a resetting cue is called a zeitgeber (German for a time-giver; external synchronizer) and synchronization to a zeitgeber cycle is termed entrainment. Lastly, circadian rhythms maintain ~ 24-hour periodicity in the range of physiological temperature.

Light influence on circadian rhythms

In nature, except in extreme environments (e.g., polar regions and deep ocean), circadian rhythms of a free-running period close to, but not exactly in most species 24 hours, are entrained

to 24-hour light-dark cycles, as light is the most dominant zeitgeber among others such as temperature, feeding time, and exercise. For example, nocturnal locomotor behavior rhythms in mice are aligned with a light-dark cycle even when mice are fed only during the daytime such that feeding timing is the opposite of the normal alignment with the light cycle[4]. Mice with a 24-hour access to food and water typically show dispersed feeding activity throughout the night. Daytime-fed mice, however, wake up briefly for a few hours during the daytime for food intake, while they maintain overall nocturnality[4].

Circadian rhythms are very sensitive to light. Single light signals such as a 15-minutes flash of light can cause changes in circadian rhythms[3]. Interestingly, the photic response in circadian rhythms varies depending on timing of light[3]. When a light pulse is given during subjective night (i.e., night in internal circadian time [CT]), circadian rhythms shift in phase: light exposure during early night causes a phase delay (e.g., activity onset arises later in time on subsequent rhythmic cycles), while light at late night causes a phase advance in which activity onset arises earlier on subsequent cycles[2]. In contrast, light pulses during the circadian daytime cause almost no phase shifts[2], referred to as 'the dead zone.' Such a daily pattern of light responsiveness in the phase of circadian rhythms is termed the phase response curve (Figure 1.1). Remarkably, phase response curves have a similar shape across many different species including invertebrates[3,5], vertebrates[2,6,7], and plants[8,9], although the ratio of delay to advance zones can vary[10], suggesting a universal design principle of the light-responsive endogenous circadian oscillator. Within the same species, the phase response curve can differ depending on light intensity, duration, and prior light history[3].

In addition to brief light pulses and light-dark cycles, constant lighting (LL) influences circadian rhythms. Its effects depend on light intensity and whether organisms are diurnal or

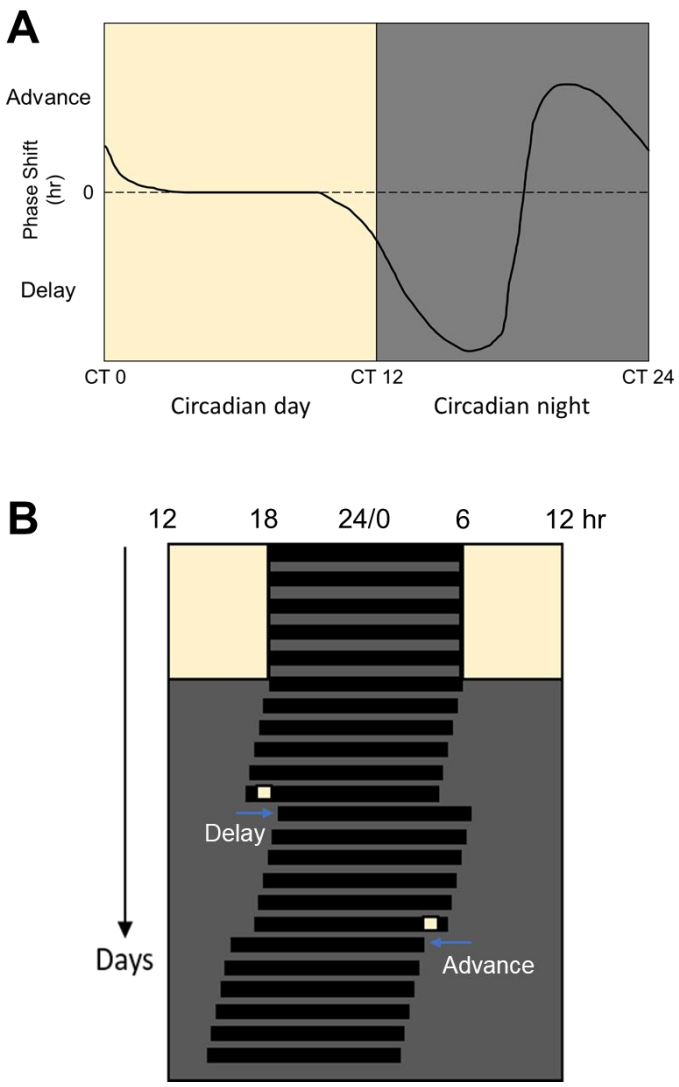

Figure 1.1. Phase resetting of circadian rhythms to light exposure.

Phase response curve **(A)** depicts the direction and magnitude of phase shifts in circadian rhythms in response to a light pulse at certain times of the day. Time of the day on the x axis is in circadian time (CT) where CT 0 to 12 denotes circadian day (yellow zone) and CT 12 to 24 indicates circadian night (gray zone). For example, mouse locomotor behavior displays circadian rhythms as seen in an actogram **(B)**. An actogram is a graphical representation of an activity record (black bars) plotted on an x-axis in hours and a (*Figure legend continues.*)

(*Figure legend continued.*) y-axis in days. Yellow and gray areas indicate light and dark. Locomotor behavior rhythms persist in constant darkness and reset their phase to short light pulses delivered during circadian night. Light during early night (e.g., CT 14) causes a phase delay, while light at late night (e.g., CT 22) causes a phase advance. Transients following a phase advance and period after-effects following phase shifts are not shown in this figure for simple illustration.

nocturnal[11]. In general, LL causes a period shortening of circadian rhythms in diurnal organisms, while it causes a period lengthening in nocturnal organisms. Increased light intensity in LL generally enhances its effects and can even result in arrhythmicity.

Light entrainment: discrete and continuous mechanisms

The phase response curve described above underlies how entrainment of circadian rhythms to a cycle of light and dark is achieved[12]. In principle, light entrainment can be achieved by daily phase shifts if they compensate for the difference in period between circadian rhythms and a light cycle. Organisms with a circadian period of shorter than 24 hr entrain to a 24 hr light cycle by phase delays, while those with a longer-than-24 hr period entrain by phase advances. Limits of entrainment in terms of a light cycle period are thus largely defined by the magnitude range of phase shifts. One remarkable example is that mouse locomotor rhythms (FRP = ~ 23.7 hr) can entrain to a 22 hr cycle of 1 hr light pulses, but they cannot entrain to a 20 hr cycle (Figure 1.2A). Entrained rhythms establish a stable phase relationship with a 22 hr cycle as light pulses at late circadian night cause ~ 1.7 hr phase advances every cycle. However, a 20 hr light cycle is not entrainable as advance phase shifts to these light stimulation parameters cannot compensate for the 3.7 hr period difference. This discrete model of entrainment predicts that a light cycle consisting of brief light pulses in the morning and evening would entrain circadian rhythms even without continued light across the day. Indeed, such a two-pulse entrainment has been shown in many species including flies and mammals[12] (Figure 1.2B). Two-pulse entrainment is achieved if net phase shifts in the morning and evening are equal to the difference between the FRP and a light cycle period. Two-pulse light cycles (also known as skeleton photoperiods) can mimic photoperiods (light cycles with a variable duration of daylight) of shorter than a 14 hr light phase (LD 14:10; 14 hr light and 10 hr dark cycle; Figure 1.2B), suggesting that light-dark transition of

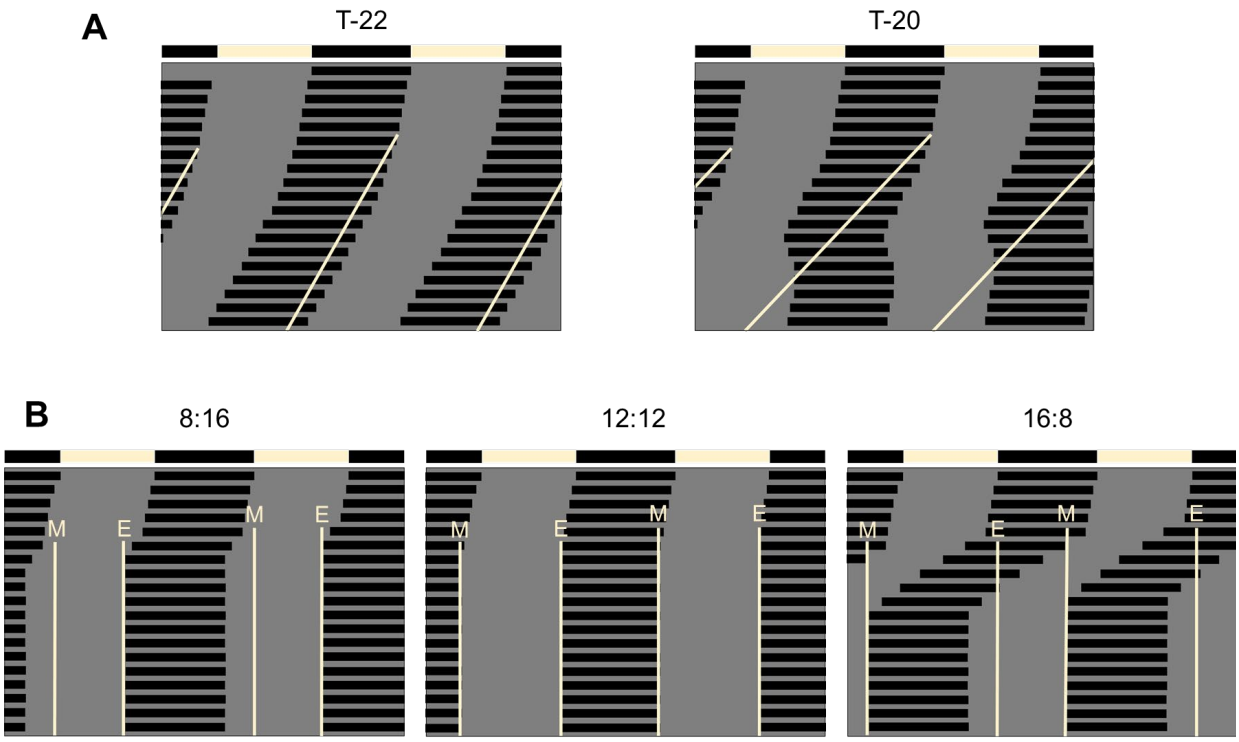

Figure 1.2. Entrainment of circadian rhythms to discrete light pulses.

As predicted by the discrete model of entrainment, circadian rhythms can entrain to discrete light pulses given at intervals with limits as shown in graphical illustrations of actograms of mouse locomotor behavior in constant darkness (gray box) followed by either one-pulse light cycles **(A)** or two-pulse light cycles (skeleton photoperiods, **B**). As actograms are double-plotted on a 24hr time scale, the x-axis shows 48hr and data are duplicated. Yellow and black bars on top of actograms indicate an LD 12:12 cycle in which mice were previously entrained. Tilted yellow lines in actograms depict pulsed light cycles **(A)** Mice are exposed to a one-pulse 22hr light cycles beginning at CT 0 (circadian dawn). As light pulses are aligned at late circadian night, where induced phase shifts compensate for time difference between FRP and 22hr cycle period, circadian rhythms entrain to a T-22 light cycle. In contrast, (*Figure legend continues.*)

(*Figure legend continued.*) a T-20 light cycle is not entrainable as phase shifts cannot offset the large difference between FRP and 20 hours. Circadian rhythms instead show relative coordination with the light cycle as rhythms are alternatively light-influenced and free-running. **(B)** Mice are exposed to skeleton photoperiods mimicking LD 8:16, 12:12, or 16:8 light cycles. Morning light pulses (M) for 8:16, 12:12, and 16:8 skeletons are given at CT 2, CT 0, and CT 22, respectively. Evening pulses (E) for 8:16, 12:12, and 16:8 skeletons are respectively delivered at CT 10, CT 12, and CT 14. 8:16 and 12:12 skeleton photoperiods entrain circadian rhythms; 16:8 skeletons, however, cause a phase jump in circadian rhythms, leading to a similar phase relationship with light pulses to that of 8:16 skeletons.

a light cycle is critical for entrainment.

Another potential mechanism of entrainment is continuous action of light on circadian rhythms such as acceleration and deceleration of circadian cycles[12]. This continuous model provides a good explanation for entrainment to a low-amplitude sine wave of light intensity in LL. The continuous model also explains a discrepancy in entrainment between skeleton and complete photoperiods with a long daytime interval such as LD 16:8. Unlike complete photoperiods, skeleton long photoperiods can cause a phenomenon called a phase jump: the subjective night interval of circadian rhythms does not stably align with the shorter light interval but instead it falls into the longer light interval (Figure 1.2B). This suggests that continuous light actions on circadian rhythms prevent phase jumps and help entrainment to summer-like long photoperiods.

In nature, whether entrainment mechanisms are discrete, continuous, or both would depend on light exposure patterns of organisms. Discrete mechanisms would be primary for nocturnal rodents going in and out of a burrow around dawn and dusk while staying away from their diurnal predators. In contrast, circadian rhythms in diurnal organisms might be sensitive to changes in light intensity throughout the day, achieving light entrainment via continuous mechanisms. As mentioned above, entrainment of circadian rhythms in nocturnal organisms by discrete phase shifts around dawn and dusk can cause a phase jump under long photoperiods in Summer. In fact, some nocturnal species living at high latitude where seasonal variation in day length is high such as microtine rodents switch their behavior between nocturnal and diurnal patterns in different seasons, suggesting that phase jumps occur in nature[12]. Interestingly, however, certain nocturnal rodents such as deer mice can tolerate long photoperiods well[12]. Comparisons of the phase response curve and maximum tolerable skeleton photoperiods with fruit flies *Drosophila pseudoobscura* suggested that an overall small magnitude of the phase response in those rodents can reduce a

chance of phase jumps as theoretically predicted[12,13]. Another possible, but underappreciated strategy to avoid phase jumps for nocturnal animals is exposure to light in the middle of the day in addition to twilight, although the theoretical and empirical evidence remains to be accumulated.

1.2 The molecular and cellular architecture of the SCN

Discoveries that circadian rhythms are internally driven in the organism and can reset to environmental time cues led to formulation of a three-component model of the circadian timekeeping system—input pathways, circadian oscillators, and output pathways—and raised a fundamental question: Where are circadian oscillators (or metaphorically circadian clocks) located in the body? In principle, the lack of either circadian oscillators or output pathways can cause arrhythmicity in overt circadian rhythms. Thus, a circadian oscillator must be proven in both its necessity and sufficiency to produce circadian rhythms. In mammals, lesioning[14,15] and transplantation[16–18] studies have shown that the suprachiasmatic nucleus (SCN) in the hypothalamus is necessary and sufficient to generate circadian rhythms in many facets of physiology and behavior[19–21], demonstrating that the SCN is a central circadian oscillator in mammals. When a donor SCN was transplanted into the third ventricle of an SCN-lesioned recipient with a different FRP from the donor's, indeed, circadian locomotor rhythms in the recipient were restored with a donor's FRP[16]. This indicates that the SCN determines the period of circadian locomotor rhythms as a master clock.

The molecular basis of autonomous circadian clocks in mammals

Nearly all cells in mammals, including SCN neurons, express a set of genes generating autonomous circadian rhythms at the molecular level. These genes are called 'clock genes'. Clock

genes are present across different species from unicellular cyanobacteria to humans although a list of clock genes and their DNA sequence vary[1,22]. The mammalian clock genes form multiple autoregulatory feedback loops where their transcription is regulated by their own protein products[23] (transcription-translation feedback loops [TTFL]; Figure 1.3). The most essential loop consists of *Brain and muscle aryl hydrocarbon receptor nuclear translocator (ARNT)-like 1* (*Bmal1*), *Circadian Locomotor Output Cycles Kaput* (*Clock*), *Period 1/2* (*Per1/2*), and *Cryptochrome 1/2* (*Cry1/2*). BMAL1 and CLOCK act together as a heterodimeric transcription factor with the basic helix–loop–helix (bHLH) and PER-ARNT- single-minded protein (SIM) (PAS) domains[24]. During the daytime, BMAL1-CLOCK heterodimer activates the transcription of *Per* and *Cry* genes via an enhancer box (E-box). As PER and CRY proteins accumulate, they are translocated into the nucleus at early night and bind to BMAL1-CLOCK[25,26]. This causes formation of co-repressor complexes containing histone deacetylases, leading to transcriptional repression of *Per* and *Cry* genes[25,26]. With a combination of transcriptional repression and proteasomal degradation, PER and CRY protein levels decline during the night, relieving negative feedback on *Per* and *Cry* gene transcription. BMAL1-CLOCK then restarts a new transcriptional cycle next morning. This negative feedback loop with time delay sets the circadian period of molecular clockworks.

The second autoregulatory loop induces *Bmal1* rhythmic expression. *Bmal1* transcription is regulated by two types of transcription factors binding to RevDR2 and retinoic acid-related orphan receptor-binding elements (RORE): RORα/β/γ[27] and reverse strand of Leukemia Viral oncogene homolog (REV-ERB) α/β[28,29]. RORs activates *Bmal1* transcription, BMAL1-CLOCK heterodimer activates transcription of *Rev-erb*s, and REV-ERBs repress ROR-mediated *Bmal1* transcription[28]. This, and the first feedback loops, create an anti-phase relationship between Bmal1

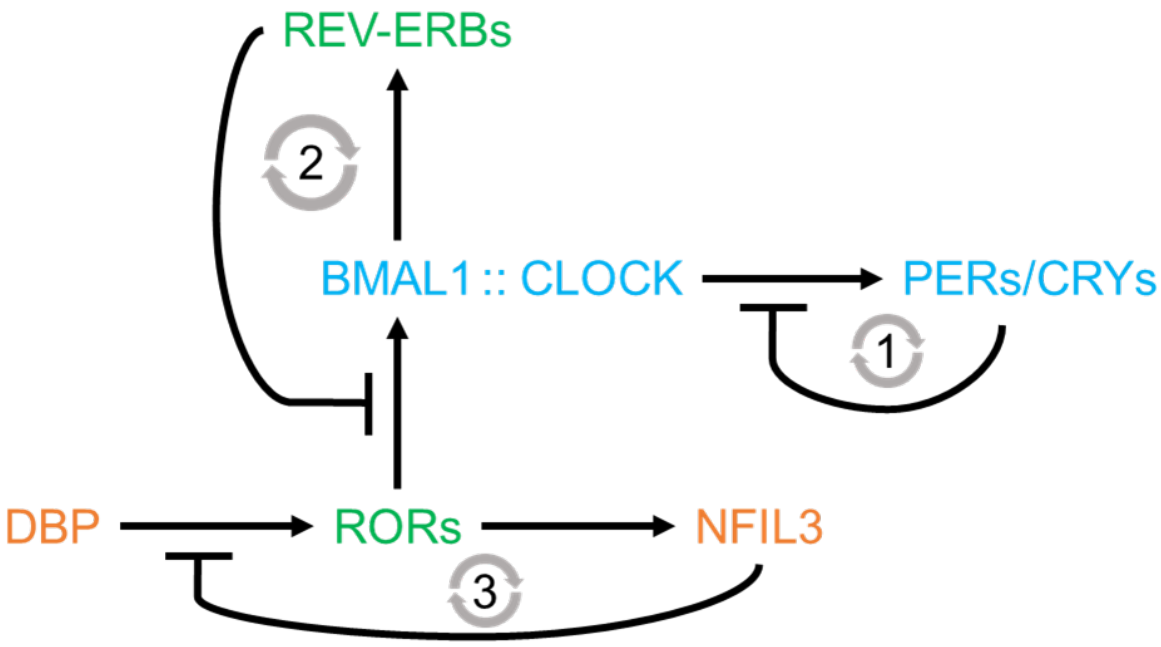

Figure 1.3. Transcription-translation feedback loops for mammalian circadian clockworks.

The first and core loop (1) consists of BMAL1, CLOCK, PERs, and CRYs. The second (2) and third (3) loops are auxiliary loops stabilizing the core loop and circadian outputs. The second loop contains RORs and REV-ERBs. The third loop involves DBP and NFIL3. Pointed and block arrows indicate transcriptional activation and inhibition, respectively. Blue, green, orange colors indicate different DNA elements involved: E-box, RORE, and D-box, respectively.

and PER/CRY protein expression rhythms.

The third feedback loop is interlocked with the two other autoregulatory loops described above. It involves basic leucine zipper (bZip) transcription factors. Proline and acidic amino acid-rich bZIP (PAR-bZip) transcription factors, including albumin D-box binding protein (DBP), activate *Ror* genes, RORs activate transcription of another bZIP transcription factor *nuclear factor, interleukin-3 regulated* (*NFIL3*)[30], and NFIL3 negatively regulates RORs. DBP and NFIL3 indirectly regulate *Bmal1* transcription via RORs.

Taken together, autonomous circadian rhythms at the molecular level are produced by multiple autoregulatory feedback loops of transcription factors and their repressors acting on E-box, RORE, and D-box. Remarkably, about 40% of the entire mouse genome has a circadian gene expression in some tissues and about 5-20% of the genome in a given tissue is clock-controlled[31], revealing a widespread circadian regulation in gene expression. As the circadian clock is critical for normal physiology and behavior, however, genes composing the TTFLs have functional redundancies. Deletion studies revealed that *Bmal1* deletion is the only single mutation that totally disrupts the circadian clockwork, leading to arrhythmic molecular and behavioral phenotypes[32,33] although rescue experiments in *Bmal1* knockout mice with its paralogue *Bmal2* suggested that *Bmal1* knockout is functionally similar to *Bmal1/2* double knockout[34]. Other single TTFL gene knockout mice still show circadian rhythms with an aberrant period (Table 1.1), revealing the robustness of TTFLs. Despite not necessary for generating circadian rhythms, multiple accessory TTFLs further stabilize rhythmicity of clock-controlled genes. In fact, a number of clock-controlled genes having E-boxes are also found to have ROREs[35], suggesting that they could be regulated by RORs and REV-ERBs as well as BMAL1-CLOCK. Also, *Bmal1* rhythmic expression

by RORs and REV-ERBs is not essential for maintaining the core BMAL1-CLOCK-PER/CRY loop[36].

The retinohypothalamic tract for light input to the SCN

In mammals, the eye is the light-receptive organ that transforms light signals into electrochemical signals at the retina. For image-forming functions, light signals are first received by photoreceptors and transmitted to retinal ganglion cells (RGCs) via bipolar cells. For circadian modulations, however, a population of RGCs expressing a photopigment melanopsin can directly detect light signals. This subpopulation of RGCs is called intrinsically photosensitive RGCs (ipRGCs) and occupies about 5% of the total RGC population[50]. There are at least five subtypes (M1-M5) of ipRGCs, differentiated by their varying morphology and electrophysiology. The M1 ipRGCs innervate the SCN. X-gal staining of axonal projections from M1 ipRGCs showed that most of the mouse SCN is densely and bilaterally innervated by M1 ipRGCs[37]. A more recent study using single M1 ipRGC labeling by alkaline phosphatase staining revealed a retinotopic map in the SCN where the dorsotemporal and ventromedial regions of the retina send axons to the dorsal and ventral SCN, respectively[38]. This contradicts earlier studies using anterograde tracing of retinal axons with cholera toxin B that the ventrolateral SCN predominantly receive retinal afferents in hamsters and rats[39,40,41]. It remains unclear if this contradiction is due to methodological differences or species-specific characteristics.

Null mutation	Phenotype	References
Bmal1	Arrhythmic	[42]
Clock	Shortened period	[43]
Per1	Shortened period or arrhythmic	[44–46]
Per2	Shortened period	[47]
Per1/2	Arrhythmic	[46]
Per3	Shortened period	[48]
Cry1	Shortened period	[49,50]
Cry2	Lengthened period	[49,51]
Cry1/2	Arrhythmic	[50]
Rorα	Shortened period	[27]
Rorβ	Lengthened period	[52]
Rev-erbα	Shortened period	[28]
Rev-erbβ	Not different from WT	[53]
Rev-erbα/β	Arrhythmic	[53]
Dbp	Shortened period	[54]
Nfil3	Not different from WT	[55]

Table 1.1. Effects of knocking out TTFL genes in mice.

A single gene and paralogous genes in the transcription-translation feedback loops were knocked out in mice and locomotor activity rhythms were measured to assess effects on behavioral phenotypes. For phenotypes in *Nfil3* knockout mice, clock gene expression and the number of rhythmic genes in the liver were assessed. Except *Bmal1*, no single gene knockout causes arrhythmicity in behavior. When paralogous genes such as *Per1* and *Per2* were knocked out together, however, circadian rhythms were abolished. WT = wild type.

The SCN neural network

The SCN is a small region in the anterior and ventral hypothalamus right above the optic chiasm and located bilaterally to the third ventricle. The SCN contains about 20,000 neurons based on Nissl staining[56], and almost all SCN neurons are GABAergic[57]. Remarkably, neuropeptide characterization using mass spectrometry revealed that there are approximately 190 endogenous peptides expressed in the SCN including vasoactive intestinal peptide (VIP), arginine vasopressin (AVP), and gastrin-releasing peptide (GRP)[58]. By percentage of total SCN population, neuromedin S (NMS)-positive neurons are the most abundant (~40%) followed by AVP+ (20%) and VIP+ (10%)[59]. Neurons expressing an individual neuropeptide have a specific spatial pattern in the SCN with some overlaps[60] (Figure 1.4). VIP is mainly localized in the ventral SCN, GRP is located in the central SCN, and AVP is expressed in the dorsal SCN[60]. GRP expression overlaps with that of both VIP and AVP[60]. In contrast, there is by far no evidence of neurons co-expressing VIP and AVP in the SCN, strongly suggesting that VIP+ and AVP+ neurons are functionally segregated.

The SCN has traditionally been thought to have two functional subdivisions: the core and shell[56,61]. This concept is mainly based on neuropeptide expression patterns, clock gene rhythmicity, and connections to extra-SCN regions[56,61]. In mice and rats, the core is anatomically located in the ventrolateral SCN and the shell is in the dorsomedial SCN[56] (Figure 1.4). The core expresses VIP and GRP, whereas the shell expresses AVP[61]. In addition, the core shows very low or undetectable amplitude in the constant darkness but the shell has rhythmic oscillations[12], although a recent study examining spatial differences in real-time clock gene rhythms in the SCN showed that both the core and shell have rhythmic clock gene expression[63]. Light induction of the clock gene *Per1* is predominant in the core, while *Per2* induction is comparable between the core and shell[64]. The core and shell receive distinct afferents from other brain regions. The core gets

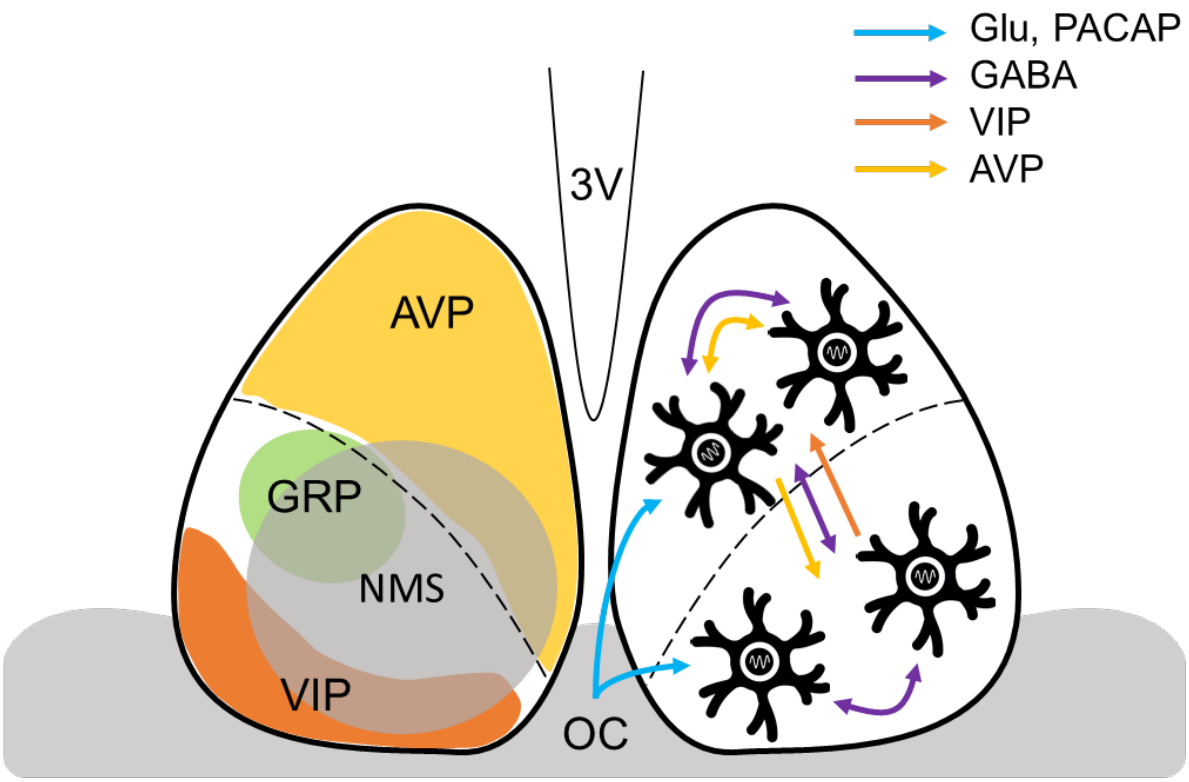

Figure 1.4. The SCN neural network.

The SCN in the hypothalamus has bilateral nuclei just above the optic chiasm (OC) and surrounds the third ventricle (3V) as illustrated in a coronal view. The SCN is a network of about 20,000 neuronal oscillators (arborized cells) and has overlapping functional divisions (dashed lines): the ventrolateral core and dorsomedial shell. Neuropeptide expression in the core includes VIP (orange area), NMS (grey area), and GRP (green area); the shell includes NMS and AVP (yellow area) expressions. Retinal light input via ipRGCs (blue arrows) is received by both the core and the shell neurons and entrains their rhythms to external light cycles. Internal synchronizers such as GABA, VIP, and AVP (purple, orange, yellow arrows, respectively) mediate intercellular coupling within the SCN.

direct photic input from the retina and non-photic inputs from the intergeniculate leaflet (IGL), lateral geniculate nucleus, pretectal nuclei, and raphe nucleus[60,61]. In contrast, the shell is innervated by the cerebral cortex, basal forebrain, hippocampus, medullary noradrenergic areas, and brainstem cholinergic nuclei[60,61] as well as the retina[37,38]. The core and shell SCN share output brain regions including the subparaventricular zone (SPVZ) and dorsomedial hypothalamus (DMH)[60,61]. Interestingly, a recent study showed that the dorsal SCN expresses c-fos induction mediated by light input from both eyes, whereas the ventral region responds to monocular light input[38]. Given that ipRGC innervation is dense across the SCN[38], this suggests intrinsic differences in light responsiveness of the circadian clock between the core and shell neurons.

Studying the connections between different subpopulations of SCN neurons, or between the core and shell, has been very challenging as the SCN is a very small brain region and its neuronal size is also small. Biocytin staining of neurites showed that AVP+ neurons have compact dendritic arborization, and their axons mostly terminate inside the SCN[65]. GRP+ neurons form a dense local network within the core but not with the shell[66]. A neuronal tracing study using biotinylated dextran amines injected into the shell showed that the core was not entirely labeled, suggesting that chemical synapses between the core and shell might be sparse[67]. Furthermore, another study found that firing patterns from SCN neurons were not cross-correlated[68], suggesting that fast synaptic transmission mainly by GABA is sparse and weak within the SCN. Non-synaptic volume transmission of neurotransmitters, in fact, plays an important role in intra-SCN communication. Particularly, the role of VIP in the core-shell interaction has been extensively studied as VIP is expressed in the core and most SCN neurons express VIP receptor type 2 (VPAC2). VIP- and VIP receptor type 2 (VPAC2)-null mice show arrhythmic behavior[69,70] and the individual neurons show desynchronized clock-gene rhythms at the molecular level[71], pointing

to the necessity of VIP signaling for synchronizing cellular circadian rhythms across the SCN. Interestingly, paracrine VIP signaling induced by WT graft SCN can restore molecular circadian rhythms in SCN slices from CRY1/2 double knockout mice that are arrhythmic at the molecular and behavioral levels[72], suggesting that rhythmic VIP signaling can compensate for loss of circadian rhythms caused by defects in the TTFLs.

As described above, individual SCN neurons themselves are circadian oscillators containing autonomous circadian clockworks. Interestingly, their circadian rhythms show very similar circadian periods, but they are differentially phased, displaying peaks at different times[73]. Such phase dispersion creates a spatiotemporal pattern of individual cellular circadian rhythms in the SCN such as clock gene rhythms[73]. The degree of phase dispersion depends on exposed light cycles: it increases if the day phase of light cycles is longer than 12 hours[74] (e.g., LD 16:8; photoperiodic effects) or the period of light cycles deviates from 24 hours[75] (e.g., LD 11:11; T-cycle effects). Notably, a defined spatiotemporal wave of peaks in SCN cellular rhythms moves roughly from dorsomedial to ventrolateral regions each cycle[76,77], suggesting that SCN coupling dynamics is more complex than the traditional idea of core-shell coupling: the core shifts its rhythms first by direct retinal light input and the shell later by an input from the core such as VIP.

Mechanisms underlying how SCN neurons are differentially phased have been extensively studied in the context of different photoperiods. Patch clamp recordings of SCN slices from animals entrained to short and long photoperiods revealed that long photoperiods shift the equilibrium potential of GABA-evoked currents towards GABA being more excitatory[78]. Later studies suggested that increased excitatory GABA transmission by long photoperiods arises in the dorsal SCN but not significantly in the ventral SCN, as changes in chloride transporters expression and intracellular chloride concentration are dominant in the dorsal SCN[79,80]. This provides a model

suggesting that long photoperiods cause phase dispersal among SCN rhythms via GABA switching from being inhibitory to excitatory in the dorsal region. However, it remains to be directly tested whether such GABA switching mediates long photoperiod entrainment. Interestingly, pharmacological blockade experiments revealed that excitatory GABA is necessary for restoration of *ex vivo* SCN phase distribution from long photoperiod-induced phase divergence, and suggested involvement of circadian period changes in SCN core neurons[81]. This suggests that excitatory GABA signaling drives compression and dispersion of SCN cellular clock phases in a context-dependent manner.

Furthermore, gap junctions play an important role in intercellular coupling in the SCN as shown among other GABAergic neurons[82]. Dendro-dendritic and dendro-somatic gap junctions between GABAergic interneurons are common in the cerebral cortex, although excitatory neurons generally lose gap junctions throughout development[82]. Indeed, gap junction proteins including connexins help SCN neurons electrically synchronize with each other and such a coupling is necessary for normal circadian behavior[83]. However, it remains elusive how electrical synapses integrate photic information from retinorecipient SCN neurons and contribute to light resetting and entrainment of circadian rhythms.

Molecular pathways underlying light-induced resetting of the SCN clock

Light inputs to the circadian system are transmitted to the SCN via the M1 ipRGCs. Interestingly, conventional rod and cone photoreceptors are not necessary for circadian synchronization[84] but do serve as complimentary players[85]. M1 ipRGCs directly respond to mid- and long-wavelength visible light through the photopigment melanopsin and release glutamate and pituitary adenylate cyclase-activating peptide (PACAP) at the synapses of retinorecipient SCN

neurons (Figure 1.5). VIP+ neurons in the SCN are mainly characterized as retinorecipient neurons, although SCN neurons expressing other neuropeptides also receive retinal light inputs.

Retinorecipient neurons express both glutamate and PACAP receptors. Glutamate receptors expressed in these neurons include AMPA (α-amino-3-hydroxy-5-methyl-4-isoxazolepropionic acid) receptors (GluA1, GluA2, GluA4), kainate receptors (GluK2, GluK3), NMDA (N-Methyl-D-aspartic acid) receptors (GluN1, GluN2C) as well as metabotropic receptors (mGluR1, mGluR5)[86]. Antagonists of either NMDA or non-NMDA receptors block light-induced resetting of the circadian clock[87,88], suggesting that all ionotropic glutamate receptors are necessary for this process. Activation of the ionotropic glutamate receptors by glutamate release from retinal afferents triggers membrane depolarization, and it causes calcium influx directly via NMDA receptors and indirectly via voltage-gated calcium channels (VGCCs; Figure 1.5). Pharmacological blockade of VGCCs is sufficient to abolish glutamate-induced clock resetting[89], suggesting that glutamate resets the circadian clock via VGCC-induced calcium influx.

PACAP receptors are widely expressed in the SCN. There are three types of PACAP receptors: PACAP receptor type 1 (PAC1), VIP receptor type 1 (VPAC1), and VIP receptor type 2 (VPAC2)[90]. PAC1 and VPAC2 are expressed in the SCN[91,92]. PAC1 has a stronger affinity to PACAP than VIP and its expression is widespread in the SCN with the highest occurrence in the ventral region[92]. In contrast, VPAC2 binds equally to VIP and PACAP, and its expression is ubiquitous with a higher level in the dorsal SCN[92]. Both PAC1 and VPAC2 are Gs-coupled receptors that activate adenylyl cyclase (AC) and increase intracellular cyclic adenosine monophosphate (cAMP) levels[90] (Figure 1.5). PAC1-deficient mice show impairment in light-induced clock resetting in a similar manner to PACAP knockout mice[93,94], suggesting that PACAP signaling is mainly mediated by PAC1. Interestingly, PACAP- or PAC1-null mice show relatively

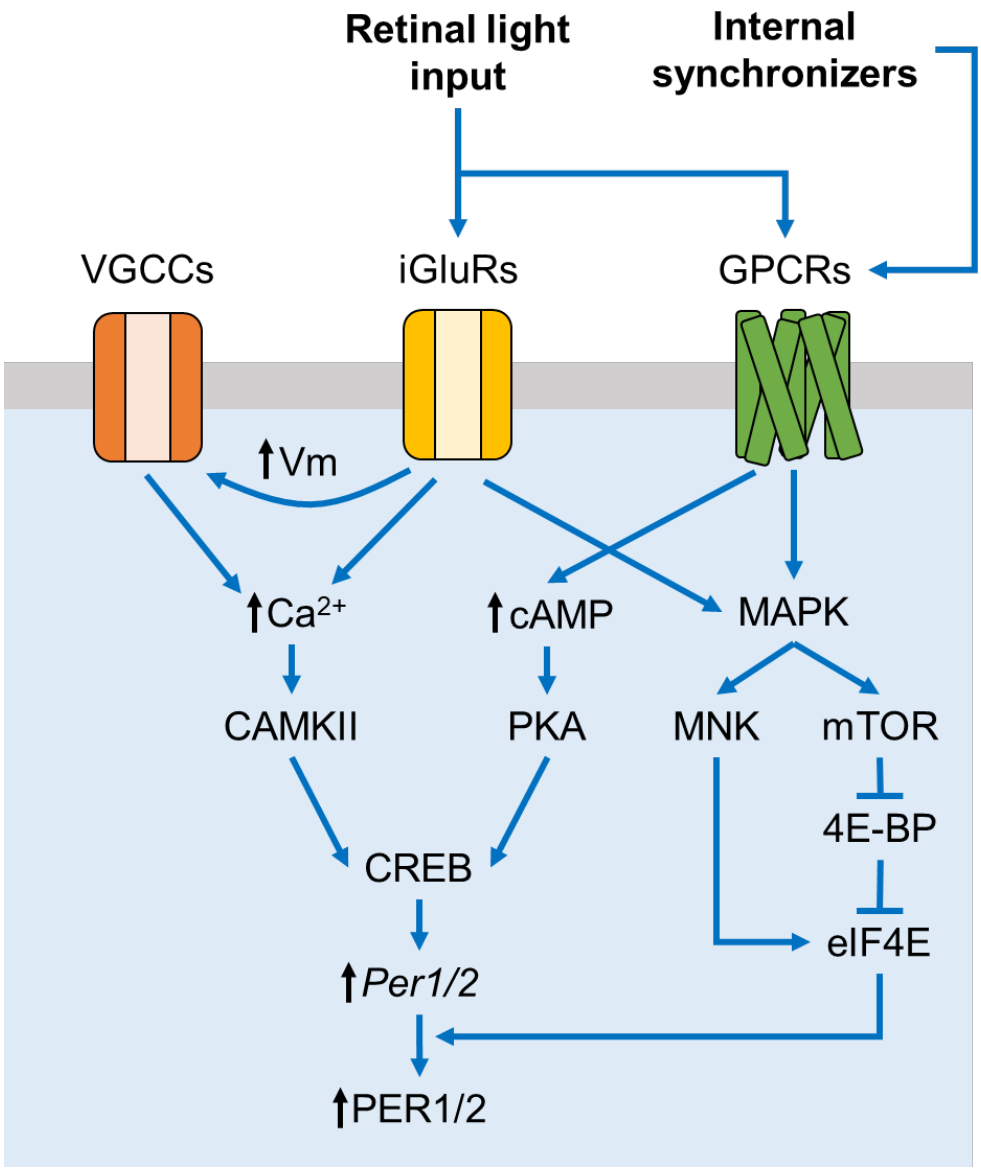

Figure 1.5. Molecular pathways underlying light-induced resetting of the SCN clock.

Retinal light input leads to release of glutamate and PACAP at retinohypothalamic synapses, causing activation of neurotransmitter receptors on SCN neurons including ionotropic glutamate receptors (iGluRs) and Gs-coupled GPCRs. Internal synchronizers such as VIP also cause GPCR activation. Activated iGluRs increase intracellular calcium (*Figure legend continues.*)

(*Figure legend continued.*) levels via NMDA receptors and open voltage-gated calcium channels (VGCCs) by depolarizing the SCN neuronal membrane. VGCCs increase intracellular calcium levels as well. Increased calcium levels lead to CREB phosphorylation via CAMKII. Also, GPCR activation leads to CREB phosphorylation through a cAMP-PKA-CREB pathway. Phosphorylated CREBs induces *Per1/2* expression, causing a phase shift in the circadian clock. In addition to CREB induction of *Per1/2*, enhanced *Per1/2* translation causes phase resetting. MAPKs activated by iGluRs and GPCRs lead to eIF4E phosphorylation via MNK and mTOR pathways. Phosphorylated eIF4Es increase PER1/2 expression. Blue pointed and block arrows indicate activation and inhibition, respectively.

a normal response to light stimulation at early night, although the late-night response is significantly decreased[93]. This indicates that PACAP signaling is critical for light-induced phase advances at late night.

Both glutamate and PACAP signaling upon light input to the SCN converge onto phosphorylation of cAMP-response element binding protein (CREB; Figure 1.5). Calcium influx mediated by glutamate receptors activates $Ca2^{+}$/calmodulin-dependent protein kinase II (CaMKII), which then phosphorylates CREB. Increased cAMP levels mediated by PACAP receptors activate protein kinase A (PKA), which also targets CREB. CREB phosphorylation is critical for light resetting of the circadian clock. CREB is phosphorylated only when light induces c-fos expression and phase shifts in circadian behavior[95], suggesting that CREB phosphorylation might gate light responsiveness in the circadian clock. Phosphorylated CREBs induce *Per1/2* gene expression by binding to CREB-responsive element (CRE) on their promoter[96,97], leading to phase shifts in the circadian clock[98,99]. Experiments using CRE decoy and clock gene antisense oligonucleotides[99] revealed that CRE activation is critical for light-induced phase shifts *in vivo*. Interestingly, CRE-mediated *Per1* induction, but not *Per2* induction, is required for glutamate-induced phase shifts *in vitro*[99]. Recent work, however, showed that PER2 mediates light induction of *Per1* by facilitating formation of a transcriptional activation complex containing CREB and CREB-binding protein (CBP)[100], suggesting that both PER1 and PER2 are critical for circadian clock resetting.

In addition to transcriptional mechanisms, translational mechanisms are involved in light-induced clock resetting. Light exposure at night involves multiple signaling cascades converging on phosphorylation of eukaryotic translational initiation factor 4E (eIF4E), a critical regulator of protein translation (Figure 1.5). In one pathway, light signals at night induce activation of mitogen-

activated protein kinases (MAPKs) such as extracellular signal–regulated kinase (ERK)[101]. ERK then activates MAPK-interacting kinase (MNK), which phosphorylates eukaryotic translational initiation factor 4E (eIF4E). Phosphorylated eIF4E enhances PER1/2 translation[102]. Blocking eIF4E phosphorylation significantly decreases light-induced clock resetting[102], suggesting that eIF4E-mediated regulation of PER translation is a critical step for clock resetting. Another pathway converging on eIF4E phosphorylation is through the mammalian target of rapamycin (mTOR) signaling. mTOR is critical for regulating protein translation via inhibiting eukaryotic translation initiation factor 4E-binding protein 1 (4E-BP1), an eIF4E repressor[103], and mediates light resetting of circadian rhythms[104]. In addition to PER translation, VIP translation is also increased by the mTOR/4E-BP1/eIF4E pathway, facilitating intercellular coupling among the SCN neurons[105]. Interestingly, 4E-BP1 knockout mice lacking its negative regulation of VIP translation show accelerated re-entrainment of circadian behavior to shifted light cycles and resistance to circadian rhythm desynchrony in behavior under constant light[105]. However, it remains an open question how translational mechanisms regulate clock synchronization within the SCN at the cellular level.

1.3 After-effects of light exposure on circadian rhythms

Light signals are strong zeitgebers that can phase-shift and entrain circadian rhythms as described in Section 1.1. Furthermore, light exposure can cause differences in circadian period measured in constant darkness (free-running period; FRP) between prior to and following the exposure, referred to as after-effects[3]. After-effects are long-lasting effects as changed FRPs gradually revert to a genetically determined value over months[2]. There are four kinds of after-effects that are well documented. The first one is after-effects of constant light. As described above,

circadian rhythms in nocturnal organisms generally show a longer period under constant light (LL) than in constant darkness. LL-induced lengthened period persists when nocturnal animals are released in constant darkness[3]. The second one is after-effects of non-24hr T-cycles. Entrainment to short T-cycles (T < FRP) shorten subsequent FRP, whereas long T cycles (T > FRP) elongate subsequent FRP. When a T-cycle period is too short or long to entrain animals, however, FRP does not change as described above[12,106], indicating that after-effects of T-cycles depends on entrainment, not just light exposure. The third kind of after-effects can arise following photoperiod entrainment. Long photoperiods shorten subsequent FRP; short photoperiods lengthen it[12]. Skeleton photoperiods have similar effects on FRP to those of complete photoperiods[12]. Lastly, the fourth kind is after-effects of single light pulses. Single light pulses can cause phase shifts immediately and induce changes in circadian period on subsequent cycles. Light at early night induces a phase delay and subsequent period lengthening, while light at late night causes a phase advance and period shortening[12]. The magnitude of period changes is positively correlated with that of phase shifts[107,108].

As the discrete model of entrainment based on the phase response curve and constant circadian period explains most aspects of light entrainment, several potential functional benefits for having after-effects have been discussed in the literature. First, as phase delays cause a period lengthening and advances cause a period shortening, after-effects are additive to phase shifts for cancelling out the difference between FRP and a period of external light cycles[12]. After-effects can thus further stabilize entrainment. Another potential benefit is that period shortening after-effects following skeleton long photoperiods can enhance tolerance to a short night length, preventing a phase jump. This idea came out from modeling work of circadian rhythms in nocturnal animals[12]; however, it remains to be experimentally validated.

As described above, after-effects of constant light are in the opposite direction of those of long photoperiods: constant light lengthens FRP, while long photoperiods shorten it. This contradicts the continuous model of entrainment where light signals continuously influence on FRP for the duration of light exposure. If circadian rhythms indeed slowed down during light exposure, long photoperiods should lengthen subsequent FRP. This discrepancy led to a reasoning that the continuous action of light is not a dominant factor to produce after-effects of long photoperiods[12]. FRP shortening by both skeleton and complete long photoperiods[12,109] suggests that light in the morning and evening might primarily induce shortening after-effects. However, it is unknown how such two-pulse entrainment can cause after-effects in the opposite direction depending on whether circadian rhythms are aligned with a shorter or a longer night interval.

Molecular mechanisms of after-effects

Although after-effects are pervasive in many forms of light entrainment, they tend to be ignored as they are much smaller in magnitude than phase shifts and therefore are harder to measure. Because of this challenge, molecular mechanisms underlying light-induced circadian after-effects are poorly understood. In contrast, it has been extensively studied and well characterized how light can induce phase shifts in circadian rhythms at the molecular level as described in Section 1.2. Given that circadian period is the most fundamental parameter of the circadian oscillators, it is significant to understand how light modulates circadian period.

There have been largely two research directions toward understanding mechanisms of after-effects. One direction is focused on persistence of after-effects. As mentioned above, after-effects last over months, indicating that they are a form of long-term neural and behavioral plasticity, such as learned behaviors. When animals are given a reward paired with an audio tone

(a neutral stimulus), for example, they develop an association between the two stimuli, showing a reward-seeking behavior in the absence of a reward if the audio tone is provided. In other fields in neuroscience, long-term behavioral plasticity has been recently found to involve epigenetic mechanisms where gene expression is altered without changes in DNA sequence. Particularly, DNA methylation is essential for long-term behavioral plasticity in many contexts such as fear conditioning[110], reward-associated learning[111], and maternal care[112].

DNA methylation is an addition of a methyl group to cytosine on DNA, and it is an epigenetic mechanism of regulation of the gene transcription via chromatin changes on the gene body or gene promoter. In general, promoter DNA methylation silences the gene expression[113,114], while gene body methylation contributes to transcriptional activation by repressing activation of intragenic cryptic promoters[115]. In mammals, DNA methylation is mediated by DNA methyltransferases (DNMTs). DNMT1, DNMT3A, and DNMT3B are three canonical DNMTs. DNMT3L in itself has no catalytic activity, but it regulates DNMT3s when it forms a complex with them[116]. DNMT1 is the most abundant isoform and essential for maintaining DNA methylation patterns[117], whereas DNMT3s are critical for establishing those patterns in the first place[118]. Recent work has revealed that this functional dichotomy seems to be an over-simplification, although it is correct for their major roles: all the isoforms are in fact involved in both de novo and maintaining DNA methylation in a context-dependent manner[119,120].

As the SCN is a master clock regulating light entrainment, the SCN and its locomotor behavior output have been examined for the role of DNA methylation in after-effects. As T-cycle entrainment causes robust after-effects, Azzi and colleagues examined differences in transcriptome of the SCN between animals entrained to 22-hour light T-cycles and those entrained to 24-hour cycles[106]. Ontological analyses showed that differentially expressed genes are enriched for

neuronal functions and chromatin regulation such as neurotransmitter receptors and DNMTs. Genome-wide assays for promotor DNA methylation patterns revealed that many differentially methylated genes between 22h and 24h cycle conditions are involved in neuronal functions. Interestingly, the ventral SCN showed a significantly higher number of differentially methylated regions on the genome compared to the dorsal SCN[75], suggesting that the ventral SCN might play an important role in after-effects of T-cycles. Further, pharmacological inhibition of DNA methylation in the SCN *in vivo* showed a reduced magnitude of after-effects on locomotor behavior rhythms[106]. This provides direct evidence that DNA methylation mediates expression of after-effects.

Examining the role of DNA methylation in the after-effects on SCN molecular rhythms, however, had a significant challenge. Conventionally, after-effects on SCN rhythms have been examined by manipulating light cycles in intact animals and then measuring free-running rhythms in explanted SCN slice culture. However, after-effects on *ex vivo* SCN rhythms from animals entrained to T-cycles are inversely correlated with those on their behavioral rhythms[75,121,122]. Short T-cycles produce a longer *ex vivo* SCN period than do long T-cycles, although in principle SCN period should reflect the behavioral period. Separate period measurements of the ventral and dorsal SCN revealed that period of the ventral SCN matches behavioral period, while those of the dorsal SCN display inverse after-effects[75], suggesting that reorganization of SCN slices during culture might cause an abnormal expression of after-effects *ex vivo*, as predicted by modeling analyses. Blocking DNA methylation in *ex vivo* SCN abolishes period differences between T-22, T-24, and T-26 *in vivo* entrainment conditions, suggesting that DNA methylation is essential for maintaining after-effects on SCN rhythms. Interestingly, this contradicts a finding that inhibition of DNA methylation in the SCN *in vivo* after T-cycle entrainment does not cause changes in after-effects

on behavioral rhythms[106]. Future studies will need to address this contradiction and whether DNA methylation is involved in establishing after-effects, maintaining them, or both.

Another direction towards understanding mechanisms of after-effects is focused on relationships with phase synchrony among SCN neurons. As described above, entrainment to long photoperiods causes a period shortening and a larger phase dispersion in free-running SCN rhythms in DD, compared to entrainment to an LD 12:12 cycle. Previous work using mathematical modeling of circadian oscillators showed that a larger phase difference among oscillators can shorten an ensemble period[123–125]. Beersma and colleagues created a simple phase-only model of two coupled oscillators of electrical firing activities. This model is based on two assumptions: (1) an early-phased oscillator phase-advances a late-phased oscillator, (2) two synchronous oscillators phase-delay themselves most. The first assumption makes sense as a firing cell can initiate firing of the other; however, the second assumption needs to be validated. Based on the assumptions, synchronized oscillators show a longer ensemble period than individual oscillators with no interactions. In contrast, differentially phased oscillators display a shorter ensemble period than uncoupled individual oscillators, as large phase advances and small phase delays arise every cycle. Thus, large phase differences among SCN neurons in long photoperiods could produce daily phase advances as a net effect, thus causing a short ensemble period.

A more realistic multiscale, multicellular model of SCN oscillators[79,80] supports an explanation that the SCN period decreases as the phase dispersion increases under long photoperiods. This model takes basic properties of SCN neurons (e.g., neurophysiology and transcription-translation feedback loops) into account, and it is based on phase repulsion from the slow-oscillating, ventral SCN to the fast-oscillating, dorsal SCN and phase attraction from the dorsal to the ventral SCN. In theory, when fast oscillators phase-lead slow oscillators, fast

oscillators run faster via phase repulsion and slow oscillators run faster as well via phase attraction. Such period shortening effects increase with larger phase differences between oscillators. Thus, a high degree of regional phase dispersion under long photoperiods induces a significant period shortening in SCN rhythms. Empirical evidence supporting such opposing phase couplings among SCN neurons comes from GABA switching predominantly arising in the dorsal SCN[80]. As described in Section 1.2, GABA signaling can be inhibitory or excitatory, depending on intracellular chloride concentration: high intracellular chloride makes GABA excitatory, whereas low intracellular chloride makes it inhibitory. Long photoperiods induce increases in the ratio of chloride importers to exporters and increase intracellular chloride specifically in the dorsal SCN, but not in the ventral SCN, suggesting that GABA signaling is excitatory in the dorsal SCN and inhibitory in the ventral SCN. Opposing GABA signaling between the dorsal and ventral SCN explains well increased phase dispersion under long photoperiods, as excitatory GABA transmission would facilitate synchronization in the dorsal SCN, while inhibitory GABA would desynchronize the ventral SCN. However, it remains to be determined whether GABA signaling is necessary for establishing phase dispersion and causing after-effects of long photoperiods. Also, unlike the assumption of the realistic SCN model, the dorsal-ventral difference in a period of SCN slices from animals entrained to long photoperiods appears marginal: *Bmal1* reporters show that the dorsal region has a slightly shorter period than does the ventral region[126], whereas PER2 reporters do not[74]. Notably, periods of SCN subregions are comparable across different long photoperiods from LD 16:8 to LD 22:2, although phase distribution in SCN is more polarized as daytime lengths get longer[74]. This suggests that there might be a ceiling effect of phase synchrony on the magnitude of after-effects, and it will be interesting to see whether a realistic model can provide any explanation.

In addition to long photoperiods, non-24h T-cycles cause phase dispersion and after-effects in the SCN[75]. In short T-cycles the ventral SCN phase-leads the dorsal SCN, while in long T-cycles the dorsal SCN is phase-leading. Inverse after-effects *ex vivo* described above are prominent in the dorsal SCN with having a shorter period following long T-cycles than short T-cycles. In contrast, the ventral SCN shows a long period following long T-cycles. Period differences in free-running SCN rhythms from animals between T-22, T-24, and T-26 cycle conditions are abolished when $GABA_A$ receptors are blocked, suggesting that GABA signaling is involved in maintaining after-effects of T-cycles. Given that GABA switching is a potential mechanism of long photoperiod-induced phase dispersion[80], it will be worth examining whether GABA switching plays a role in T-cycle-induced phase dispersion. Also, it is an interesting and important question whether and how T-cycle after-effects are mechanistically linked to phase distribution in the SCN.

Two research directions towards understanding mechanisms of after-effects described above are apparently intertwined. Differentially methylated genes across different T-cycles include genes involved in ion channels, neurotransmitter receptors, and transporters[75,106], suggesting that DNA methylation might regulate after-effects via modulation of intercellular rhythm coupling in the SCN such as changes in phase synchrony. Future studies will need to address how photoperiodic and T-cycle after-effects converge at the molecular level. This will deepen our understanding of network plasticity of cellular clocks in the SCN.

In summary, classical studies in behavioral circadian rhythms have provided a foundation of how light as a zeitgeber influences circadian endogenous oscillators, such as the phase response curve, models of entrainment, and after-effects. Discoveries of the molecular and cellular identity of the mammalian circadian oscillators have expanded our understanding of how they contribute to light entrainment of circadian behavior in mammals. At the master SCN clock level, it is well

characterized how the SCN maintains circadian periodicity in free-running conditions, and how SCN molecular rhythms are phase-shifted by acute light exposure or stimulations. However, it is not fully understood how the SCN clock shows light-induced changes, achieves light entrainment, and produces after-effects at the molecular and network levels. In Chapter II, I present my work describing how the SCN achieves entrainment and show canonical forms of circadian clock plasticity at the very basic level of a core clock gene. In addition, I describe regional differences in phase shifts and after-effects within the SCN neural network. Chapter III presents my work on the role of DNA methylation in after-effects of photoperiods and single light pulses on circadian behavior and SCN molecular rhythms. Lastly, Chapter IV provides conclusions and discusses future directions.

CHAPTER II

Light sets the brain's daily clock by regional quickening and slowing of the molecular clockworks at dawn and dusk

This work presented here is published as:

Kim, S., & McMahon, D. G. (2021). Light sets the brain's daily clock by regional quickening and slowing of the molecular clockworks at dawn and dusk. eLife, 10, e70137. https://doi.org/10.7554/eLife.70137.

2.1 Abstract

How daily clocks in the brain are set by light to local environmental time and encode the seasons is not fully understood. The suprachiasmatic nucleus (SCN) is a central circadian clock in mammals that orchestrates physiology and behavior in tune with daily and seasonal light cycles. Here, we have found that optogenetically simulated light input to explanted mouse SCN changes the waveform of the molecular clockworks from sinusoids in free-running conditions to highly asymmetrical shapes with accelerated synthetic (rising) phases and extended degradative (falling) phases marking clock advances and delays at simulated dawn and dusk. Daily waveform changes arise under *ex vivo* entrainment to simulated winter and summer photoperiods, and to non-24 hr periods. *Ex vivo* SCN imaging further suggests that acute waveform shifts are greatest in the ventrolateral SCN, while period effects are greatest in the dorsomedial SCN. Thus, circadian

entrainment is encoded by SCN clock gene waveform changes that arise from spatiotemporally distinct intrinsic responses within the SCN neural network.

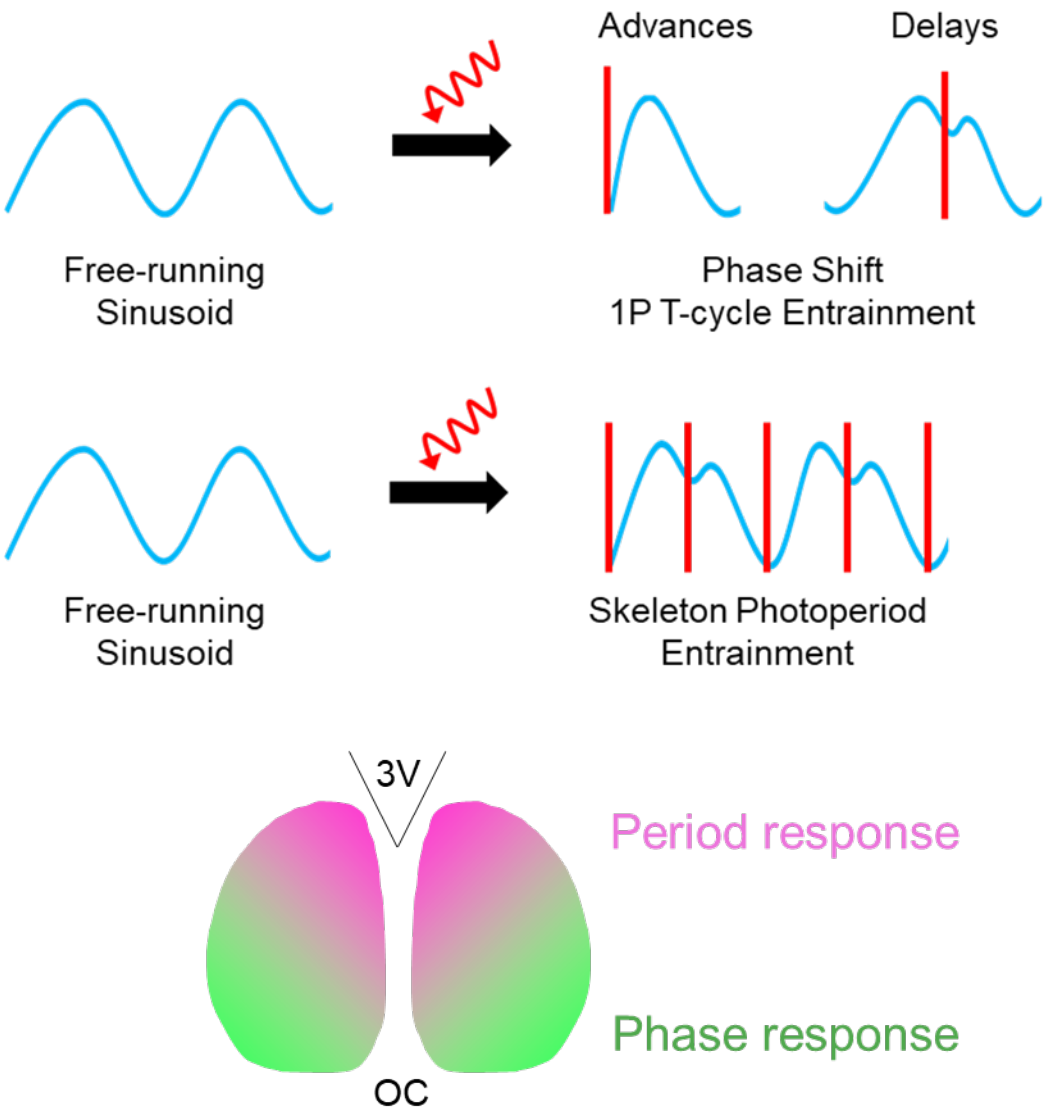

Figure 2.1. Graphical abstract.

2.2 Introduction

A key biological function of circadian clocks is to encode local environmental time, and the seasons, through interactions with the daily light cycle. Most organisms live in a rhythmic environment where daily environmental changes occur corresponding with solar time, and their endogenous 24-hour timing mechanism, or the circadian clock, enables adjustment of their physiology and behavior accordingly. In mammals, the central clock—the suprachiasmatic nucleus (SCN) of the hypothalamus—represents solar time to synchronize peripheral tissue clocks in the rest of the body, and it drives the expression of daily and seasonal behaviors in tune with the temporal structure of the environment.

Classical behavioral studies performed by manipulating light cycles have revealed fundamental principles in how circadian rhythms are reset and synchronized by external time cues at the level of behavioral outputs[2,12], but the molecular basis of clock setting and synchronization remains to be fully explained. Entrainment or alignment of circadian locomotor behavior with light cycles is achieved based on differential sensitivity of the circadian rhythm to the timing of light exposure – phase delays result from light exposure in the early circadian night, phase advances from light in the late night, and there is a "dead zone" in the mid-day where light does not reset the rhythm[12]. At the molecular level, the basis of the mammalian circadian clock is self-sustained circadian oscillations of core clock genes arranged in an autoregulatory transcription-translation feedback loop, with transcription factors *Clock* and *Bmal1* driving the circadian expression of *Period* (*Per*) and *Cryptochrome* (*Cry*) genes that mediate negative feedback within the clockworks[23]. Light stimulation results in acute induction of *Per1/2*[23]. Conventional time-point clock gene expression profiling from animals under different light cycles has provided a snapshot of how the clock gene rhythms in the SCN are influenced by various lighting conditions[127,128], but

with limited temporal resolution that does not fully capture dynamic changes in the clock gene rhythms induced by different light cycles.

The advent of clock gene reporters (e.g., *Per1*::GFP, PER2::LUC)[129,130] enabled assaying the motion of the circadian clock in real time and with low variability. However, to date the fundamental question of how clock genes in the SCN encode different lighting conditions has been primarily approached by manipulating light exposure *in vivo* and subsequently explanting the SCN into slice culture in constant darkness to retrospectively infer the *in vivo* entrained state, due to technical challenges in mimicking retinal light input *ex vivo*. While much progress has been made with this paradigm, this approach can have significant limitations. The SCN activity observed in a free-running condition reflects relaxation of the explanted SCN network back toward baseline, rather than active encoding of entrainment[81], and explantation can disrupt expression of the *in vivo* state[131].

Here, combining long-term organotypic explant culture, cyclic red light optogenetic stimulation, and the PER2 bioluminescent reporter, we assess how the clock gene rhythms in the *ex vivo* SCN change in real time to achieve entrainment to light cycles. We have instituted an *ex vivo* optogenetic experimental system that provides precise timing, duration and intensity of recurring input stimulation to the explanted SCN while tracking clock gene rhythms at high temporal resolution. Acute optogenetic channelrhodopsin-2 (ChR2) stimulation of SCN neurons with 470nm blue light to make them fire at light-driven spike frequency (e.g., 8–15Hz)[132,133], as does retinal light input, has been shown to be effective to reset circadian rhythms *in vivo* and *ex vivo*. However, long-term blue light illumination in culture (without opsins) results in phototoxicity, reducing cell viability (470 nm, 1 Hz)[134] and degrading many biological processes, including cell growth (470 nm, continuous)[135] and respiration (425–500 nm, continuous)[136].

Notably, red light is more tolerable *in vitro* (488nm vs 558 or 640 nm, continuous)[137] and *in vivo* (440–500nm vs. 540–660 or 655–695nm, continuous)[138138]. Recent development of optogenetic actuators responding to red light[139,140] prompted us to test whether red light can be utilized for long-term optogenetic stimulation, and to study how core clock gene PER2 rhythms in the *ex vivo* SCN are dynamically altered and reset by repeated light stimulation to achieve light entrainment.

Here we uncover that PER2 rhythms in the *ex vivo* SCN under entrainment to optogenetic light cycles show contraction of the rising phase and elongation of the falling phase depending on the timing of light exposure, and reveal *ex vivo* SCN plasticity at the clock gene level similar to canonical features of light-induced plasticity in circadian behavior. Aspects of circadian plasticity to light entrainment and regional heterogeneity of light responsiveness are apparently intrinsic to the SCN clockworks.

2.3 Results

An integrated system for long-term optogenetic stimulation and bioluminescence recording

To entrain the SCN slice with optogenetic stimulation, light pulses must be given periodically for multiple days to weeks. While repeated and long-term optogenetic stimulation of the SCN with ChR2 has been used to successfully entrain circadian locomotor behavior[132,141], long-term blue light exposure in culture can decrease cell viability via toxic byproducts[134]. To test the effects of sustained blue light exposure on SCN slices, we delivered blue light pulses (470nm, 1.2mW/mm^2) for 12h to SCN slices expressing a bioluminescent translational reporter of the core clock gene *Per2*, PER2::LUC[130], but no optogenetic construct. We applied 10Hz, 10ms light pulses that can be used to optogenetically drive SCN neurons to fire at light-driven spike frequency *in vivo*[132,133,142]. We found that PER2::LUC bioluminescence became arrhythmic following the

prolonged blue light exposure (Figure 2.2A, B). This effect was not reversible with a medium change (Figure 2.2A), suggesting that long-term blue light exposure *per se* can impair circadian rhythmicity in SCN slice cultures.

Since side effects of light exposure decrease with increasing irradiation wavelength[137,143], we tested whether using red light (625nm) mitigates light impairment of SCN rhythms. 12h red light pulses (625nm, 10Hz, 10ms, 1.25mW/mm^2) did not significantly affect the PER2::LUC rhythm in SCN slices (Figure 2.2A, B), suggesting that using red light stimulation could be more feasible for prolonged optogenetic light stimulation *ex vivo*. We thus expressed a red light-activated opsin, ChrimsonR, fused with a red fluorescent protein tdTomato (tdT) throughout SCN slices using synapsin promoter-controlled AAVs targeting all SCN neurons (AAV-Syn-ChrimsonR-tdT[140]) to mimic widespread retinal photic inputs to the SCN [38,144] (Figure 2.2C).

To extend the duration over which we can observe the SCN slice throughout entrainment, we improved the quality and robustness of PER2::LUC rhythmicity by using brain slices from younger mice that usually survive longer in culture[145], and by using stabilized glutamine media that were shown to reduce ammonia production and improve cell viability in cell culture[146,147] (Figure 2.3). With these modifications, *ex vivo* SCN rhythms were stable for more than three weeks, long enough to conduct entrainment paradigms without culture medium changes that may perturb *ex vivo* SCN rhythms and entrainment. For precise temporal control of optogenetic stimulation of multiple SCN slices, we integrated an optogenetic stimulation apparatus into a multi-channel luminometer (Figure 2.2D). To minimize the potential effect of LED-generated heat on SCN rhythmicity while achieving sufficient light intensity for optogenetic stimulation, we set up a light delivery path in which an LED placed outside the incubator housing the luminometer could deliver 625nm light through a fiber optic cable and a collimation lens (Figure 2.1D). We then created a

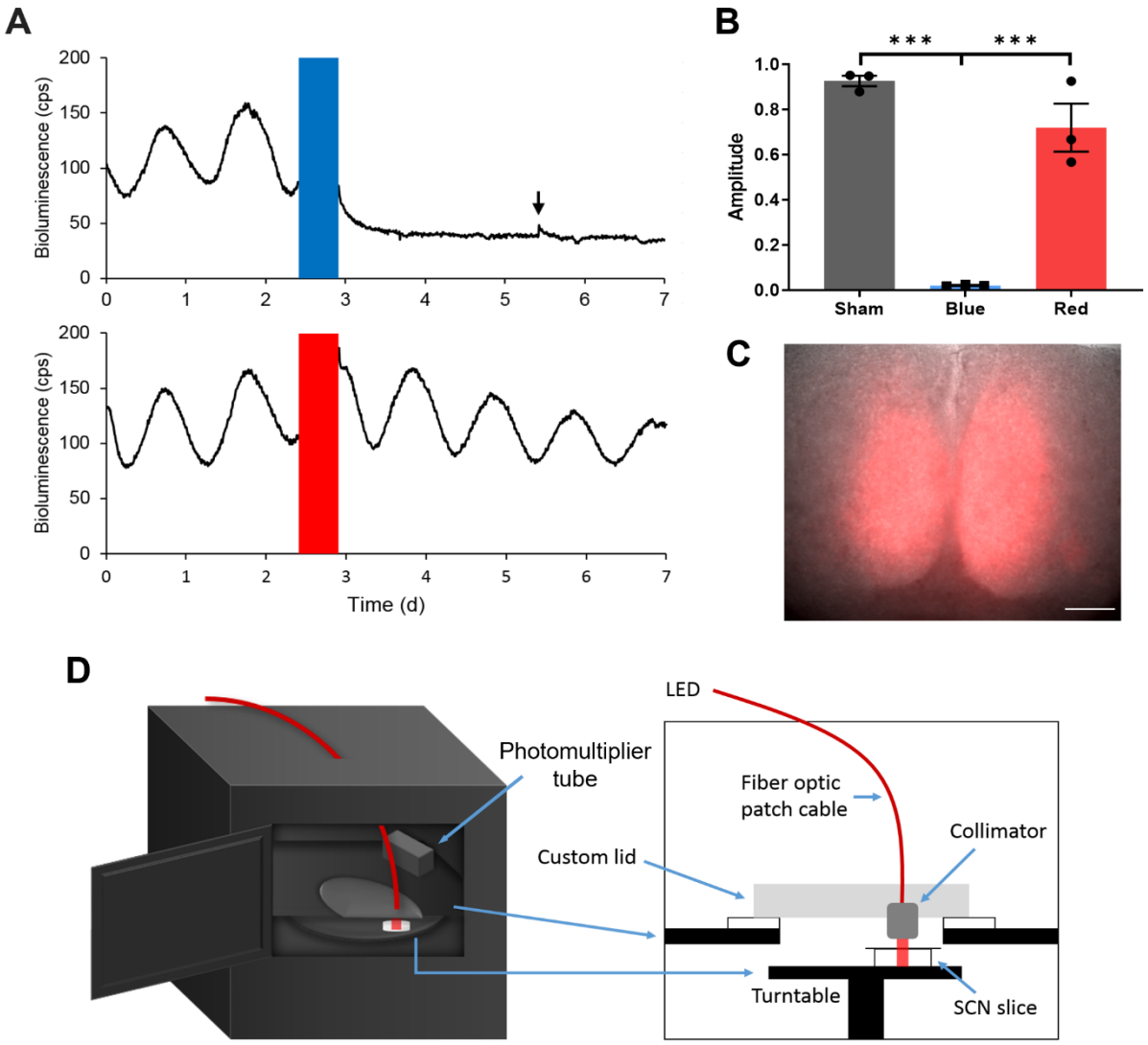

Figure 2.2. Long-term optogenetic stimulation system for circadian entrainment *ex vivo*.

(A) Representative PER2::LUC bioluminescence rhythms of adult SCN slices exposed to either red (top) or blue (bottom) 10Hz light pulses (red or blue bars) for 12h. The black arrow indicates the timing of media change. **(B)** Fold change in the rhythm amplitude following sham, blue, or red light exposure (Student t-test, mean ± SEM, n = 3, ***p < 0.001). **(C)** Merged ChrimsonR-tdT fluorescence and the brightfield images of an SCN slice. Scale = 100μm. **(D)** Diagrams showing a multi-channel luminometer integrated with an optogenetic stimulation apparatus.

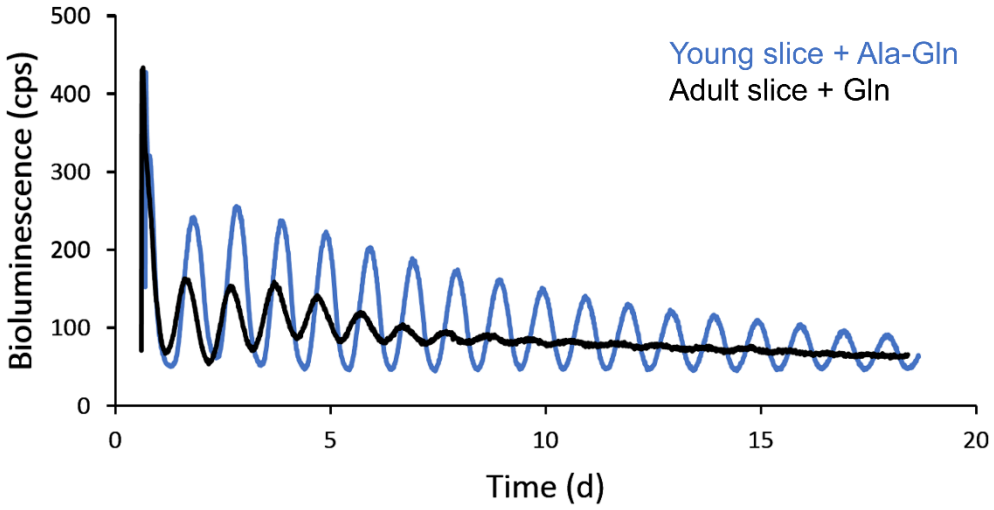

Figure 2.3. Improved PER2::LUC rhythmicity in SCN slice explanted from young mice to culture medium containing stabilized glutamine.

Representative PER2::LUC rhythms of SCN slice cultures from an adult (P60) and a young (P12) mouse. Young SCN slice cultures with stabilized glutamine (alanyl-glutamine) showed higher amplitude in PER2::LUC rhythms for a longer duration, compared to rhythms from adult SCN slices in culture medium containing regular glutamine.

program interface for remotely operating PER2::LUC luminometry and optogenetic stimulation in a coordinated manner (Figure 2.4).

Discrete optogenetic light pulses differentially alter SCN clock gene waveforms to induce the phase and period responses

To test how this integrated system induces phase resetting of circadian rhythms that fundamentally underlies circadian entrainment, we applied 10Hz optogenetic light stimulations to ChrimsonR-expressing SCN slices on the 3rd or 4th day of recording at three different circadian times (CT) as defined by the timing of the intrinsic PER2::LUC rhythm of each SCN slice. We chose 10Hz stimulation as light-driven SCN spike frequency *in vivo* ranges 7 to 13 Hz[142]. By convention, CT12 was defined as the peak time of the PER2::LUC rhythm and is correlated *in vivo* with the onset of nocturnal behavioral activity[130]. Thus, the rising phase (CT0–12) of the PER2::LUC rhythm represents the day phase of intrinsic SCN circadian time, while the falling phase (CT12–24) corresponds to physiological night. Light stimulation *in vivo* at CT6, CT14, and CT21 induces representative phase responses in the locomotor circadian rhythm (no phase shift, phase delays, and phase advances, respectively)[148,149]. We found that the phase responses to ChrimsonR-mediated stimulation in *ex vivo* SCN indeed mimicked the phase responses of circadian behavior in intact mice to light stimulations *in vivo* (Figure 2.5A, C). Optogenetic stimulation of SCN slices at CT6 induced little phase shift (0.14 ± 0.19 h; mean ± SEM), whereas optogenetic stimulation at CT14 and CT21 induced significant phase delays and advances, respectively (CT14: -4.25 ± 0.76 h, CT21: 4.38 ± 0.67 h; Figure 2.5C).

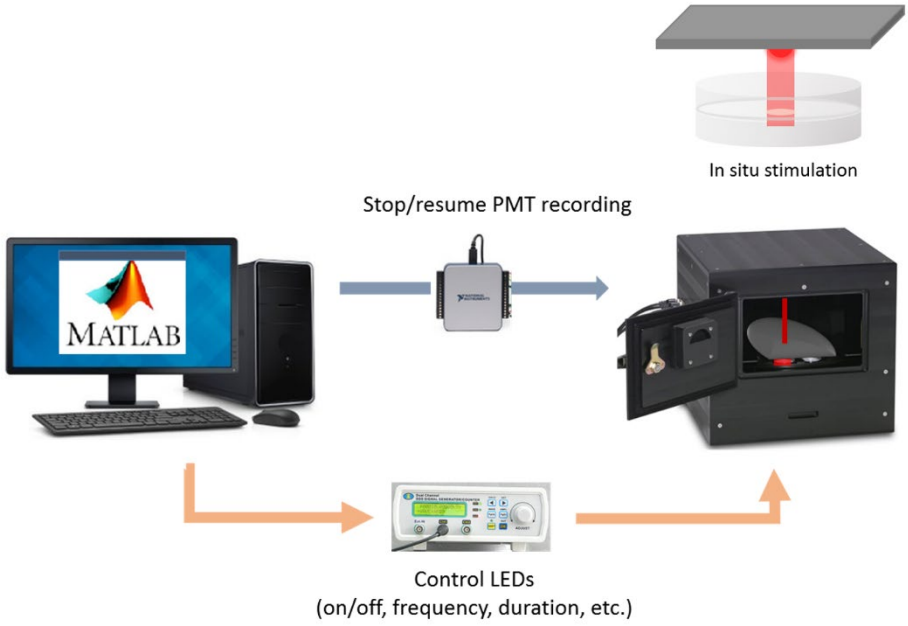

Figure 2.4. Diagram of an integrated system for long-term luminescence recording and optogenetic stimulation.

Custom-written Matlab code has access to a luminometer data collection software, a multifunction I/O device turning on/off the photomultiplier tubes (PMTs), and a signal generator controlling LEDs. Thus, it can schedule periodic stimulation and execute a series of events during optogenetic stimulation — pause PMT recording, target positioning, LED stimulation, and PMT recording resumption.

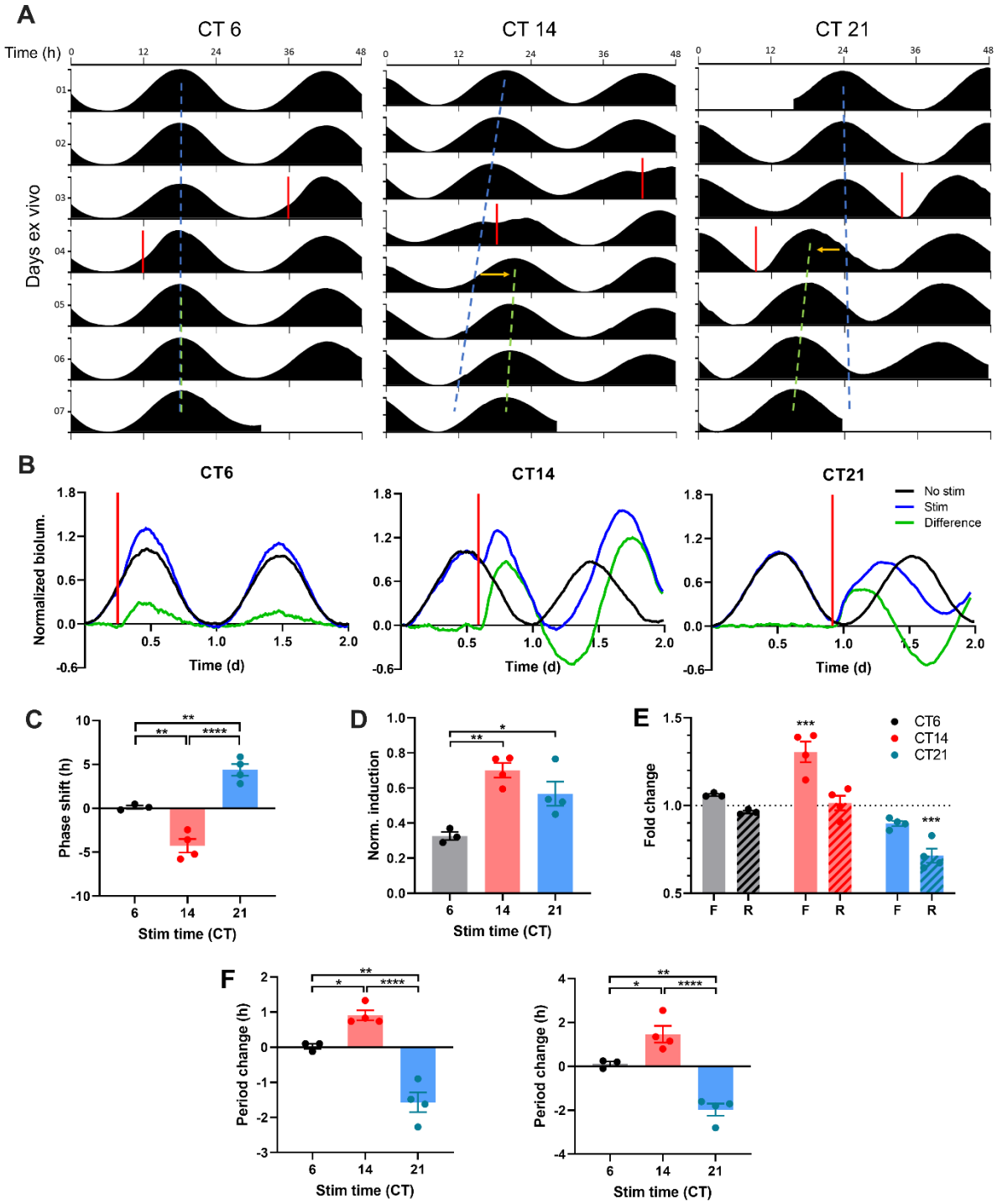

Figure 2.5. ChrimsonR-driven optogenetic stimulation alters the waveform of SCN PER2 rhythm to reset the SCN clock. (*Figure legend continues.*)

(*Figure legend continued.*) **(A)** Representative double-plotted PER2::LUC bioluminescence actograms of SCN slices stimulated with single 15min 10Hz optogenetic pulses (red bar) at CT6 (left), 14 (middle), and 21 (right). Linear regressions of the pre-stimulation and post-stimulation cycle peaks are indicated as the blue and green dashed lines, respectively. Phase shifts are depicted by a yellow arrow. **(B)** Representative PER2::LUC rhythms of SCN slices before and after stimulation (red bar). Green traces depict difference in normalized bioluminescence between the pre-stim and post-stim rhythms (black and blue traces, respectively). **(C)** Quantification of phase shifts following stimulation. Positive and negative phase shifts indicate phase advance and delay, respectively. (One-way ANOVA with Tukey's multiple comparisons test, mean ± SEM, n = 3-4, **p < 0.01, ****p <0.0001). **(D)** Normalized PER2::LUC induction following stimulation. (One-way ANOVA with Tukey's multiple comparisons test, mean ± SEM, n = 3-4, *p < 0.05, **p < 0.01). **(E)** Fold change in duration of the rising (R; dashed boxes) and falling (F; open boxes) phases of PER2::LUC rhythms following stimulation. (RM two-way ANOVA with Sidak's multiple comparisons tests, mean ± SEM, n = 3-4, ***p < 0.001). **(F)** Quantification of period changes following stimulation using linear regression of peaks (left) and Lomb-Scargle periodogram (right). Positive and negative period changes indicate period lengthening and shortening, respectively. (One-way ANOVA with Tukey's multiple comparisons test, mean ± SEM, n = 3-4, *p < 0.05, **p < 0.01, ****p <0.0001).

Strikingly, optogenetic stimulation of SCN slices differentially altered the waveform of PER2::LUC rhythms on the stimulated cycle, depending on the timing of the stimulation (Figure 2.5B). Stimulation at night (CT14, CT21) induced greater acute increases in PER2::LUC expression in SCN slices than did stimulation in the day (CT6) (CT6: 0.33 ± 0.02 artificial unit (AU), CT14: 0.70 ± 0.04 AU, CT21: 0.57 ± 0.07 AU; Figure 2D). The differential PER2::LUC induction led to differential changes in the duration of specific phases of PER2::LUC rhythms (Figure 2.5E). Stimulation at CT14 induced an acute rise in PER2, elongating the falling phase (1.31 ± 0.06 fold change (FC)) to induce a phase delay, whereas stimulation at CT21 accelerated the rising phase (0.72 ± 0.04 FC) to induce a phase advance. Stimulation at CT6, however, did not significantly alter either the rising or the falling phase duration (rising phase: 0.97 ± 0.01 FC, falling phase: 1.06 ± 0.01 FC) despite small PER2::LUC induction, thus causing little phase shift. Together, differential waveform changes in PER2 rhythms underpin time-dependent phase responses to light stimulation in the SCN.

Further, the acute phase shifts were accompanied by a subsequent sustained change in the free-running circadian period (i.e., circadian period of an oscillator in the absence of external time cues such as light) of SCN slices that persisted for multiple days as an after-effect of the acute phase-shifting stimulations (Figure 2.5A, F). Similar to after-effects of light induced phase shifts on circadian locomotive behavior[2], phase delays in PER2::LUC rhythms following stimulation at CT14 led to period lengthening on subsequent cycles, whereas phase advances following CT21 stimulation resulted in period shortening (linear regression method. CT14: 0.91 ± 0.14 h, CT21: -1.57 ± 0.28 h; Lomb-Scargle periodogram. CT14: 1.46 ± 0.38 h, CT21: -1.98 ± 0.28 h; Figure 2.5F). These after-effects on period were not the result of persistent waveform changes—the PER2::LUC waveform returned to its free-running sinusoidal form after the stimulated cycle.

Thus, the SCN itself, in isolation from extra-SCN clocks and neural inputs, has plasticity of the circadian period following acute light stimulation.

Daily phase-specific waveform changes drive entrainment at the clock gene level

Individual phase shifts by external time cues are the building blocks of circadian entrainment[12]. Daily, repeated phase shifts to light adjust the endogenous circadian period to match the 24h day and align circadian rhythms in a particular temporal relationship with the daily light-dark cycle (i.e., phase angle of entrainment). Remarkably, animals can entrain to single light pulses given repeatedly as a cycle (T-cycle), even to cycle periods that deviate modestly from 24 hours, such as a 22h light cycle[12]. This so-called one-pulse entrainment is the simplest form of entrainment well-documented in the literature and can be used to easily interpret whether biological clocks can entrain to certain external cues. To test whether optogenetic stimulation can entrain the isolated SCN clock, we delivered periodic optogenetic light stimulation at intervals (optogenetic day-night cycle lengths, or T-cycles) that significantly deviated from the near-24h endogenous period of the SCN, to clearly differentiate the entrained state from free-running. One cohort of SCN slices was stimulated every 22h (T22) while the other cohort was stimulated every 25h (T25, Figure 2.6A). SCN in both cohorts demonstrated the canonical responses defining circadian entrainment—matching of clock period to the period of the input stimulus (Figure 2.6–2.8), adopting a stable timing relationship with the repeating stimulus (stable phase angle, Figure 2.6C, 2.9), and initiating a subsequent free-run from the point in time of the entrained phase angle upon cessation of the stimulus (Figure 2.6A). Importantly, PER2::LUC rhythms in the SCN entrained to the different T-cycles with different phase angles of entrainment (Figure 2.6C, 2.9), as predicted by the non-parametric model of circadian entrainment, and previously observed at the

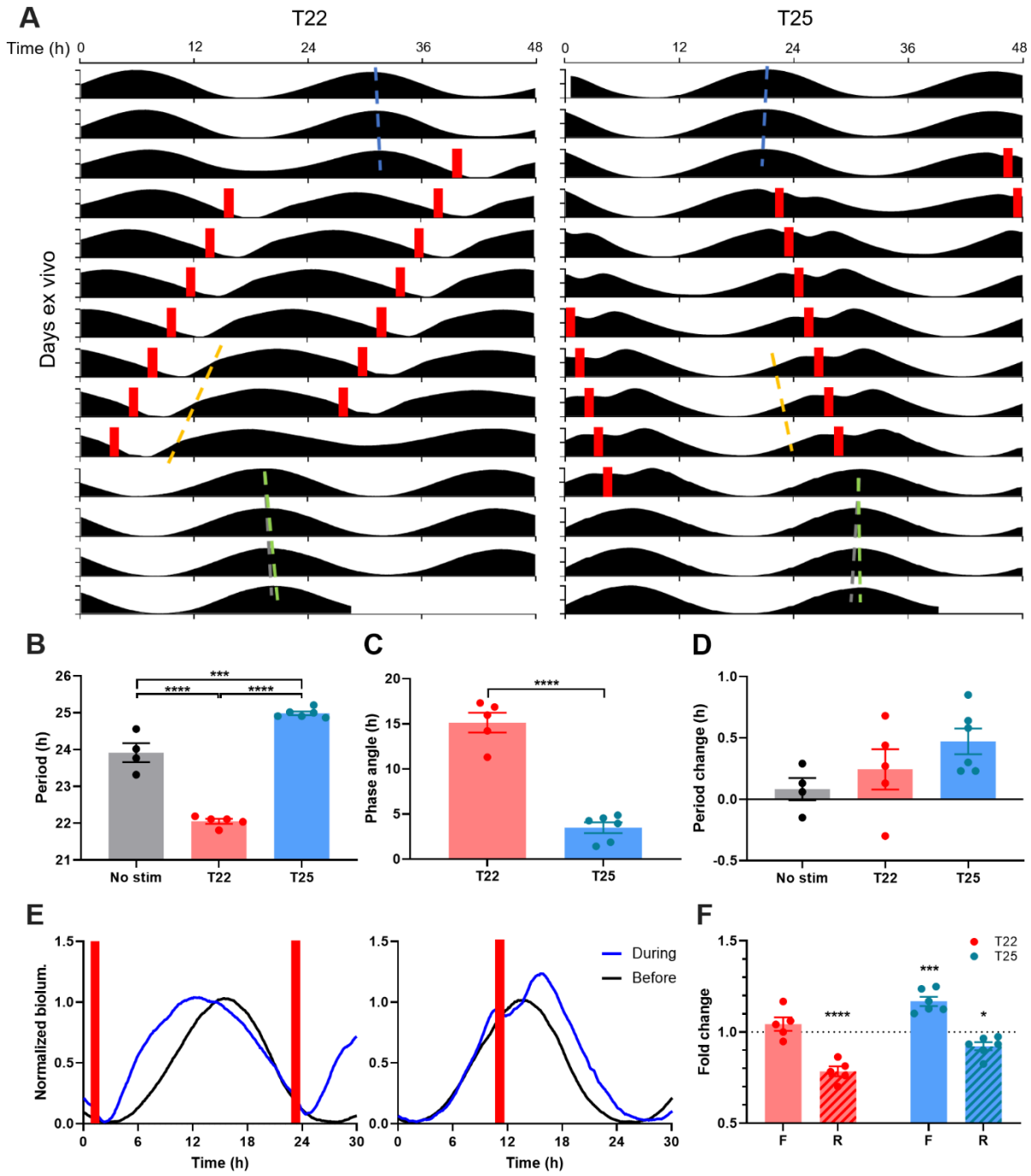

Figure 2.6. Optogenetic cycles entrain PER2::LUC rhythms in the SCN by triggering daily waveform changes that match the SCN clock to the cycle period.

(A) Representative double-plotted PER2::LUC bioluminescence actograms of the SCN slice entrained with 1–1.5h 10Hz optogenetic pulse (red bar) in every (*Figure legend continues.*)

(*Figure legend continued.*) 22h (left) or 25h (right). Linear regressions of the pre- and post-entrainment cycle peaks are indicated as the blue and green dashed lines, respectively. Yellow dashed lines indicate half-maxes on the rising phase during entrainment. Grey dashed lines indicate the pre-entrainment cycle period as a reference. **(B-D)** Quantification of period during entrainment **(B)**, phase angle of entrainment **(C)**, period change by entrainment **(D)**. **(B and D)** were analyzed using one-way ANOVA with Tukey's multiple comparisons tests (mean ± SEM, n = 4-6, ****p < 0.0001, ***p < 0.001), **(C)** was analyzed using Student t-test (mean ± SEM, n = 5-6, ****p < 0.0001). **(E)** Representative waveforms of PER2::LUC bioluminescence rhythms before (black trace) and during (blue trace) entrainment to T22 (left) and T25 cycles (right). Red bars depict optogenetic stimulation during entrainment. **(F)** Fold change in duration of the rising (R; dashed boxes) and falling (F; open boxes) phases of PER2::LUC rhythms during entrainment compared with before entrainment. (RM two-way ANOVA with Sidak's multiple comparisons tests, mean ± SEM, n = 5-6, ***p < 0.001, ****p < 0.0001).

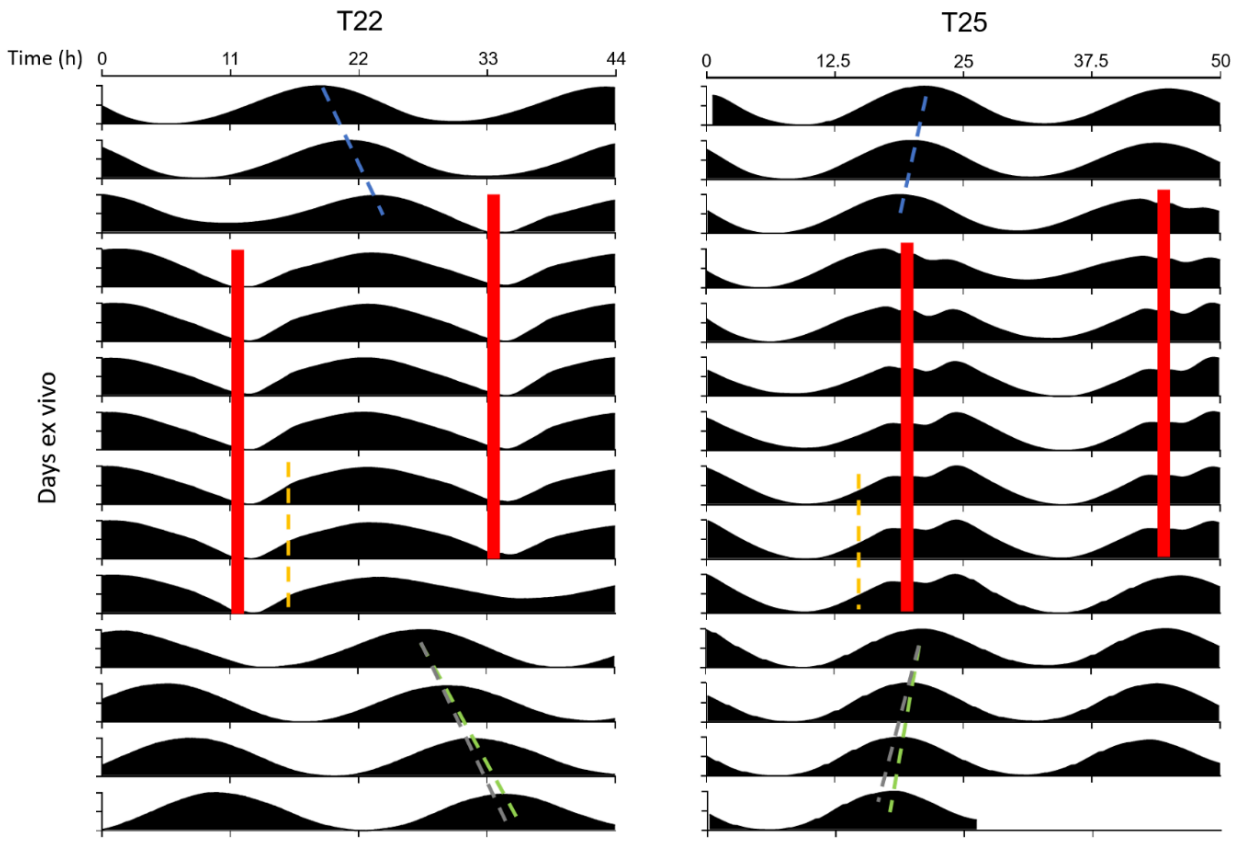

Figure 2.7. PER2::LUC rhythms in SCN slices entrain to optogenetic T-cycles.

Representative double-plotted PER2::LUC bioluminescence actograms of the SCN slice entrained with 1-1.5h 10Hz optogenetic pulse (red bar) in every 22h (left) or 25h (right). Actograms are plotted against a 22h (left) or 25h (right) time scale. Linear regressions of the pre- and post-entrainment cycle peaks are indicated as the blue and green dashed lines, respectively. Yellow dashed lines indicate half-maxes on the rising phase during entrainment. Grey dashed lines indicate the pre-entrainment cycle period as a reference.

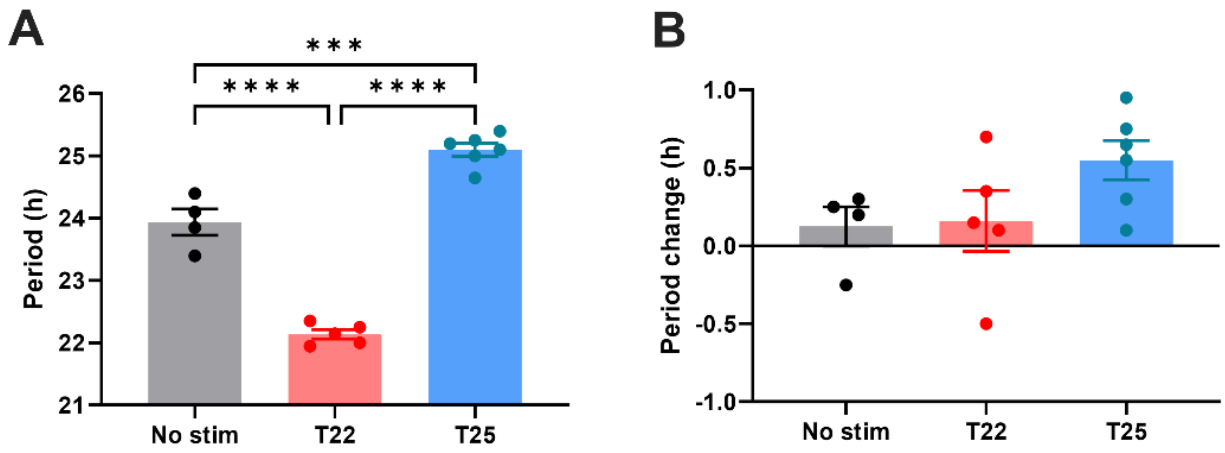

Figure 2.8. Quantification of period during entrainment (left) and period changes following entrainment (right) using Lomb-Scargle periodogram. (One-way ANOVA with Tukey's multiple comparisons tests, mean ± SEM, n = 4-6, ****p < 0.0001, ***p < 0.001)

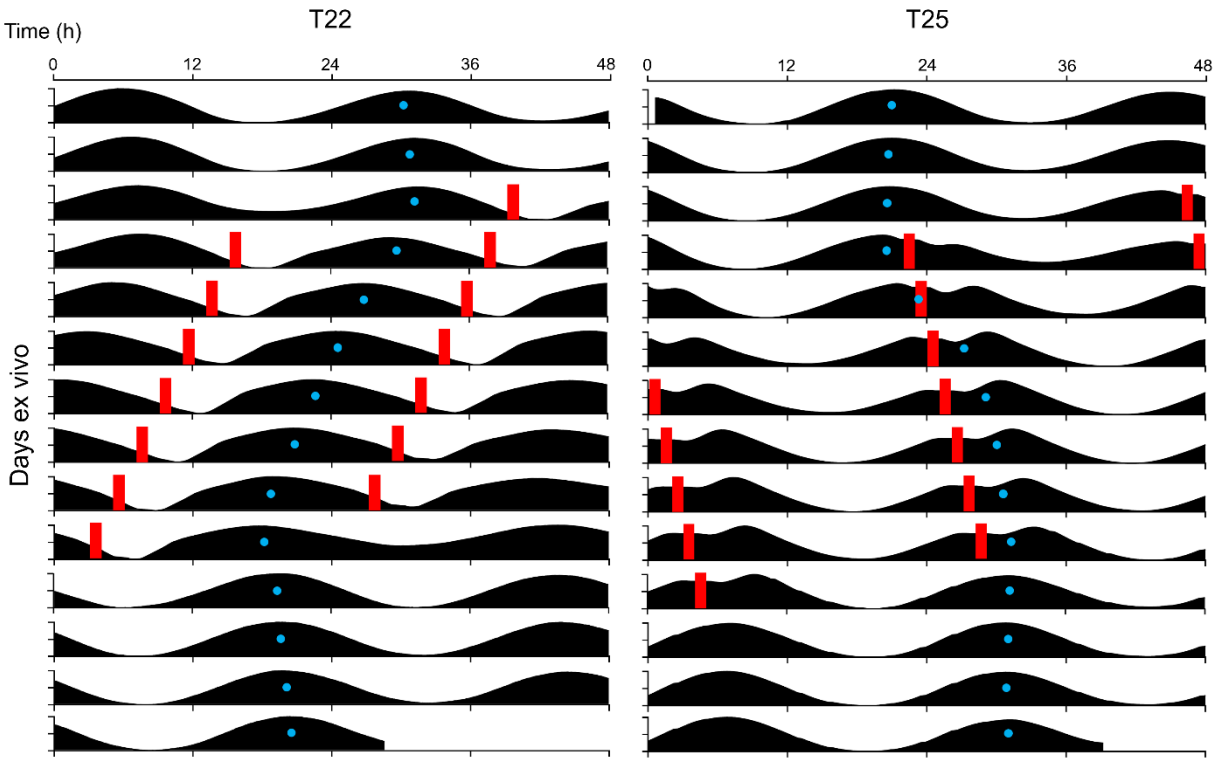

Figure 2.9. Acrophase fitting of PER2::LUC bioluminescence actograms from Figure 2.5.

Blue dots denote acrophases.

level of behavioral outputs[12]. PER2::LUC rhythms under T22 and T25 cycles showed that the periodic stimulation was aligned with the late falling and the late rising phases, where acute stimulation produces a phase advance and a delay, respectively (Figure 2.6A). Indeed, PER2::LUC rhythms in the SCN were entrained to short and long period cycles by daily phase advances and delays, respectively. The daily phase advances and delays were respectively derived from repeated acceleration of the PER2::LUC rising phase (0.79 ± 0.03 fold change) and elongation of the falling phase (1.17 ± 0.03 fold change; Figure 2.6A, E, F). Taken together, our results demonstrate that PER2::LUC rhythms in SCN slices can entrain to periodic optogenetic stimulation, and reveal that PER2 rhythms in the SCN encode different input cycle lengths via repeated rising phase shortening or falling phase lengthening.

We also tested whether PER2 rhythms in SCN slices show plasticity of endogenous clock period in constant darkness following the T-cycle entrainment. T-cycle entrainment by repeated light pulses *in vivo* produces after-effects on the period of circadian locomotive behavior: short and long T-cycles produce period shortening and lengthening, respectively[12,128]. As phase shifts by single stimulation had profound period after-effects on PER2::LUC rhythms (Figure 2.5D), repeated phase shifts by periodic stimulation were expected to have significant period after-effects. Surprisingly, however, repeated phase advances in PER2::LUC rhythms in SCN slices during T22 entrainment and phase delays during T25 entrainment did not produce statistically significant period after-effects (Figure 2.6D, 2.8). This suggests that phase shifts (rather than changes in the endogenous period) are a primary driver of matching circadian PER2 rhythms in the SCN to the period of T-cycles, as proposed by non-parametric model of entrainment[12].

The SCN clock entrains to skeleton photoperiods with a minimum tolerable night

Circadian oscillators in the SCN encode the length and timing of the daily light period (i.e., photoperiod)[19,150], thereby promoting seasonal changes in physiology and behavior. Strikingly, light cycles consisting of only brief light pulses defining dawn and dusk (i.e., skeleton photoperiods) have been shown to simulate most aspects of full photoperiods at the behavioral level, with the interval between the brief dawn and dusk pulses determining the photoperiodic state of circadian behavior[12]. This remarkable ability of the circadian system to lock onto the timing of light transitions can, in principle, result from properties of circadian photoreception in the retina (input), downstream behavioral modulation (output), or properties of the SCN clock itself. Here we have tested directly whether the SCN clock itself can be entrained to different photoperiods by brief daily transitions that simulate dawn and dusk.

We applied to SCN slices an optogenetic equivalent of skeleton photoperiods mimicking short (winter-like), equinox, or long (summer-like) photoperiods (8h, 12h, and 16h daylight per day), respectively (Figure 2.10A, B). For the 12:12 skeleton photoperiod entrainment, we gave short optogenetic stimulations twice per day (12h apart). We initiated entraining stimulations with one stimulation at the trough of the free-running PER2::LUC rhythm to mimic dawn, and the other stimulation at the peak to mimic dusk (Figure 2.10A, B, 12:12). The 12:12 skeleton indeed entrained SCN slices such that PER2::LUC rhythm period during entrainment became matched to the 24h optogenetic light cycle length (Figure 2.10C, 2.11), and the phase angle of entrainment (measured as the difference in time between the dusk pulse and the half-max on the rising phase of PER2::LUC rhythm) was stable (Figure 2.10D, 2.12). To test for 8:16 short day skeleton photoperiod entrainment, we initiated twice-daily optogenetic stimulations 8h apart, with the "dawn" pulse given 2h after the trough of the free-running PER2::LUC rhythm, and the "dusk"

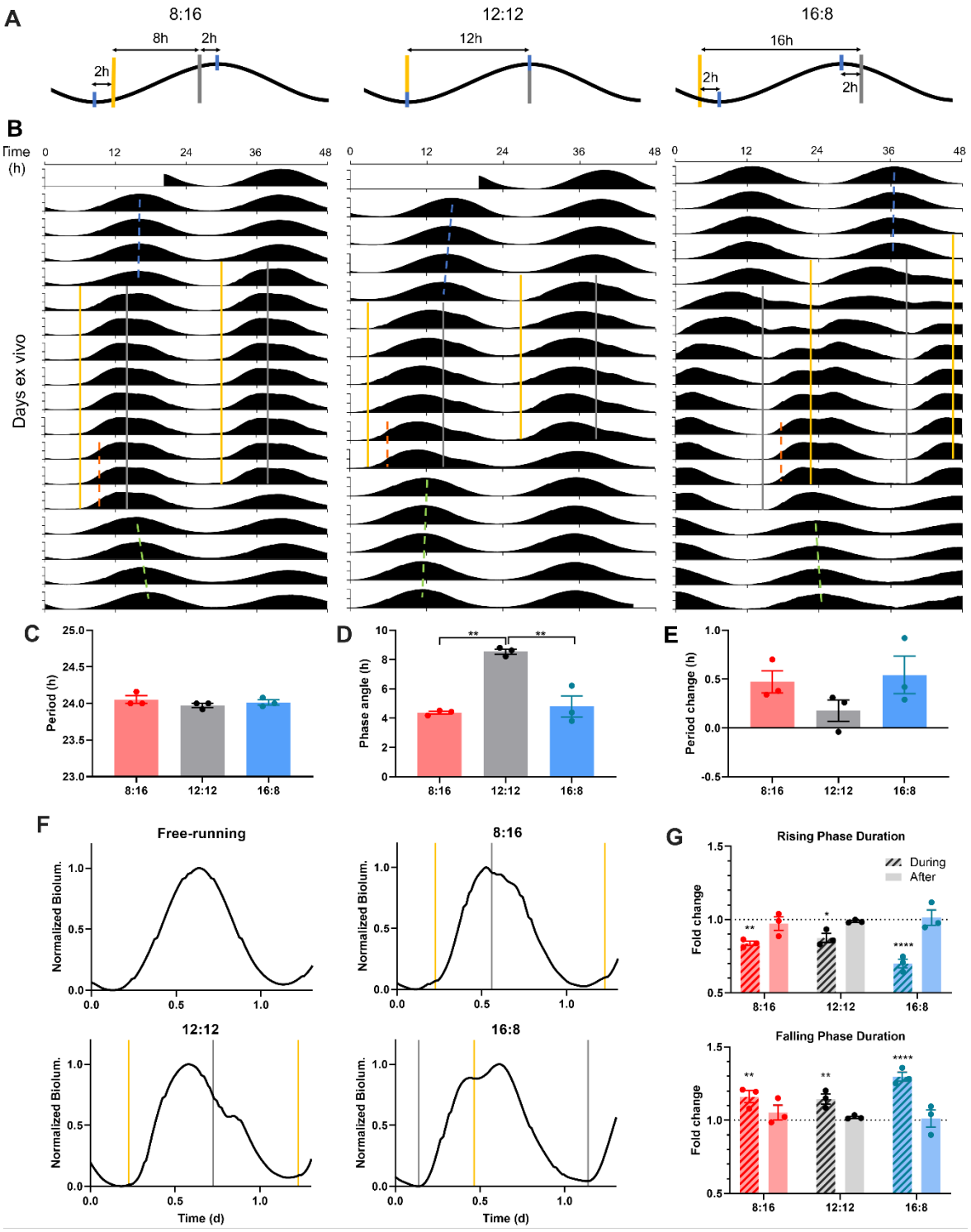

(*Figure legend is on the next page.*)

Figure 2.10. SCN entrain to optogenetic simulation of dawn and dusk via differential PER2::LUC rhythm waveform changes.

(A) Schematic diagram of optogenetic stimulation paradigm for 8:16 (left), 12:12 (middle), and 16:8 (right) skeleton photoperiod entrainment. Optogenetic pulses (yellow and grey bars for nominal dawn and dusk pulses, respectively) were given twice (8h, 12h, or 16h apart) every 24h, targeting near the peak and trough (blue ticks) of PER2::LUC rhythms (black). **(B)** Representative double-plotted PER2::LUC bioluminescence actograms of SCN slices entrained with 15-min 10Hz red optogenetic pulses at 8:16 (left), 12:12 (middle), or 16:8 (right) interval of 24h. Linear regressions of the pre-, post-entrainment cycle peaks and during-entrainment cycle half-maxes are indicated as the blue, green, and orange dashed lines, respectively. **(C-E)** Quantification of period during entrainment **(C)**, phase angle of entrainment **(D)**, period change following entrainment **(E)**. (One-way ANOVA with Tukey's multiple comparisons test, mean ± SEM, n = 3, **p < 0.01). **(F)** Representative waveforms of PER2::LUC rhythms in SCN slices in a free-running condition (before and after entrainment), and those entrained to optogenetic 8:16, 12:12, 16:8 photoperiod entrainment. Optogenetic light pulses were given at times indicated by yellow and grey lines marking nominal dawns and dusks, respectively. **(G)** Fold changes in the duration of the rising phase (top) and the falling phase (bottom) during and after entrainment, compared to before entrainment. (RM two-way ANOVA with Sidak's multiple comparisons tests, mean ± SEM, n = 3, *p < 0.05, **p < 0.01, ****p < 0.0001).

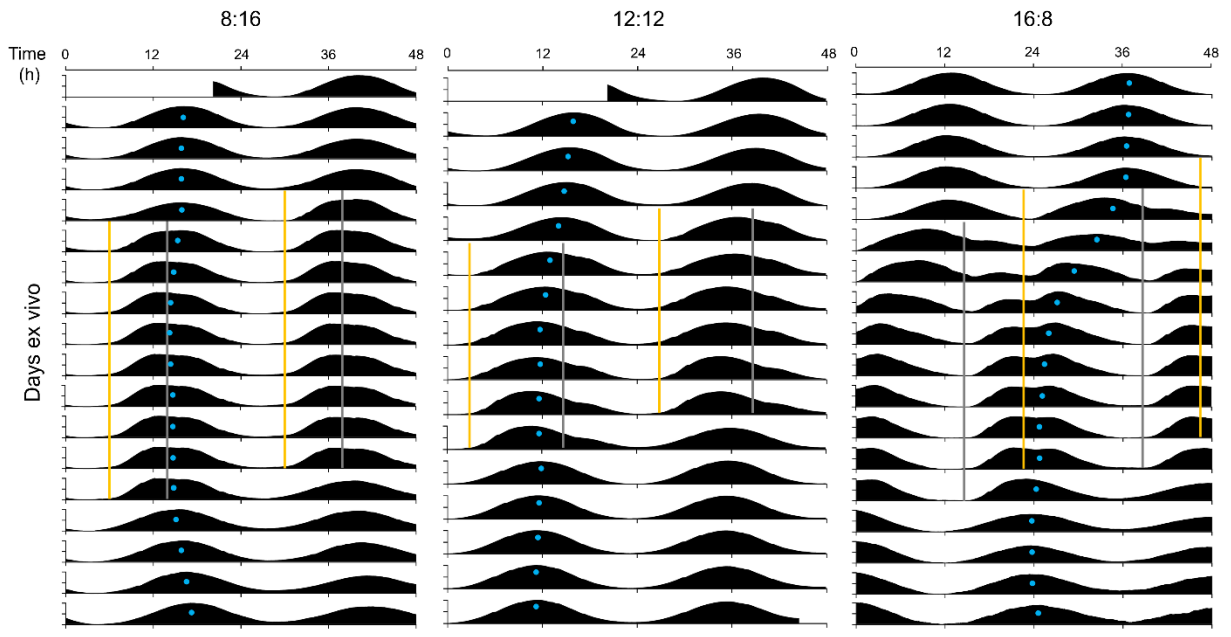

Figure 2.11. Acrophase fitting of PER2::LUC bioluminescence actograms from Figure 2.10. Blue dots denote acrophases.

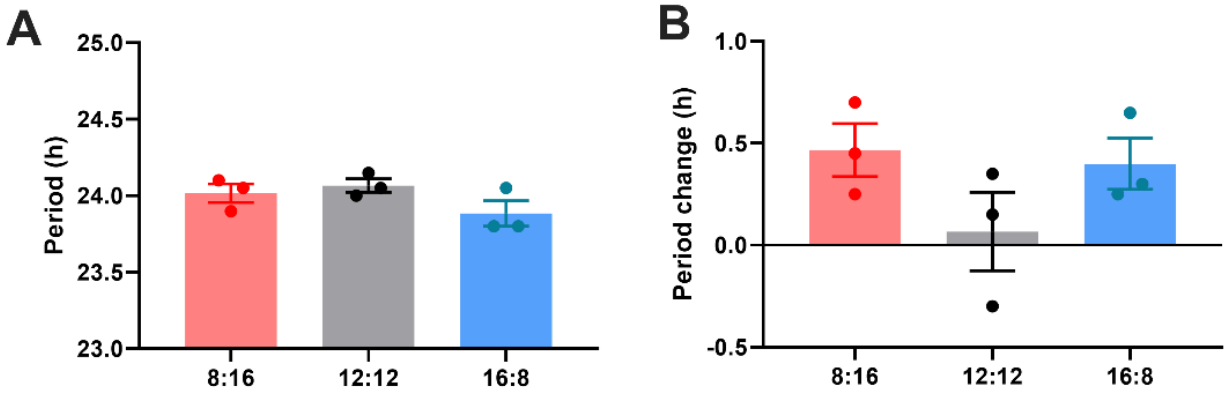

Figure 2.12. Quantification of (A) period during entrainment and (B) period changes following entrainment using Lomb-Scargle periodogram.

pulse given 2h before the peak (Figure 2.10A, B, 8:16). The 8:16 skeleton photoperiod entrained PER2::LUC rhythms to 24h period (Figure 2.10C, 2.11) with a stable phase angle (Figure 2.10D, 2.12) such that the rising phase (SCN day) was encompassed within the 8h "short day" interval between the "dawn" and "dusk" stimulations (Figure 2.10B). To test for entrainment to 16:8 long day skeleton photoperiods, we initiated optogenetic stimulations twice daily 16h apart, with the "dawn" stimulation applied 2h before the trough and the "dusk" stimulation applied 2h after the peak (Figure 2.10A, B). In contrast to the 12:12 and the 8:16 skeletons, when SCN were presented 16:8 skeleton photoperiods they did not maintain alignment of the PER2::LUC rising phase (SCN day) with the "daytime" interval (16h), but instead rapidly phase-advanced across the "dawn" pulse until achieving similar phase angles to the 8:16 skeleton, stably aligning the SCN day (rising) phase within the 8h short day interval (Figure 2.10B–D). This phenomenon in SCN slices replicates the phase jump of circadian locomotor behavior in rodents[12] (Figure 2.13) and flies[13] during attempted entrainment to long-day skeleton photoperiods, a characteristic expression of circadian plasticity in which entrainment to short-day skeleton photoperiods is more stable. Together, our results show that the SCN clock itself can entrain to different photoperiods by dawn and dusk light pulses, and suggest that the phase-jumping behavior during skeleton periods is derived from SCN-intrinsic clock plasticity.

Entrainment to different skeleton photoperiods also altered the molecular waveform of the SCN clock (Figure 2.10F). Stimulations at dawn shortened the PER2::LUC rising phase (8:16 skeleton: 0.84 ± 0.02 fold change (FC), 12:12 skeleton: 0.88 ± 0.03 FC, 16:8 skeleton: 0.70 ± 0.03 FC), while stimulations at dusk lengthened the falling phase (8:16 skeleton: 1.16 ± 0.04 FC, 12:12 skeleton: 1.15 ± 0.03 FC, 16:8 skeleton: 1.30 ± 0.03 FC), to match the clock period to 24h and set the phase angle of entrainment (Figure 2.10F, G). The net effect was that PER2 rhythms show

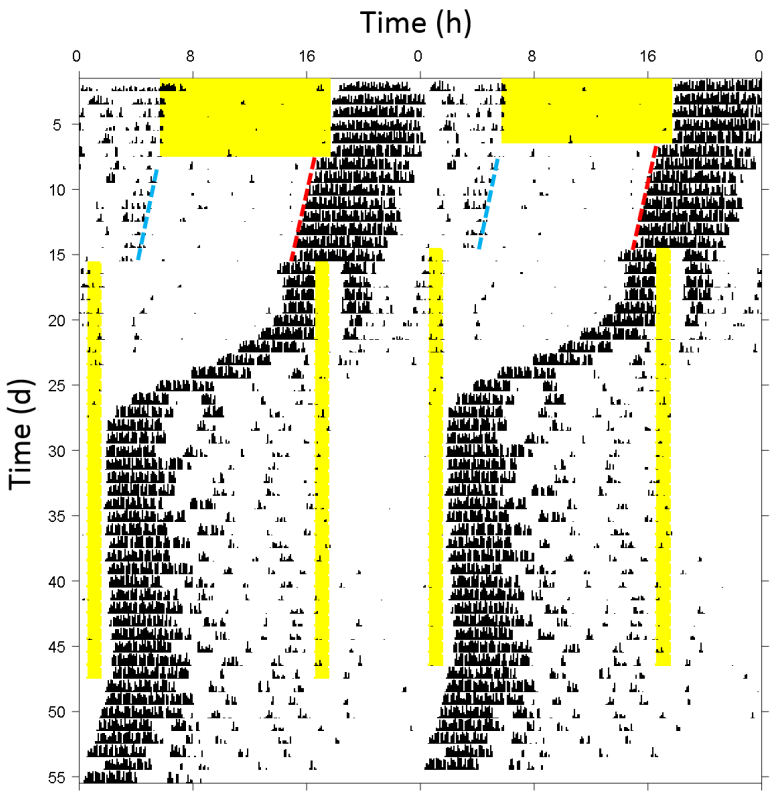

Figure 2.13. Phase jump in circadian behavior during long skeleton photoperiod entrainment.

Representative double-plotted wheel-running actogram showing a behavioral phase jump to the preferred phase angle of 16:8 long skeleton photoperiod entrainment. The black tick marks indicate 6 min-binned wheel-running activity. A mouse under a light cycle of 12h light (yellow bar) and 12h darkness was released into constant darkness and then presented with a 16:8 skeleton photoperiod. The 16h interval between 1h light pulses defining dawn and dusk was initially aligned with the subjective day (i.e., the time from the nocturnal behavioral offset (blue dashed line) to the onset (red dashed line)). As the circadian rhythm rapidly phase-advanced across the nominal dusk pulse, the shorter 8h interval became aligned with the subjective day instead of the night.

asymmetric waveforms with the falling phase longer than the rising phase in all skeleton photoperiods (Figure 2.10F, G). However, changes in the waveform did not persist when the rhythms were free-running in constant darkness following entrainment (Figure 2.10G), indicating that the waveform changes are direct effects of optogenetic light stimulation accelerating and decelerating different phases of the molecular clock during entrainment. Additionally, as entrainment to 8:16 skeleton photoperiods causes period lengthening of circadian behavior *in vivo*[12], it induced a trend toward period lengthening of PER2::LUC rhythms as an after-effect (0.47 ± 0.11h), although these did not reach statistical significance (Figure 2.10E, Figure 2.12). Taken together, skeleton photoperiods entrain PER2 rhythms in the SCN via opposing actions of light pulses on the duration of the rising and the falling phases to match the clock period to 24h.

To determine the waveform of PER2::LUC rhythms in SCN stably entrained to a long skeleton photoperiod, we entrained SCN slices to skeleton photoperiods whose daytime interval was gradually extended from 12h to 14h to 16h (Figure 2.14). All 9 SCN slices tested entrained to the 12:12 skeleton photoperiod, and most (8 out of 9) maintained entrainment when the skeleton was expanded to 14:10, while only a few (2 out of 9) maintained entrainment when the skeleton was expanded to 16:8, and most (7 out of 9) executed a phase jump to the 8:16 phase angle (Figure 2.14A, C). This is consistent with previous findings in fruit flies and mice that a phase jump in circadian behavior is more likely to occur as the daytime interval of skeleton photoperiods gets longer than 12h, a phenomenon called the "minimum tolerable night"[12,151].

SCN slices that did stably entrain to the 16:8 long skeleton photoperiod exhibited a broader PER2::LUC rhythm waveform with more prominent PER2::LUC inductions following stimulation at each dawn and dusk transition, compared to the same slices under the 12:12 skeleton photoperiod (Figure 2.14B). Providing SCN slices with simulation of dawn and dusk transitions

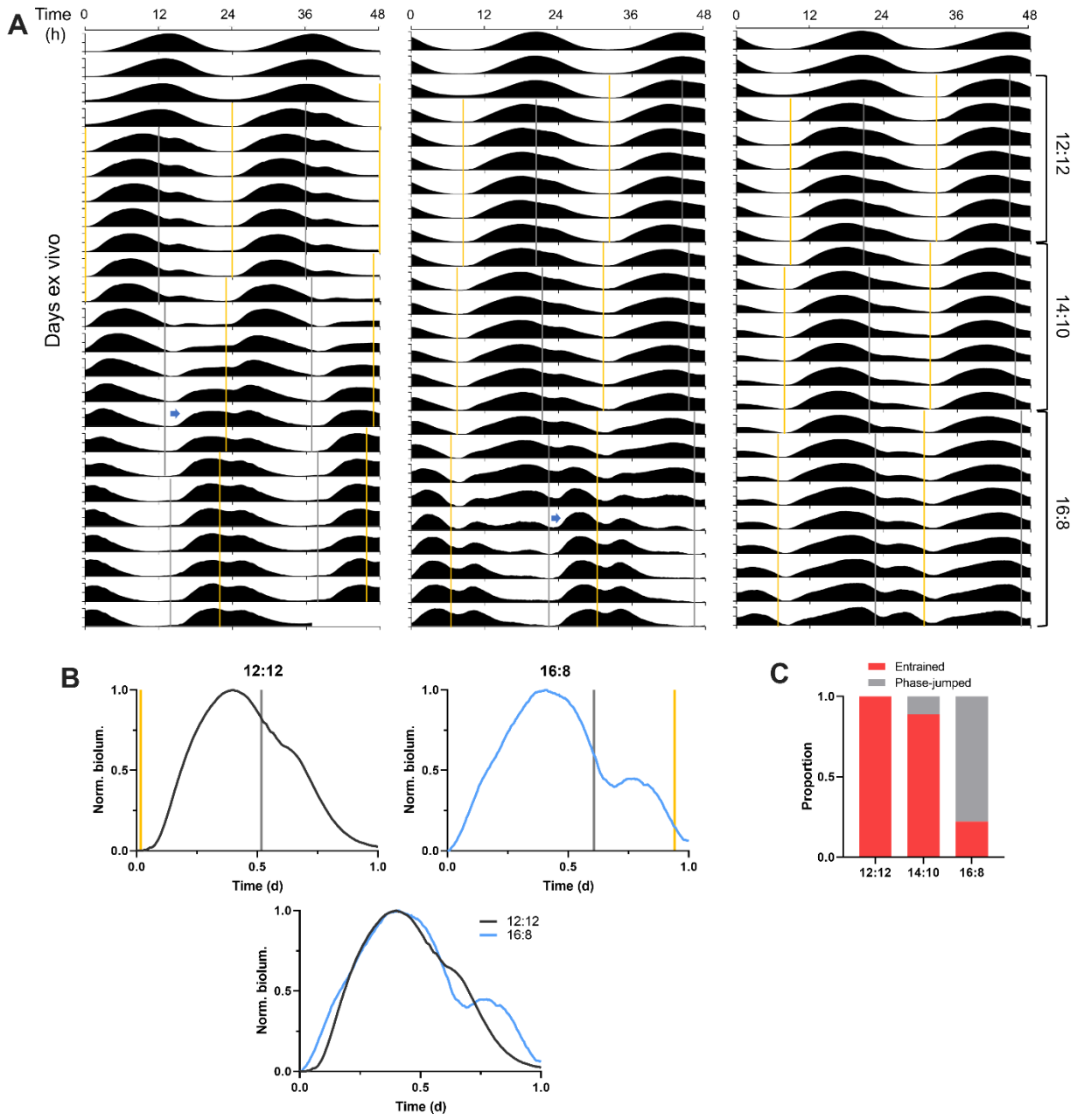

Figure 2.14. Gradual shifts from equinox to long optogenetic skeleton photoperiods reveal SCN PER2::LUC rhythms stably entrained to long skeleton photoperiods.

(A) Representative double-plotted PER2::LUC bioluminescence actograms of SCN slices entrained to optogenetic skeleton photoperiods (yellow and grey bars [*Figure legend continues.*]

[*Figure legend continued.*] for nominal dawn and dusk pulses, respectively) from the 12:12 skeleton to the 14:10 to the 16:8. The left and the middle actogram show that a phase jump (blue arrow) begins during the 14:10 and the 16:8 skeleton photoperiods, respectively. The right actogram depicts SCN PER2::LUC rhythms entrained to all the three skeleton photoperiods without a phase jump. **(B)** Representative waveforms of the PER2::LUC rhythms entrained to the 12:12 (upper left) and the 16:8 (upper right) skeleton photoperiods simulated by optogenetic stimulation (yellow and grey bars for nominal dawn and dusk pulses, respectively). The bottom plot shows a superimposed image of the two upper plots. **(C)** Proportion of entrained SCN slices (without a phase jump) and the phase-jumped slices for the 12:12, 14:10, and 16:8 skeleton photoperiods (n=9).

was sufficient to mimic waveform broadening of the clock gene rhythms induced by complete long photoperiods (e.g., a cycle of 16h light and 8h darkness)[152,153]. Dawn stimulation for the 16:8 skeleton aligned with the late falling phase of the rhythms and led to a greater increase in the slope of the rising phase than did the 12:12 dawn stimulation aligned with the trough (Figure 2.14B). At dusk, the timing of the 16:8 skeleton stimulation at the early falling phase was later than that of the 12:12 stimulation, triggering greater PER2::LUC induction (Figure 2.14B). Our results show that the timing of light-dark transitions at dawn and dusk differentially drives photoperiodic effects on the clock gene rhythm waveform in the SCN likely via the observed changes in the magnitude of *Per* induction.

The SCN clock expresses regionally distinct clock-resetting capacities

The SCN clock is a functional network of heterogenous cellular oscillators which themselves are autonomous clocks. Recently, genetic dissection approaches (e.g., cell type-specific knockouts)[154] and real-time imaging of the *ex vivo* SCN[74] further revealed aspects SCN timekeeping at the network level broadly defining the ventral region marked by vasoactive intestinal polypeptide (VIP) secreting neurons, and the dorsal region marked by arginine vasopressin (AVP) secreting neurons as distinct functional nodes within the SCN network. SCN slices explanted from mice entrained to extreme lighting conditions such as 20:4 photoperiods (20h light:4h darkness) or 22h light cycles (11h light:11h darkness) showed regional phase differences and coupling profiles in PER2::LUC rhythms within the SCN distinct from those of SCN slices explanted from mice under a standard light cycle (12h light:12h darkness)[74,75]. However, these post-hoc *ex vivo* studies assay the relaxation of previous light cycle encoding, not the process of entrainment itself[81], and it remains unclear how light input alters network function

of the SCN clock in real time. As phase shifts in circadian rhythms by such light pulses underlie light entrainment[12], we assessed how the circadian phase shifts by single light pulses impact the network state of the SCN clock. To do that, we combined optogenetic stimulation of the SCN *ex vivo* with spatially imaging real-time PER2::LUC bioluminescence in SCN using a light-tight microscope equipped with an LED illumination system.

Pan-neuronal optogenetic stimulation of SCN neurons was applied at CT14 or CT21 and the subsequent network-level changes in the SCN clock were observed following this phase-delaying or phase-advancing stimulation. Subregional bioluminescence rhythm analysis and subsequent hierarchical clustering analysis revealed the spatiotemporal distribution of circadian phase, period, phase response, and period response within the SCN (Figure 2.15). Before stimulation, the circadian oscillator network in SCN slices exhibited a baseline phase distribution where the dorsomedial lip was most phase-leading and the ventrolateral area the most phase-lagging, and the distribution of circadian period was almost uniform across the SCN (Figure 2.15A). Optogenetic stimulation induced phase shifts and the period changes of different magnitudes in different regions of the SCN (Figure 2.15A).

Following CT14 stimulation, the lateral region showed larger phase delays than did the medial region. In contrast, period lengthening effects were more prominent in the medial SCN than in the lateral SCN, indicating an inverse correlation between phase change and period plasticity among SCN subregions (Figure 2.15A, C). To classify the SCN into subregions with different rhythmic properties in an unsupervised manner, we performed group-averaged clustering analysis and identified a lateral-medial axis with 3 clusters for phase shifts (lateral shell: -1.33 ± 0.18 h, lateral core: -1.64 ± 0.17 h, medial: -0.64 ± 0.30 h) and a ventrolateral-dorsomedial axis with 3 clusters for period changes (dorsomedial: 0.36 ± 0.16 h, ventrolateral: 0.08 ± 0.14 h,

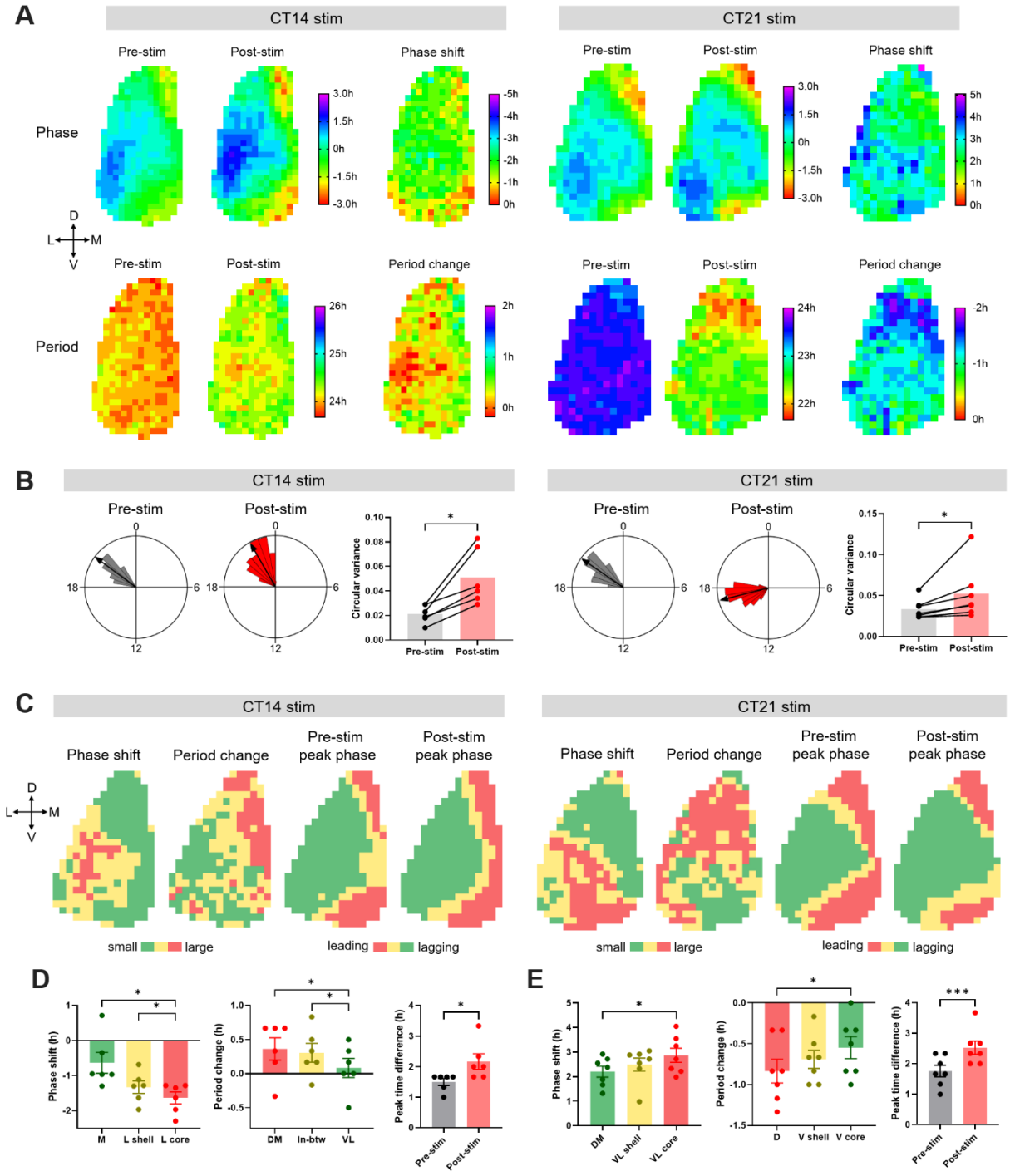

Figure 2.15. Regional distribution of circadian phase and period in the SCN, and heterogeneity of the phase and the period responses in the SCN (*Figure legend continues.*)

(*Figure legend continued.*) **to Optogenetic Light Pulses.**

(A) The upper row shows phase maps of PER2::LUC bioluminescence rhythms in the unilateral SCN before and after optogenetic stimulation at CT14 (left) or CT21 (right), and regional distribution of the phase shifts in response to corresponding stimulation. The lower row displays the period maps before and after the stimulation, and the period change maps. The crossed arrows denote the SCN orientation. D=dorsal, V=ventral, M=medial, L=lateral. The phase maps depict peak times in hours relative to the mean in each condition. Pre-stim and post-stim phases indicate the last peak before stimulation and the first peak after stimulation, respectively. Positive and negative phase shifts indicate phase advances and delays, respectively. Positive and negative period changes indicate period lengthening and shortening, respectively. **(B)** Representative Rayleigh plots (24h circular plots) for regional peak PER2::LUC phases in the SCN, and bar graphs of the circular variance before and after optogenetic stimulation at CT14 (left) or CT21 (right). (Wilcoxon matched-pairs test, n=6-7, *p <0.05). The arrows in the Rayleigh plots indicate mean Rayleigh vectors. **(C)** Group-averaged clusters of the phase shift, period change, pre-stimulation peak phase, and post-stimulation peak phase for CT14 (left) or CT21 (right) stimulation (n=6-7). Clusters were hierarchically formed using Ward's minimum variance method. Different colors indicate different clusters. The crossed arrows denote the SCN orientation. D=dorsal, V=ventral, M=medial, L=lateral. **(D-E)** Phase shifts (left) and period changes (middle) in corresponding clusters in **(C)**, and peak time differences between the phase-leading and the phase-lagging clusters (right) for CT14 **(D)** or CT21 stimulation **(E)**. Phase shifts and period changes were analyzed using RM One-way ANOVA with Tukey's multiple comparisons test, mean ± SEM, n=6-7, *p<0.05. Peak time differences were analyzed using paired t-test, mean ± SEM, n=6-7, *p<0.05, ***p<0.001.

in-between: 0.31 ± 0.14 h; Figure 2.15C, D). In terms of changes in phase coupling, the phase variance within the SCN was increased following stimulation (Figure 2.15B), indicating a larger phase desynchrony in the SCN. The phase difference between the medial and the lateral regions increased following stimulation (pre-stim: 1.50 ± 0.11 h, post-stim: 2.17 ± 0.25 h) as larger phase delays occurred in the phase-lagging, lateral region than in the phase-leading, medial region (Figure 2.15C, D).

Following CT21 stimulation, the ventrolateral or ventral SCN showed larger phase advances and smaller period shortening than did the dorsomedial or dorsal SCN, indicating again an inverse correlation in magnitude between the phase shift and the period change among SCN subregions (Figure 2.15A, C). Clustering analysis identified a ventrolateral-dorsomedial axis with 3 clusters for phase shifts (ventrolateral shell: 2.49 ± 0.27 h, ventrolateral core: 2.87 ± 0.29 h, dorsomedial: 2.21 ± 0.22 h) and a ventral-dorsal axis with 3 clusters for period changes (ventral shell: -0.69 ± 0.11 h, ventral core: -0.55 ± 0.13 h, dorsal: -0.83 ± 0.15 h; Figure 2.15C, E). Also, the phase variance was increased following stimulation (Figure 2.15B) as the phase difference between the phase-leading and the phase-lagging clusters increased (pre-stim: 1.76 ± 0.19 h, post-stim: 2.52 ± 0.22 h; Figure 2.15C, E). This increased phase desynchrony can be explained by two phenomena: the ventral part of the phase-leading medial lip region showed large phase advances, while the dorsal part of the phase-lagging lateral region exhibited smaller phase advances (Figure 2.15C).

Taken together, the network-level changes in the circadian phase and period distributions within the SCN in response to discrete light pulses reveal that the lateral or ventrolateral SCN exhibits large phase shifts and small period changes, whereas the medial or dorsomedial SCN displays small phase shifts and large period changes. To test whether a higher regional expression

of the ChrimsonR optogenetic construct in the lateral or ventrolateral SCN might be associated with the larger phase shifts of this region, we analyzed the ChrimsonR-tdT fluorescence intensity in different subregions corresponding to phase-shift clusters and compared with the magnitude of phase shifts. For both CT14 and CT21 stimulations, subregions exhibiting large phase shifts had lower levels of ChrimsonR-tdT expression (Figure 2.16), suggesting that regionally different phase responses are not directly derived from spatial ChrimsonR expression patterns. Given this distribution, and that we applied synchronous stimulation across the entire SCN, our results suggest that this subregional heterogeneity in resetting responses is intrinsic to the neurons or circuits in the ventrolateral and dorsomedial SCN.

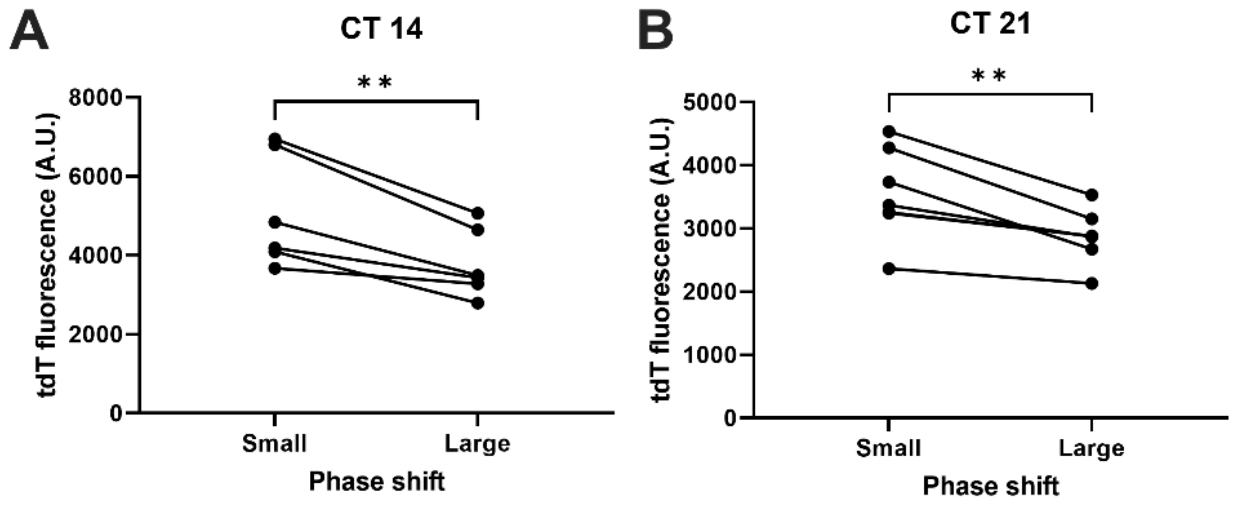

Figure 2.16. ChrimsonR-tdT fluorescence levels in different phase shift clusters in the Figure 2.15C for (A) CT14 and (B) CT21 stimulation. (Paired t-test, n=6-7, **p<0.01).

2.4 Discussion

In this study, we assessed at high-resolution temporal and spatial dynamics of core clock gene rhythms in the ex vivo SCN following single optogenetic light exposures and various forms of optogenetic light cycles to gain further insights into light resetting and entrainment of clock gene rhythms in the SCN. Using real-time bioluminescent recording of PER2 expression combined with recurring optogenetic stimulation, we confirmed that the isolated SCN strikingly recapitulates many of the canonical features of circadian clock entrainment in intact animals, including 1) phase responses with period after-effects, 2) period matching and phase angle differences to stimuli of non-24-hour cycles, and 3) differential entrainment to skeleton photoperiods with a minimum tolerable night. Entrainment is expressed as transformation of the ongoing rhythmic waveform of the clock protein we monitored, PER2, from approximately sinusoidal in free-running conditions to highly asymmetrical trajectories with accelerated synthetic (rising) phases and extended degradative (falling) phases of PER2 protein abundance mediating clock advances and delays, respectively. Spatiotemporal analysis revealed intrinsic regional differences in light resetting within the SCN neural network, with the magnitude of acute phase shifts that underlie ongoing waveform changes being greatest in the ventrolateral SCN core, while the magnitude of subsequent period after-effects is greatest in the dorsomedial SCN shell.

A key question addressed in our study was how exactly light input changes the clock gene rhythms in the SCN to drive phase shifts and to achieve entrainment to external light cycles. Previous studies[127,128] have assayed the clock gene rhythms under lighting conditions by time-point sampling clock gene expression from populations of animals for each time point at low temporal resolution (e.g., 4hr sampling intervals), making it difficult to fully capture dynamic waveform changes in the rhythms induced by light input. Using bioluminescent recording of PER2

expression at an interval of minutes, while optogenetically providing the SCN explant with simulated light signals, we directly showed that discrete light input induces acute induction of PER2 expression and differential waveform changes in PER2 rhythms in a phase-dependent manner, leading to a time-dependent phase shifts: high PER2 induction by early-night light exposure induces phase delays by elongating the falling phase of the molecular clockworks, while late-night light induces phase advances by accelerating the rising phase of the clockworks, and mid-day light does not affect the rhythm phase due to low PER2 induction. These differential waveform changes in specific PER2 phases differentiate PER2 waveforms under light cycles from those in free-running conditions. PER2 rhythms express typical sinusoidal waveforms in free-running conditions, whereas under light entrainment they show asymmetric waveforms with elongated falling phases, abbreviated rising phases and dramatic waveform changes aligned with light stimulation events. Given that a pulse of retinal light input can induce PER gene expression in the SCN and PER induction is required for the SCN clock resetting[98,99], our results suggest that the SCN clock rhythms such as neural activity rhythms can phase-shift to acute light exposure and entrain to a light cycle via single and regular events of the aforementioned waveform changes, respectively, as a result of light induction of PER gene expression.

As daily phase shifts underlie adjustment of the endogenous period of circadian behavior to different day-night cycle lengths, daily waveform acceleration in the rising phase of PER2 aligned with dawn, and daily elongation in the falling phase of PER2 abundance aligned with dusk express the entrainment of circadian PER2 rhythm to light cycle periods. Stable alignment of the SCN clock with repeated light stimulations at a phase-delaying circadian time achieved circadian entrainment to a longer-than-24h cycle mainly via repeated lengthening of the falling phase of PER2, whereas repeated shortening of the rising phase at a stable phase angle accompanied short

T-cycle entrainment. For photoperiodic encoding, as brief light pulses defining dawn and dusk can entrain circadian behavior, daily brief optogenetic simulations of light transitions at dawn and dusk shortened PER2 rising phase and lengthened the falling phase in the SCN, respectively, thereby matching PER2 rhythms to a 24h period. PER2 waveform widths were different between equinox and long skeleton photoperiods. Previous studies suggested that long photoperiod induces *Per* waveform broadening as high *Per* gene expression gets extended throughout long light periods[152,153]. However, our results from skeleton photoperiods suggest that light-dark transitions at dawn and dusk are sufficient to alter PER2 waveform width. Light exposures at earlier dawns and later dusks for long photoperiods drive more PER2 induction than do light exposures in equinox photoperiods, thus expanding PER2 waveform. This is consistent with waveform broadening of neural activity rhythms in animals under a long photoperiod[155].

Another important point of this study is that plasticity in circadian behavior following alteration of lighting conditions is intrinsic to the SCN clockworks. Key principles of circadian entrainment and plasticity in mammals have been discovered by classical behavioral studies that assessed circadian locomotor behavior under different lighting conditions. Circadian behavior, however, is a product of multiple oscillators involving different brain areas, and the SCN receives both extensive feed-forward and feedback from other brain nuclei *in situ*[156]. Our results from ex vivo entrainment of isolated SCN strongly suggest that many of the classically studied forms of circadian plasticity and properties of entrainment apparently reside intrinsically within the SCN molecular and neural network themselves. As previously reported[132], differential phase responses of circadian rhythms depending on the timing of light input is evident even though the SCN neurons are directly stimulated, rather than them receiving retinal input. Furthermore, as entrainment of circadian behavior to different T-cycles is achieved by different phase angles of

entrainment, the SCN clock itself establishes different entrained phase angles to the T-cycles, consistent with non-parametric model of entrainment[12]. Daily light stimulations fall in the phase-advancing zone (late falling PER2 phase) and the phase-delaying zone (late rising PER2 phase) during short and long T cycles, respectively. Also, the SCN clock itself can indeed be entrained directly by the light-dark transitions in skeleton photoperiods as mimicked by optogenetic stimulation, and a higher-order aspect of entrainment, such as the bias of the circadian system to resolve ambiguous skeleton light cycles in favor of short-day entrainment[12], also resides in the SCN clockworks.

We also uncovered whether and how the SCN clock itself expresses light-induced after-effects on the endogenous clock period. Acute phase shifts produce after-effects on the endogenous period of the SCN clock itself, and interestingly, the magnitude of the period after-effects (up to several hours) is larger than that at the level of behavioral rhythms (less than an hour)[2]. This suggests that the after-effects on circadian behavior following single light pulses become diminished as light signals are transmitted downstream of the SCN, or that the plasticity of the in vivo SCN is constrained by interactions with extra-SCN oscillators or circuits. In the case of entrainment to non-24 hour periods (T-cycles), surprisingly, we did not detect significant period after-effects in the SCN clock, although T-cycle entrainment produces most significant period after-effects in circadian behavior[12]. It is an unexpected finding that repeated stimulation does not produce large period after-effects, while single light stimulation does. Period after-effects of circadian locomotive behavior are expressed after more than a month of exposure to different T-cycles[106,128], suggesting that our one-week entrainment paradigm might not be sufficient to drive T-cycle period aftereffects. Notably, previous findings indicate that the clock period of SCN explanted from animals entrained to T-cycles does not represent circadian behavioral period of

those animals[75,121,122,157], suggesting the possibility that extra-SCN clocks are a critical influence on the period after-effects of T-cycles. Our results from direct entrainment of isolated SCN to T cycles also suggest that there may be additional non-SCN influences underlying the T cycle period after-effects at the behavioral level.

We also revealed how light exposure alters the network state of the SCN clock to induce phase shifts and period plasticity, and directly showed that the SCN itself has subregional heterogeneity in clock-resetting capacity. Previously, it is assumed that retinal light input is mainly received by the ventral SCN, creating differences light-induced clock resetting between the ventral and dorsal regions due to differential input[61]. For example, in the in vivo SCN light induction of *Per1* mRNA expression is more prominent to the ventral region, whereas *Per2* induction is widespread[64]. More recent studies using intrinsically photosensitive retinal ganglion cell (ipRGC) labeling[38,144], however, showed that the retinal projections are widespread across the entire SCN and neuronal activation following light exposure was ubiquitous, suggesting the possibility of intrinsic differences in responsiveness between the SCN subregions. Using pan-neuronal optogenetic stimulation that was synchronous across the entire SCN, we found that the lateral or ventrolateral SCN exhibits large phase responses and small period responses, while the medial or dorsomedial SCN exhibits small phase responses but large period plasticity, revealing an intrinsic nature of the clock-resetting heterogeneity in the SCN. As the VIP and AVP neurons are respectively located in the ventral and dorsal SCN, this suggests that regionally differential phase and period responses in the SCN might be derived from intrinsic differences between the VIP and AVP neuronal clocks. The period response, inversely correlated with the phase response, could serve to help the SCN recover back to its baseline network phase state from decreased synchrony following phase shifts. Decreased phase synchrony among SCN neurons following light exposure

has been observed in the case of VIP-induced phase shifts[158] and entrainment to long photoperiods or non-24h light cycles[74,75]. Interestingly, stimulating VIP neurons reset the ensemble SCN phase, while stimulating VPAC2 neurons located in the dorsal SCN do not[159], suggesting regionally different phase-resetting capacity. Future studies will be needed to address whether and how the subregional heterogeneity in light responsiveness fulfills encoding of various lighting conditions in the SCN.

Technical limitations of our methods are twofold. We used ~P12 SCN slices to achieve long-term monitoring of real-time clock gene rhythms throughout optogenetic entrainment. Although the SCN astrocytes become fully mature by P20–25 and they are recently identified as an important component for entrainment in vivo[160–162], the SCN maturity reaches near-adult levels at P12 in many aspects including retinal innervation, clock gene rhythmicity, neuropeptide expression profile, and photic responses[60]. Additionally, our current system is not readily applicable to studying real-time SCN rhythms under a full optogenetic light cycle (e.g., 12 hours of stimulation every day) as excitation light for optogenetics interrupts bioluminescence detection. Moving forward, overcoming such a limitation will further extend the usage to studying SCN-intrinsic mechanisms of entrainment. Interestingly, real-time clock gene rhythms in the in vivo SCN re-entrain to a new light cycle during experimental jet lag[163]. Future waveform analyses of clock gene rhythms in such an in vivo setup would allow comparison with our observations in the isolated SCN.

Lastly, our study provides technical contributions to studies of SCN entrainment and plasticity and to the study of neural plasticity in general. Our system that employs long-term red optogenetic stimulation and photomultiplier tube-based bioluminescence recording from cultured neural tissues enables *ex vivo* entrainment of the isolated SCN neural network over intervals of

days to weeks in a similar way to light entrainment in animals, and high-resolution assessment of plasticity in the SCN clock gene rhythms throughout entrainment. As the SCN explant is more accessible to genetic or pharmacological manipulations than in vivo SCN, our method will provide a great opportunity to further study molecular mechanisms of the SCN entrainment. Our system can also be adapted for long-term optogenetic stimulation with other bioluminescent readouts, such as bioluminescence resonance energy transfer (BRET) Ca^{2+} sensors[164,165], and thus it is potentially widely applicable to studying induction of long-term neural plasticity in different regions of the brain.

2.5 Materials and methods

Reagent type (species) or resource	Designation	Source or reference	Identifiers
Animal strain (*M. musculus*)	PER2::LUC	[130]	RRID: IMSR_JAX:006852
Transfected construct (*M. musculus*)	AAV1-Syn-ChrimsonR-tdT	[140]	Addgene viral prep # 59171-AAV1
Software, algorithm	MATLAB	Mathworks	RRID:SCR_001622
Software, algorithm	ClockLab Analysis	Actimetrics	Matlab-based ClockLab Analysis ver. 2.72
Software, algorithm	LumiCycle	Actimetrics	
Software, algorithm	Signal Generator	Mhinstek	
Software, algorithm	Prism	GraphPad	RRID:SCR_002798
Software, algorithm	SPSS	IBM	RRID:SCR_002865
Software, algorithm	OptoLumicycle	This study	https://github.com/SuilKim/OptoLumicycle
Other	LED driver	Thorlabs	LEDD1B

Other	Fiber-coupled LEDs	Thorlabs	M470F3 (470nm), M625F2 (625nm)
Other	Fiber collimation package	Thorlabs	F230SMA-B
Other	Multi-mode fiber cable (Ø1500µm, 0.39NA)	Thorlabs	M93L
Other	Relay switch	Sensata-Crydom	DC60S5-B
Other	Multi-functional I/O device	National Instruments	USB-6001

Table 2.1. Key resources table.

Animals and housing

P11-14 heterozygous PER2::LUC knock-in mice[130] were used for organotypic slice culture and subsequent procedures as the PER2::LUC knock-in allele can alter circadian functions such as free-running period and entrainment[166]. All animals were housed in a 12:12 LD cycle, and had food and water provided ad libitum. Both male and female mice were used in experiments. Experiments were performed in accordance with the Vanderbilt University Institutional Animal Care and Use Committee and National Institutes of Health guidelines.

Organotypic slice culture and AAV viral transduction

Removed brains were mounted and cut into coronal slices (300µm) on a vibrating blade microtome (Leica) in cold HBSS supplemented with 100 U/ml penicillin/streptomycin, 10 mM HEPES, and 4.5 mM sodium bicarbonate. The SCN slices were dissected out and transferred onto a PTFE membrane insert (Millipore) in 35-mm culture dishes with 1.2 ml of DMEM (D5030,

Sigma) supplemented with 3.5 g/L D-glucose, 2mM Glutamax (Gibco), 10 mM HEPES, 25 U/ml penicillin/streptomycin, 2% B-27 Plus (Gibco), and 0.1 mM D-Luciferin sodium salt (Tocris). The SCN slice position was adjusted to the center of the dish and 1.5µl AAV (pAAV1-Syn-ChrimsonR-tdT, Addgene)[140] was placed directly onto the SCN slice. The culture dishes were then sealed with an optically clear PCR plate film (Bio-Rad) and maintained in a non-humidified incubator at 36.8 °C for about 10 days. The opsin expression was checked after about 10 days of viral transduction by imaging tdT fluorescence.

Bioluminescence recording and in situ optogenetic stimulation

After viral transduction, bioluminescence from firefly luciferase in each of PER2::LUC SCN slices was recorded in 6 min intervals by a 32-channel/4-photomultiplier tube luminometer LumiCycle (Actimetrics) in a non-humidified, light-tight incubator at 36.8°C. Baseline rhythms were recorded for at least three days before optogenetic stimulation. For optogenetic stimulation, 625nm LED light (10Hz, 10ms pulse width, 1.5mW/mm^2) was delivered at the center (6mm illumination radius) of a target culture dish by a fiber-coupled LED (M625F2, Thorlabs). The LED was located outside the incubator and coupled to a multimode fiber cable (Ø1500µm, 0.39NA) (M93L, Thorlabs) and a fiber collimation package (F230SMA-B, Thorlabs) tethered above samples. Light pulses were generated by an LED driver (LEDD1B, Thorlabs) and a signal generator (Mhinstek). For remotely turning on and off the photomultiplier tubes in the luminometer, a relay switch (Sensata-Crydom) was added in the electrical circuit of the luminometer and connected to a multi-functional I/O device (National Instruments). Custom-written code in Matlab (Mathworks)[167] was used to access luminescence data collection software (Actimetrics), the multi-functional I/O device, and a signal generator software (Mhinstek). The

Matlab code loaded a spreadsheet having stimulation settings and time schedules, and executed a series of events during optogenetic stimulation: pause bioluminescence recording, target positioning, stimulation initiation, stimulation termination, and resumption of the recording. For a long light exposure test, 12h blue or red light pulses (10Hz, 10ms pulse width, 1.2mW/ mm^2) were illuminated onto PER2::LUC SCN slices by LEDs (M470F3 or M625F2, respectively, Thorlabs) coupled to a multimode fiber cable (Ø1500μm, 0.39NA) (M93L, Thorlabs). Blue light-illuminated samples were given a medium change two days after illumination.

Bioluminescence recording data analysis and visualization

Raw bioluminescence data were baseline-subtracted using 24h running averages and smoothed by 2.4h moving averages using LumiCycle Analysis software (Actimetrics), and then they were loaded as normalized actograms into Matlab-run ClockLab software (Actimetrics) for further analyses. Phase shifts were determined as the time difference between the observed post-stimulation peak of the bioluminescence rhythm and the predicted peak from a linear regression of at least three cycles before stimulation. Period changes were determined as the difference in the period length between the pre-stim and the post-stim cycles. Period length was calculated using a linear regression of at least three peaks or using Lomb-Scargle periodogram in ClockLab software. If peaks were not obvious, the period length was determined using half-maxes of the rising phase. Acrophases were calculated using ClockLab software. For data visualization, smoothed and baseline-subtracted bioluminescence rhythms were represented as double-plotted actograms normalized to min and max values of the data for each line of the actograms, using Excel (Microsoft) and Prism (Graphpad). The actograms were 24h-plotted unless otherwise stated. Bioluminescence rhythms of 12h light-exposed slices were visualized using Excel and LumiCycle

Analysis software. For quantifying the effect of a long light exposure on the rhythm amplitude, the amplitude of the first post-treatment cycle was normalized to the amplitude of the last pre-treatment cycle. For waveform analyses of single phase shifts, smoothed bioluminescence rhythms with and without stimulation were normalized to extrapolated peak and trough values based on the average dampening rate of the rhythm amplitude over time. Then the rhythms with stimulation were subtracted from those without stimulation. Normalized induction following stimulation was calculated as the first-cycle amplitude of the subtraction data. For waveform analyses of bioluminescence rhythms during T cycle entrainment, smoothed bioluminescence rhythms before T22/T25 entrainment and during T22 entrainment were normalized to peak and trough values, and the rhythms during T25 entrainment were normalized to actual troughs and interpolated peaks based on the first cycle of the free-running rhythms released in constant darkness. For waveform analyses of bioluminescence rhythms during skeleton photoperiods, the smoothed first derivatives were taken from the smoothed, baseline-subtracted bioluminescence rhythms normalized to min and max values, using Excel and Prism. The duration of the rising and falling phases was determined using the time duration between the zero crossings of the first derivatives. If the first derivatives were close to zero but did not make a zero crossing due to an increase immediately following an optogenetic stimulation, the local minimum was defined as the end of the rising phase. Waveform data were visualized using Excel and Prism.

Time-lapsed bioluminescence imaging with optogenetic stimulation and data analyses

SCN slices expressing PER2::LUC and pAAV-ChrimsonR-tdT were cultured in the sealed 35mm dishes as described above, and the dishes were transferred into a temperature-controlled chamber of the LV200 microscope system (Olympus) equipped with an imaging software

(CellSens, Olympus), an EM-CCD camera (Hamamatsu) and an LED light illumination system (CoolLED). Bioluminescent images were acquired every ten minutes using 40x objective lens and 0.2x tube lens. For optogenetic stimulation, 10Hz 635nm LED light pulses with 10ms pulse width were illuminated for 15 minutes using real-time controllers (Olympus) and the experimental manager of CellSens imaging software. Stimulation time was determined using at least three cycles of PER2::LUC bioluminescence rhythms before stimulation. For regional analyses in ImageJ (NIH), background noise of bioluminescent image series was removed using grouped Z project with group size 2 and minimum intensity method, and 15x15 pixels ROIs were generated based on average intensity projection of the image series. Mean intensity data from each ROI was 0th-order smoothed in Prism, and peak times of the bioluminescence rhythms were determined using Excel. To create a circadian phase map, peak time data were normalized to the mean and plotted as a rainbow-colored heat map in Prism. A circadian period map was created using period values calculated from three cycle peaks for each ROI. Phase shifts and period changes were calculated as described above. To determine the overall phase dispersion within the SCN slice, circular variance (=1 – mean vector length) was calculated and Rayleigh plots were generated using Oriana (Kovach Computing Services).

For cluster analyses in each dimension (e.g., phase shift), two clusters were formed from each SCN slice using Ward's minimum variance method in SPSS (IBM) to separate ROIs with larger values from ROIs with smaller values, and then two-clustered SCN slices were color-coded in Excel. The color-coded clusters were group-averaged using ImageJ, and the group-averaged was clustered again in SPSS to divide into three regions. To calculate the difference in each dimension among the three clusters, bioluminescent image series were re-analyzed using ROIs corresponding to each cluster.

Statistical analysis

All statistical analyses were performed in Prism (Graphpad). Statistical tests used for each experiment are provided in the figure legend. Data are presented as a mean ± standard error of mean (SEM) and differences between groups were considered statistically significant when $p < 0.05$.

CHAPTER III

DNA methylation is a widespread mechanism of light-induced period plasticity of circadian behavior and SCN rhythms

3.1 Abstract

The suprachiasmatic nucleus (SCN) in the hypothalamus is a principal light-responsive circadian clock that adjusts circadian rhythms in mammalian physiology and behavior to changes in external light signals. Although mechanisms underlying how light acutely resets the phase of circadian rhythms are well characterized, it remains elusive how light signals induce lasting changes in circadian period, or period after-effects. Here we have found that period after-effects of altered daytime periods (photoperiods) on circadian behavior require DNA methylation in the SCN, an epigenetic mechanism of the gene regulation. At the level of single light pulses or clock-resetting stimulations, DNA methylation in the SCN mediates period after-effects following acute phase shifts in SCN clock gene rhythms and behavioral output rhythms. Phase shifts themselves, however, do not necessitate DNA methylation at the SCN and behavioral levels. Given previous studies showing that DNA methylation in the SCN is essential for period after-effects of non-24hr light cycles (T-cycles), our results suggest that DNA methylation in the SCN is a widespread mechanism of light-induced period after-effects regulating all major types: after-effects of T-cycles, photoperiods, and single light pulses.

3.2 Introduction

Circadian rhythms are pervasive in mammalian physiology and behavior in anticipation of daily environmental cycles. Nearly all mammalian cells including neurons and glia have the endogenous 24-hour timing mechanism, or the circadian clock, whose molecular basis is self-sustained circadian oscillations of the clock genes including *Period* (*Per*) and *Cryptochrome* (*Cry*) genes via autoregulatory transcription-translation feedback mechanisms[23]. Individual cellular circadian rhythms in the body are adjusted in tune with daily light cycles by the suprachiasmatic nucleus (SCN) in the hypothalamus which receives retinal light input[57]. The period length of circadian rhythms, or circadian period, is genetically defined but can be modified by external light signals[2,12]. Brief light exposures at night causing phase delays or advances in circadian rhythms lead to enduring changes in circadian period, or period after-effects, in constant conditions without external timing cues. Phase delays cause period lengthening after-effects, while phase advances cause period shortening after-effects[2]. In addition, synchronization of circadian rhythms or entrainment to different light-dark (LD) cycles, such as non-24h light-dark cycles (T-cycles; e.g., 11 hr light and 11 hr dark per 22 hr [T22]) and altered durations of daylight (photoperiods; e.g., 16 hr light and 8 hr dark per 24 hr [LD 16:8]), cause pronounced period after-effects[12].

Previous work[106] showed that DNA methylation in the mouse SCN is necessary for after-effects on circadian period of behavioral rhythms following weeks of entrainment to non-24h light cycles, suggesting that epigenetic regulation of gene expression might mediate long-lasting changes in circadian clock properties. However, it remains an open question whether DNA methylation is involved in other types of period after-effects. Also, it remains unclear whether DNA methylation regulates period after-effects at the level of single light pulses, or it does so only after chronic light exposures such as light entrainment.

Here, we show that DNA methylation in the SCN is necessary for photoperiodic aftereffects on circadian period of behavioral rhythms and uncover that DNA methylation regulates period plasticity of SCN clock gene rhythms and behavioral output rhythms at the level of acute clock-resetting stimulations without influencing induced phase shifts. Our results suggest that DNA methylation is a fundamental mechanism of period after-effects of prior light history.

3.3 Results

DNA methylation in the SCN is essential for after-effects of photoperiods on a period of circadian behavior

Entrainment of mouse circadian locomotor behavior to long summer-like photoperiods (e.g., 16 hr light per 24 hr) causes a subsequent shortening of the endogenous circadian period when measured in constant darkness[12]. To test whether DNA methylation is involved in period after-effects of long photoperiod entrainment, we blocked DNA methylation in the mouse brain via infusion of RG108, a pan-inhibitor of DNA methyltransferases, into the third ventricle surrounded by the SCN during entrainment of wheel-running behavior rhythms to LD 16:8 photoperiods (Figure 3.1A). Mice which had been maintained in LD 12:12 light cycles were placed in running wheel cages and allowed to free-run for 7 days in constant darkness to establish their baseline circadian locomotor rhythm period. Mice were then re-entrained to a LD 12:12 light cycles for 9-10 days, with infusion of RG108 started on day 4 or 5, and either continued for an additional 10 days in LD 12:12 (Control), or entrained to LD 16:8 light cycles for 12 days (LD 16:8), and then allowed to free-run for 7 days to assay for period after-effects. Control group RG108-infused mice did not show a significant difference in endogenous period change compared to vehicle controls (Figure 3.1B), suggesting that DNA methylation itself does not affect the

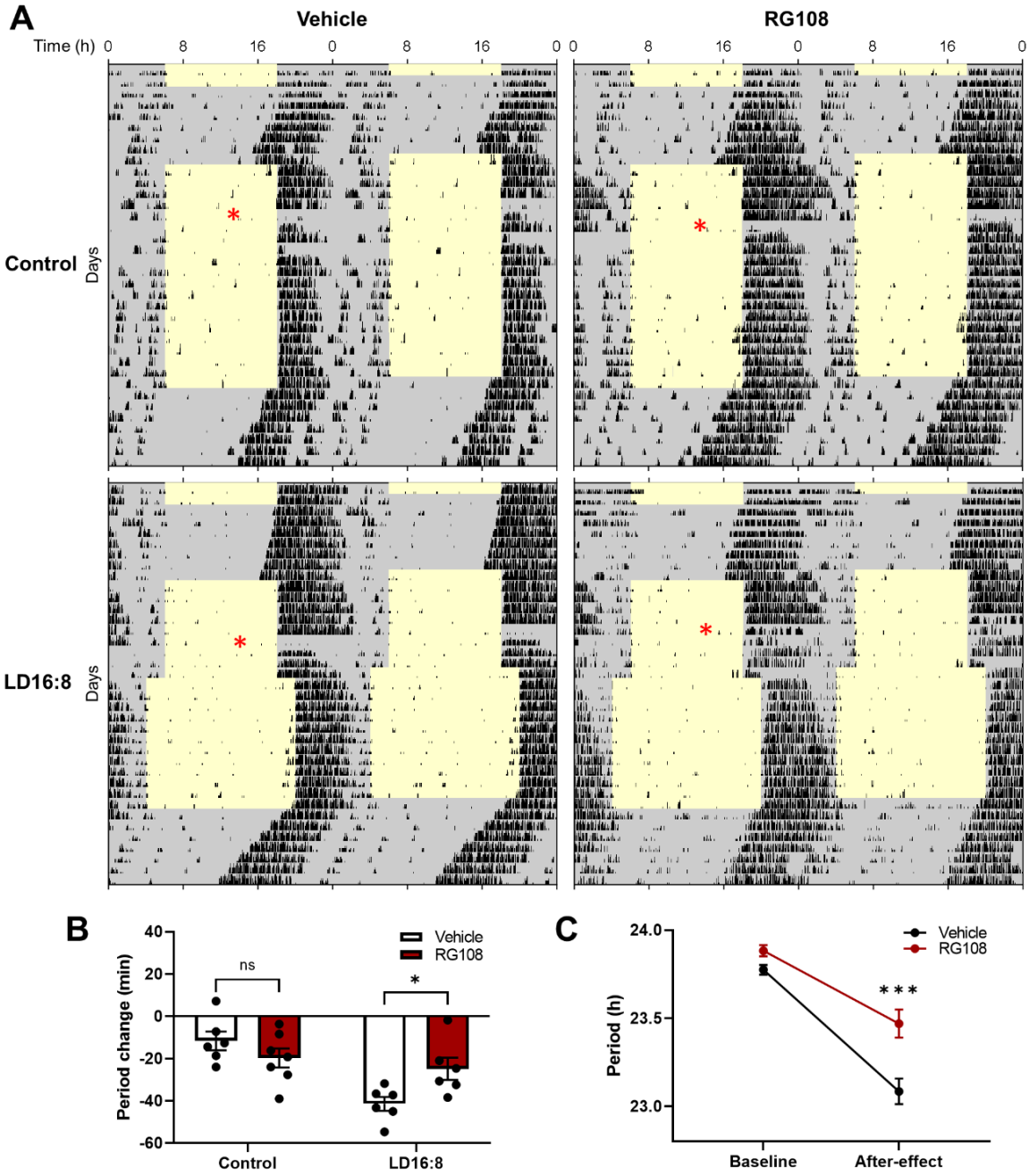

Figure 3.1. DNA methylation mediates after-effects on circadian period following long photoperiod entrainment.

(A) Representative double-plotted mouse locomotor actograms under different lighting conditions (a 12h light cycle, a 16h light cycle, constant darkness). (*Figure legend continues.*)

(*Figure legend continued.*) Yellow and grey areas indicate a light and a dark phase, respectively. Black ticks indicate wheel-running behavior patterns. Red asterisks denote onset of RG108 or a drug vehicle infusion into the third ventricle of the brain. **(B)** Quantification of changes in the endogenous period in constant darkness in control (a 12h light cycle) and LD16:8 (a change from a 12h to a 16h light cycle) conditions with RG108 or a drug vehicle infusion. (Two-way ANOVA with Sidak's multiple comparisons tests, mean ± SEM, n = 6-7, ns: not significant, *p < 0.05). **(C)** Quantification of the endogenous period at the baseline (the first constant darkness) and the after-effect period (the second constant darkness) following long photoperiod entrainment. (RM two-way ANOVA with Sidak's multiple comparisons tests, mean ± SEM, n = 6, ***p<0.001).

baseline circadian period. In contrast, LD 16:8 vehicle control mice exhibited shortening of their circadian locomotor period, which was significantly blunted by RG108 (Figure 3.1B), suggesting that DNA methylation regulates changes to circadian period following photoperiodic entrainment.

DNA methylation in the SCN regulates expression of period after-effects in circadian behavior following acute phase shifts

Resetting of circadian rhythms by discrete light exposure is fundamental for circadian entrainment to light cycles[12]. In addition, an acute phase delay or an advance in circadian rhythms induced by a brief light exposure causes period after-effects, with a period lengthening or a shortening on subsequent cycles[2]. Interestingly, the magnitude of subsequent period changes is positively correlated with the magnitude of the preceding phase shifts[107,108]. We thus sought to investigate two questions. First, is DNA methylation involved in period changes following acute light exposure, not just following weeks of entrainment to different photoperiods (Figure 3.1), or non-24h light cycles[106]? Second, does DNA methylation regulate period after-effects by modulating the magnitude of initial phase shifts, or by directly acting on expression of period after-effects?

To test whether and how DNA methylation mediates period after-effects at the level of discrete light pulses, we inhibited DNA methylation in the mouse brain with RG108 injection into the third ventricle near the SCN and then delivered 1h light pulses in the early physiological night (~circadian time (CT) 13.5, ~CT16.5) in constant darkness to induce phase shifts and period after-effects in locomotor behavior rhythms (Figure 3.2A). Vehicle controls showed phase delays and period lengthening following light pulses as expected (Figure 3.2B-D). RG108-treated mice showed similar magnitude phase delays to vehicle controls, but period lengthening was blocked

(Figure 3.2B-D), indicating that DNA methylation regulates period changes without directly affecting phase shifts. This supports an idea that DNA methylation mediates expression of period after-effects following acute resetting of circadian rhythms.

After-effects of phase resetting on a period of SCN molecular rhythms are modulated by DNA methylation

The preceding experiments in animals showed that inhibition of DNA methylation directed at the SCN blocks expression of behavioral period plasticity to photoperiodic entrainment and single phase shifts. As circadian behavioral rhythms are regulated by interactions between a central SCN clock and other peripheral brain clocks[168,169], in principle, DNA methylation might be acting directly on expression of period plasticity in the SCN itself, or through actions on other brain clocks downstream of the SCN for behavioral outputs.

To test whether DNA methylation mediates circadian after-effects directly on SCN molecular rhythms, we used organotypic SCN slice cultures expressing a bioluminescent reporter of clock protein PER2 expression (PER2::LUC)[130], and induced phase shifts in PER2::LUC rhythms in SCN slices by applying vasoactive intestinal peptide (VIP), a neuropeptide mediating light-induced SCN clock resetting[57], at early physiological night (CT14) in the presence or absence of a DNA methylation blocker RG108 in culture medium (Figure 3.3). RG108 treatment itself without VIP application did not change the phase or period of PER2::LUC bioluminescence rhythms in SCN slices (Figure 3.3A-C), suggesting that DNA methylation is not essential for maintaining SCN rhythms in the resting state. This is consistent with a previous observation[106] and ours that blocking DNA methylation itself does not affect the endogenous period of circadian behavior. When VIP was applied to SCN slices, RG108 co-treatment did not affect VIP-induced

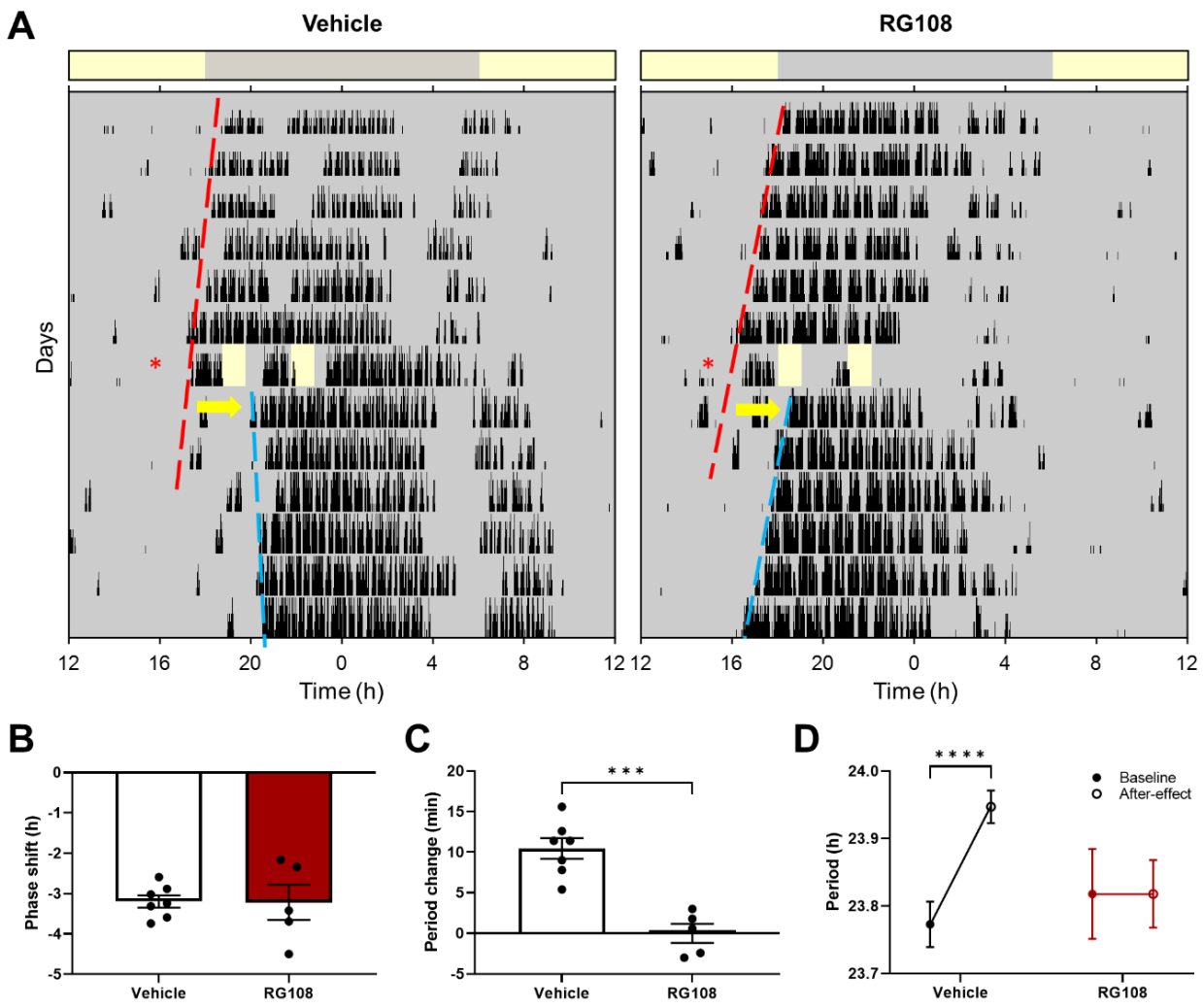

Figure 3.2. DNA methylation mediates after-effects on circadian period of locomotor behavioral rhythms without affecting acute phase delays.

(A) Representative wheel-running behavior actograms with brief light exposure (yellow bars) in constant darkness with a drug vehicle (left) or RG108 (right) injection (red asterisk) in the third ventricle. Bars above the actograms indicate the 12h light (yellow) and 12h dark (grey) cycle previously entrained to which mice were before release into constant darkness. Red and blue dashed lines indicate linear regression of locomotor activity onsets (*Figure legend continues.*)

(*Figure legend continued.*) before and after light exposure, respectively. The slopes of regression lines are the calculated activity rhythm periods. Yellow arrows denote phase shifts. **(B-C)** Quantification of phase shifts **(B)** and period changes **(C)** following light exposure in vehicle- and RG108-injected mice. (Unpaired t-test, mean ± SEM, n = 5-7, ***p<0.001). **(D)** Quantification of the endogenous period before and after light exposure (baseline, after-effect) in vehicle- and RG108-injected mice. (RM two-way ANOVA with Sidak's multiple comparisons tests, mean ± SEM, n=5-7, ****p<0.0001).

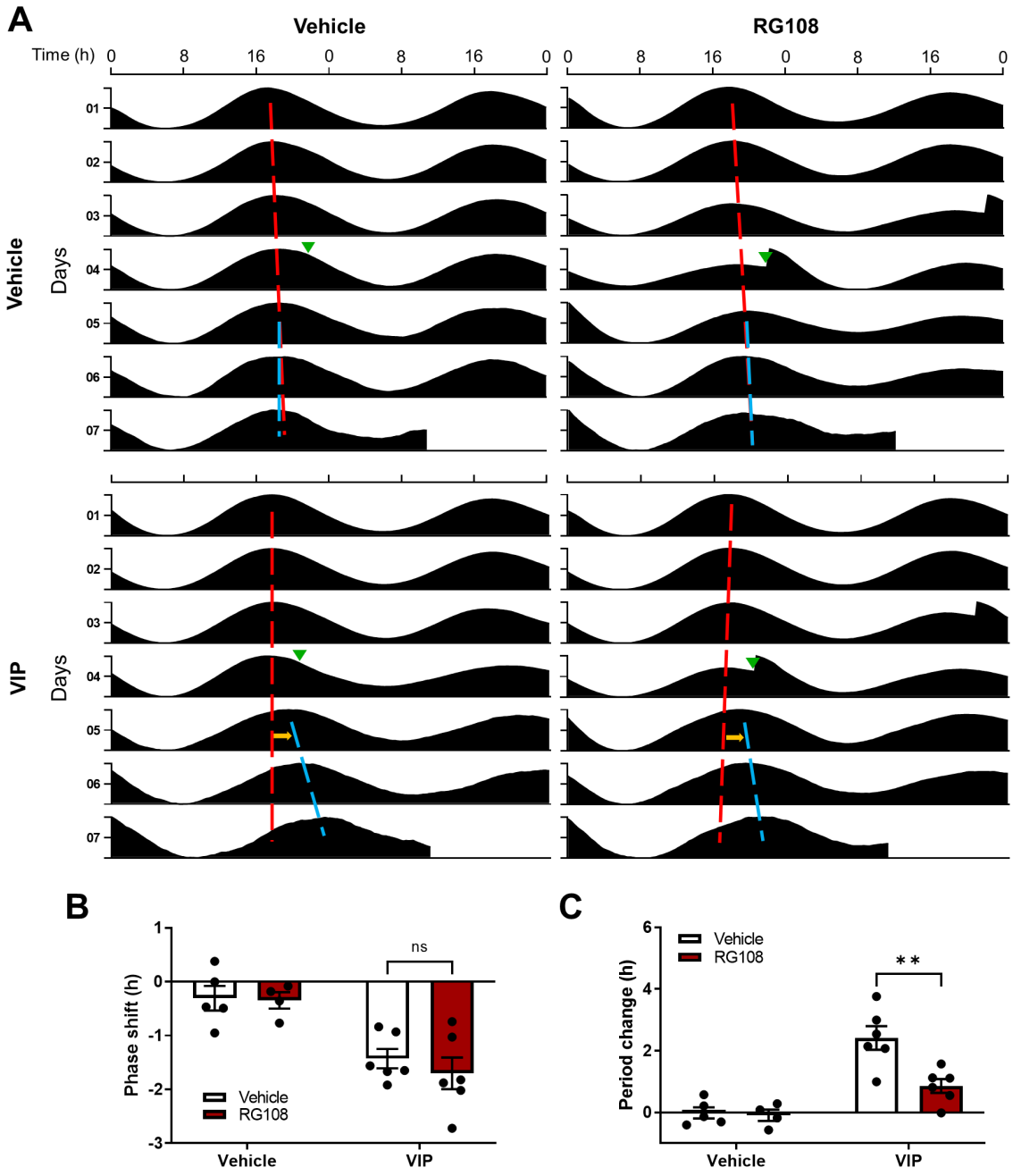

Figure 3.3. DNA methylation mediates VIP-induced after-effects on the ex vivo SCN rhythm period without affecting acute phase delays.

(A) Representative double-plotted actograms of PER2::LUC bioluminescence rhythms in SCN slices treated with one of combinations of VIP, RG108, and (*Figure legend continues.*)

(*Figure legend continued.*) their vehicles. Red and blue lines indicate linear regression of peaks before and after treatment (green triangles), respectively. Yellow arrows denote phase shifts. **(B-C)** Quantification of phase shifts **(B)** and period changes **(C)** following treatment. (Two-way ANOVA with Sidak's multiple comparisons tests, mean ± SEM, n=4-6, ns: not significant, **p<0.01).

phase shifts in SCN rhythms but it attenuated VIP-induced period changes (Figure 3.3A-C). This suggests that DNA methylation directly modulates expression of after-effects on SCN rhythms following acute phase shifts, consistent with our findings in behavioral experiments.

Since in the previous experiments VIP was applied as a bolus, and not washed out, its continued presence in the medium could potentially confound after-effects on period with persistent ongoing effects of VIP itself on period. Therefore, we sought to test these results with a more temporally precise stimulus to the ex vivo SCN. Recently, our lab showed that optogenetic stimulation of the ex vivo SCN using a red light-sensitive opsin ChrimsonR mimics light-induced resetting of circadian rhythms in vivo[170]. Here, we expressed ChrimsonR in neurons in SCN slices from PER2::LUC mice with an AAV (AAV-Synapsin-ChrimsonR-tdTomato)[140]. We then applied to the SCN slices a different class of pan-DNA methyltransferase inhibitor, SGI-1027, and one day later delivered 15-minutes of optogenetic stimulation (625 nm, 10 Hz, 10 ms pulse width) to SCN neurons in their early physiological night (CT14) to mimic retinal light input to the SCN (Figure 3.4). SGI-1027 treatment itself without optogenetic stimulation did not affect SCN PER2::LUC rhythms (Figure 3.4A-C), suggesting again that DNA methylation does not influence resting-state circadian rhythms in the SCN. SGI-1027 treatment prior to optogenetic stimulation suppressed period changes in the SCN rhythms following the stimulation, but it did not impact phase shifts (Figure 3.4A-C). This further supports the notion that DNA methylation is not essential for phase shifts in SCN rhythms following acute light input, but it is required for expression of after-effects on SCN rhythm period on subsequent cycles.

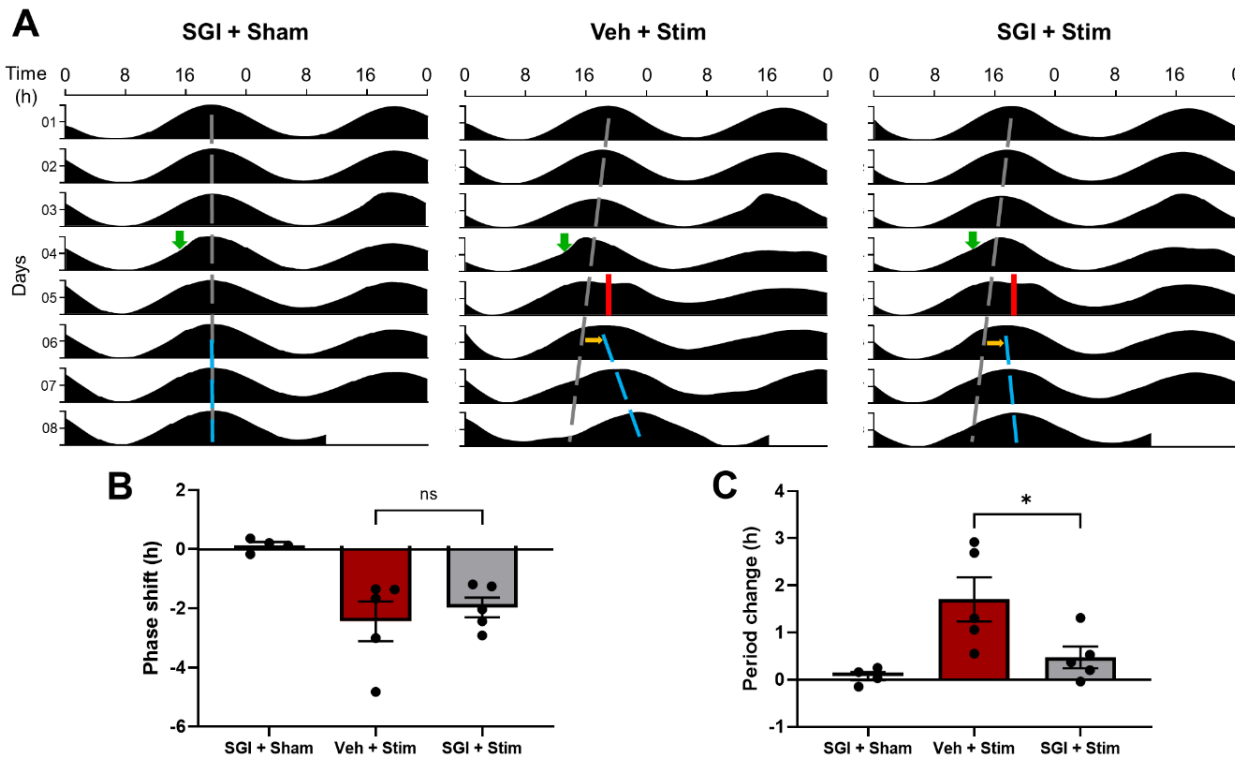

Figure 3.4. DNA methylation is critical for after-effects on the ex vivo SCN rhythm period following acute optogenetic stimulation of SCN neurons.

(A) Representative double-plotted actograms of PER2::LUC bioluminescence rhythms in SCN slices with SGI-1027 or its vehicle treatment (green arrows), and sham or optogenetic stimulation (red bars). Grey and blue dashed lines indicate linear regression of peaks before and after stimulation, respectively. Yellow arrows denote phase shifts. **(B-C)** Quantification of phase shifts **(B)** and period changes **(C)** following sham or optogenetic stimulation. (One-way ANOVA with Tukey's multiple comparisons tests, mean ± SEM, n=4-5, ns: not significant, *p<0.01).

3.4 Discussion

This study extends the understanding that DNA methylation is involved in light modulation of circadian period, a lasting form of circadian clock plasticity. Previous studies showed that DNA methylation in the SCN mediates period after-effects following months of entrainment to non-24h light cycles (T-cycles)[106]. Here we have shown that entrainment to altered daytime lengths (photoperiods) involves DNA methylation to express after-effects on circadian period, and uncovered that at the level of single light pulses the SCN produces circadian after-effects via DNA methylation. Thus, our results suggest that the SCN involves DNA methylation as a widespread mechanism of period after-effects at the molecular and behavioral output levels.

After-effects on circadian period is a prominent example of circadian clock plasticity to different lighting conditions. DNA methylation was previously shown to be necessary for period plasticity in the case of T-cycle entrainment[75,106]. However, the role of DNA methylation in period plasticity following other forms of light exposure remained uncharacterized. Unlike T-cycle entrainment, which is rarely, if ever, experienced in nature, photoperiod entrainment is a key function of the circadian clock critical for mediating seasonal changes in animal physiology and behavior. We now show that period plasticity following photoperiod entrainment likely involves DNA methylation in the SCN. Interestingly, DNA methylation plays a key role in regulating seasonal timing of reproduction in many different taxa including animals and plants[171]. In rodents, DNA methylation is critical for hypothalamic regulation of seasonal reproductive organ development[172]. This suggests that seasonal changes in DNA methylation patterns in different brain regions, including the SCN, might coordinately regulate seasonality of animal physiology and behavior. Future studies will be needed to investigate how photoperiod-induced period plasticity is coordinated with other hypothalamic regulation for seasonal physiology and behavior.

Another important point of this study is that our data suggest that DNA methylation can take place in the SCN following even a brief light exposure or a clock-resetting stimulation to mediate period plasticity. Given that DNA methylation is essential for period changes following months of T-cycle entrainment[106], this suggests that DNA methylation might universally regulate light-induced period plasticity regardless of the duration of altered lighting paradigms, although DNA methylation might act on different targets for period changes following acute light exposure than those following entrainment. Interestingly, ontological analyses of DNA methylation in the SCN following T-cycle entrainment revealed that the most significant changes in DNA methylation were found in genes encoding neurotransmitter receptors and ion channels[75], suggesting that changes in intercellular coupling within the SCN might be regulated by DNA methylation to induce period plasticity. Further investigating targets of DNA methylation for period plasticity to different lighting conditions will deepen our understanding of epigenetic regulation of circadian clock plasticity.

Lastly, our study has implications in human health. Our data suggest that DNA methylation patterns in the SCN might change dynamically following altered lighting conditions, including a brief light exposure at night or seasonal changes in daylight lengths, to mediate after-effects on circadian period. Given that animals including humans can experience highly varying circadian lighting conditions throughout their lifetime, this suggests that studying dynamics of DNA methylation patterns in the SCN might contribute to understanding the molecular basis of effects of prior light history on the circadian clock[2], and to assessing potential health impacts on human populations experiencing a high degree of changes in environmental lighting conditions including those living at a high latitude with large seasonal changes in daylight and those experiencing circadian misalignments such as shift workers and those frequently traveling across time zones.

3.5 Materials and methods

Animals and housing

Two to four months old Wild-type C57BL/6J mice (000664, Jackson Laboratory) were used for behavioral experiments. For organotypic SCN slice culture from heterozygous PER2::LUC knock-in mice[130], 2-4 months old mice were used in VIP application experiments and P11-14 mice were used in optogenetic stimulation experiments. We used heterozygous PER2::LUC mice as the PER2::LUC knock-in allele can alter circadian functions such as free-running period[166]. All animals were housed in a 12:12 light-dark cycle (except as noted), and had food and water provided ad libitum. For circadian behavioral experiments, male mice were used to avoid effects of the estrous cycle on circadian behavior and transferred from their home cages to individually housed wheel-running cages connected to a computer for monitoring locomotor activity using ClockLab software (Actimetrics). Wheel-running cages with ad libitum access to food and water were placed in light-tight chambers and exposed to various lighting conditions controlled by ClockLab including constant darkness and a 16:8 light-dark cycle. For ex vivo assays, both male and female mice were used in experiments. Experiments were performed in accordance with the Vanderbilt University Institutional Animal Care and Use Committee and National Institutes of Health guidelines.

Stereotaxic surgery and drug delivery to the brain

Mice were anesthetized with 2% isoflurane and placed securely in a stereotaxic apparatus (Kopf Instruments) with the body temperature maintained at 36°C using a homeothermic heating pad (Harvard Apparatus). Eye lubricant was applied to prevent drying during surgery. For RG108 infusion into the third ventricle, an implantable osmotic pump (Model 1004, infusion rate

0.11µl/hr, Alzet) was filled with 200µM RG108 in aCSF (0.66% DMSO) or vehicle and primed with sterile saline at 36.8°C before use as per manufacturer's instruction. RG108 concentration was chosen based on previous studies examining behavioral outcomes associated with blocking DNA methylation in a brain region[111,173]. An osmotic cannula (28 gauge, Plastics One) was stereotaxically implanted in the third ventricle near the SCN (relative to bregma, A/P: -0.5 mm, M/L: 0.0 mm, D/V: -4.5 mm) and connected to the osmotic pump via a vinyl catheter tubing (Alzet). The osmotic pump was then implanted subcutaneously under the back skin as per manufacturer's recommendations. After stereotaxic surgery, mice were returned to individually housed wheel-running cages for recovery and subsequent behavioral experiments. To ensure pump infusion, the pump reservoir was inspected after behavioral experiments.

For RG108 injection into the third ventricle, a guide cannula (26 gauge, Plastics One) was implanted in the same location as for infusion and capped with a dummy cannula (Plastics One). After stereotaxic surgery, mice were returned to individually housed wheel-running cages for recovery and subsequent experiments. On the day of light stimulation in constant darkness, mice were taken out of their cages, and while mice were held tightly under dim red light a dummy cannula was removed and an internal cannula (Plastics One) was inserted into a guide cannula and connected to a 10µl microsyringe (Model 1701, Hamilton) filled with 100µM RG108 in aCSF (0.66% DMSO) or a vehicle via PE50 tubing (Plastics One). Mice were released and allowed to move around while RG108 or a vehicle was dispensed at 0.5µl/sec using a syringe dispenser (Hamilton). After injection, the injection system was disassembled and mice were returned to their cages under dim red light.

Circadian wheel-running behavioral assays and data analyses

Mice were transferred to individually housed wheel-running cages in light-tight chambers provided with experimental lighting conditions. Mice were habituated in wheel-running cages under a 12:12 LD cycle for at least three days before experiments. For photoperiodic entrainment assays, mice were released into constant darkness for a week to measure a baseline circadian period, and they received stereotaxic brain surgery for RG108 or a vehicle infusion after four or five days of re-exposure to a 12:12 LD cycle. After additional four or five days in a 12:12 LD cycle, mice were exposed to a 16:8 LD cycle for 12 days and then released into constant darkness to measure an after-effect on circadian period. Light cycle control mice remained in a 12:12 LD cycle for a total of 20 days before a release into constant darkness. For light pulse experiments, mice received stereotaxic brain surgery and after a week of recovery in a 12:12 LD cycle they were released into constant darkness for six days to measure a baseline circadian period. On day 7, mice received RG108 or a vehicle injection under dim red light around CT10.5 (CT12 was defined as the onset of nocturnal locomotor activity) and were given two one-hour light pulses in constant darkness around CT13.5 and CT16.5. Wheel-running activity after the light pulses was recorded to measure phase shifts and period changes.

Wheel-running activity records were extracted and analyzed using ClockLab software running in Matlab (Mathworks). Single- or double-plotted 24-hour actograms with lighting information were produced and activity onsets were determined using ClockLab. Phase shifts were calculated as difference in time between the activity onsets observed following light exposure and those predicted using linear regression from activity onsets before light exposure. Period changes were calculated as differences in the period length of at least six cycles before and after changes in light exposure using Chi-square periodogram in ClockLab.

Ex vivo SCN bioluminescence rhythm assays

Organotypic SCN slice culture was performed as previously described[170]. Briefly, 300μm-thick coronal slices containing the SCN were obtained from PER2::LUC mouse brains using a vibratome (Leica) and placed on a semi-permeable membrane insert (PTFE, Millipore) in 35-mm culture dishes. The culture dishes were sealed with a transparent PCR plate film (Bio-Rad) and maintained in a multi-channel luminometer LumiCycle (Actimetrics) inside an incubator at 36.8°C. Bioluminescence from PER2::LUC SCN slices was recorded in 10 min intervals. For VIP application experiments, culture medium was 1.2ml of DMEM supplemented with 10mM HEPES, 25U/ml penicillin/streptomycin, 2% B-27 Plus (Gibco), and 0.1mM D-luciferin sodium salt (Tocris). 1μM VIP (Tocris) dissolved in sterile water was applied at CT14 to the culture medium 15 mins prior to 200μM RG108 (dissolved in 0.66% DMSO) application in the medium. CT12 was defined as the peak of PER2::LUC rhythms. CT14 was determined using at least three cycles of PER2::LUC rhythms before drug application. Drugs were pre-warmed before application and not washed off.

For optogenetic stimulation experiments, culture medium was the same as for VIP application experiments except that it contained 2mM Glutamax (Gibco) instead of L-glutamine. 1μl AAV (pAAV1-Syn-ChrimsonR-tdTomato, Addgene)[140] was applied onto SCN slices before sealing culture dishes. The opsin expression was confirmed by imaging tdTomato fluorescence 10 days after viral transduction. 10μM SGI-1027 (Tocris) dissolved in DMSO was applied to culture medium one day before optogenetic stimulation. For optogenetic stimulation, 625nm LED light pulses (10Hz, 10ms) were illuminated onto SCN slices at CT14 for 15 minutes using an integrated system of luminometry and optogenetic stimulation previously described[170].

Bioluminescence recording data analysis

Bioluminescence data were analyzed as previously described[170]. Briefly, raw data were baseline-subtracted and smoothed using LumiCycle Analysis software (Actimetrics). Then they were loaded into Matlab-run ClockLab for further analyses. Phase shifts were calculated as difference in time between the rhythm peaks observed following drug application or optogenetic stimulation and those predicted using linear regression from peaks before manipulation. Period changes were determined as difference in the period length of at least three cycles using linear regression of peaks. Bioluminescence data were visualized using Excel (Microsoft) and Prism (Graphpad).

Experimental design and statistical analysis

For all experiments, mice were randomly assigned to control and experimental groups. For circadian behavior assays, only male mice were used to avoid estrous cycle effects on circadian period. For ex vivo SCN rhythm assays, both males and females were used. For statistical comparisons, unpaired t-tests, one-way ANOVAs with Tukey's post hoc tests, or two-way ANOVAs with Sidak's post hoc tests were performed using Prism, and tests used for individual experiments are described in the figure legends. Data are presented as mean ± standard error of mean (SEM). Differences between groups were considered statistically significant when the p-value was less than 0.05.

CHAPTER IV

Conclusions and future directions

My work presented in this dissertation addresses a fundamental question in circadian biology: how light signals induce entrainment and plasticity of SCN clock gene rhythms. In Chapter II, I developed novel methods that allow tracking of clock gene rhythms in real time throughout entrainment, and which revealed that SCN clock gene rhythms under light entrainment change their waveforms from sinusoids to asymmetric shapes with accelerated synthetic phases following dawn and prolonged degradative phases following dusk. The SCN clock expresses canonical forms of circadian clock plasticity at the fundamental level of core clock genes. Also, I mapped out the spatial organization of phase resetting and after-effects in the SCN, and uncovered that phase resetting is more pronounced in the ventrolateral SCN, while after-effects are larger in the dorsomedial SCN. In Chapter III, I showed that DNA methylation mediates after-effects of photoperiods, and revealed that at the level of brief light exposure the SCN clock involves DNA methylation to produce after-effects. Taken together, these results contribute to our understanding of circadian light entrainment and clock plasticity at the molecular and network levels, and provide new directions for future studies into studying mechanisms of circadian entrainment and plasticity, as described below.

Real-time recordings of clock gene expression under entrainment conditions (Chapter II) fully revealed the dynamic nature of circadian rhythms in gene expression that had been inferred indirectly from snapshots of those rhythms. Circadian rhythms in gene expression under light entrainment have often been assumed as symmetrical sinusoidal rhythms and fitted to cosine

curves accordingly. Real-time PER2 rhythms in entrainment conditions, however, show that effects of light or clock-resetting signals on rhythmic gene expression throughout the 24-hour cycle are not uniform, but they are distinct in different clock phases, causing an asymmetry in molecular waveforms: light signals in the morning accelerate the synthetic phase, while evening light signals slow down the degradative phase. Notably, *Per1/2* expression is light-inducible via activation of cAMP-response elements (CREs)[23]. Although other clock genes do not contain CREs, their expression might be indirectly induced by light, as interlocked TTFLs influence the expression of one clock gene and another. Indeed, *Bmal1* rhythms in the SCN are gradually phase delayed by single light exposure around circadian dusk, while Per1 rhythms are immediately phase delayed[174]. However, differences in kinetics of phase shifts between *Per1* and *Bmal1* rhythms are not pronounced during a small magnitude of phase advances[174], leaving a question of whether that is because of differences in the magnitude or direction of phase shifts. Real-time measurement of *Bmal1* rhythms under entrainment conditions would allow examination of how the different phase-shifting kinetics of *Per* and *Bmal1* rhythms affects kinetics and other properties of entrainment. Furthermore, studying how rhythms in expression of clock-controlled genes are light-reset, and how they achieve light entrainment will advance our understanding of the circadian regulatory network.

The e*x vivo* entrainment assays I developed can be adapted for tracking subregional rhythms in SCN slices throughout entrainment conditions, and thus can contribute to investigating how SCN entrainment is established and maintained at the molecular and network levels. This question has been addressed using previous methods that had significant limitations. Circadian behavioral assays combined with genetic manipulations *in vivo* are limited to examining molecular mechanisms of SCN entrainment at the behavioral output level. Assessing free-running rhythms

in the SCN explanted from animals entrained to light cycles does not fully capture active encoding of entrainment in the SCN, as the network state of SCN rhythms under entrainment rapidly reverts to the baseline following a release into free-running conditions[81]. *Ex vivo* entrainment assays combined with genetic or pharmacological manipulations allow direct testing of what molecular mechanisms mediate SCN entrainment at the ensemble and individual oscillator levels. For example, previous work by Myung and colleagues suggested that GABA switching in the dorsal SCN mediates phase dispersion in SCN rhythms under long photoperiods, and that changes in chloride homeostasis induce GABA switching[80]. Given that skeleton long photoperiods mimic most aspects of complete long photoperiods including photoperiod-induced phase dispersion[109], whether such GABA switching is necessary for phase dispersion and for long photoperiod entrainment can be tested by blocking chloride transporters during *ex vivo* entrainment to skeleton long photoperiods.

Canonical forms of circadian clock plasticity expressed in the SCN at the ensemble level (Chapter II) can be further studied using real-time imaging of *ex vivo* SCN under entrainment conditions. I revealed that phase jumps during skeleton photoperiods are dynamic processes of waveform changes in SCN molecular rhythms at the ensemble level. It is completely unknown what happens to SCN rhythms at the network level during phase jumps. It would be interesting to see whether the SCN rhythm largely maintains intercellular phase synchrony or there is any regional pattern of network changes in SCN rhythms. This will give us novel insights into coupling properties of the SCN oscillator. In addition, I revealed how SCN ensemble period changes over the course of entrainment. It will be interesting to explore how circadian period is encoded in the SCN at the network level throughout entrainment. Myung and colleagues predicted using a SCN mathematical model that fast and slow oscillators are further phase-dispersed under long

photoperiods[80]. It remains an open question how circadian period organization in the SCN is modified and influences phase synchrony, and vice versa, throughout long photoperiod entrainment.

Regional heterogeneity in phase shifts between the ventrolateral and dorsomedial SCN suggested in my dissertation work can be further studied to determine the underlying mechanisms. As synchronous optogenetic stimulation of all SCN neurons produced regionally different phase responses, such heterogeneity might be derived from cell-intrinsic differences in phase-shifting capacity. Notably, the ventral and dorsal regions are respectively populated by VIP and AVP neurons[57], suggesting that those neurons show different phase responses to the same light signals. This could be tested by delivering clock-resetting stimulations to either VIP or AVP neurons and then comparing their phase shifts. Interestingly, intracellular calcium rhythms are asynchronous between the dorsal and ventral regions in free-running conditions, although voltage and firing rate rhythms are synchronous across the regions[175]. Given that an increase in intracellular calcium level in the SCN is critical for light-induced phase resetting[176] and a higher calcium level following an acute stimulation (e.g., either via a higher influx or timing of stimulation close to a peak phase) might cause a bigger amplitude of phase shifts, it might be worth examining regional differences in changes in intracellular calcium rhythms within the SCN in response to clock-resetting stimulations.

Other remaining questions from my dissertation work focus on after-effects. Real-time SCN imaging throughout single phase shifts revealed that the magnitude of phase shifts is inversely correlated with that of after-effects, suggesting that after-effects of phase shifts compensate for regional differences in initial phase shifts and thus revert phase synchrony to the baseline level. Given that after-effects of single pulses at the SCN network level suggest a role in

recovering phase synchrony, it will be informative to explore whether that is the case in entrainment conditions, and if not, what roles after-effects play in phase and period synchrony within the SCN. Surprisingly, after-effects of one-pulse T-cycles were not pronounced in the *ex vivo* SCN compared to those of a single pulse, suggesting that T-cycle after-effects might not simply be an accumulative effect of after-effects of single pulses. In fact, this result fits well with discrete mechanisms of entrainment: entrainment is achieved by discrete phase shifts without period changes[12]. As the T-cycle entrainment I have used relies on only one light response every cycle and thus is not as stable as two-pulse or complete T-cycle entrainment[12], it would be interesting to assess after-effects of two-pulse T-cycles and compare to those of one-pulse T-cycles. This might give us a clue for the origin of after-effects of entrainment. Additionally, it remains largely unexplored what is the role of different clock genes in the expression of after-effects. Given that clock genes are critical for setting circadian period, they might be involved in light modulation of circadian period. Testing after-effects in TTFL gene knockout animals (Table 1.1), for example, will address this question.

Another remaining question on after-effects from my dissertation work is mechanisms of DNA methylation regulation of after-effects. In addition to after-effects of T-cycles[106], after-effects of photoperiods and single light pulses involve DNA methylation (Chapter III). This strongly suggests that DNA methylation is a fundamental mechanism of circadian after-effects. However, it remains unknown which target genes of DNA methylation are essential for producing after-effects. Comparisons of DNA methylation profiles from the SCN between different T-cycle conditions revealed that differentially methylated genes are involved in neuronal communications[75,106], suggesting that DNA methylation might regulate after-effects via modulation of SCN rhythm coupling. Blocking GABA signaling abolishes period differences in

ex vivo SCN rhythms of animals between T-22, T-24, and T-26 cycle conditions[75], suggesting that GABA signaling is critical for maintaining after-effects of T-cycles. It will be interesting to test whether GABA signaling is essential for establishing after-effects and is regulated by DNA methylation. As VIP signaling is critical for intercellular coupling in the SCN[69–71], it is worth examining whether DNA methylation modulates VIP signaling to produce after-effects. Other than genes involved in SCN networking, genes regulating stability of clock proteins such as *casein kinase 1 delta* (*Ck1δ*) might be modulated by DNA methylation as turnover rates of clock proteins are a critical parameter of circadian oscillators for setting circadian period[23].

Lastly, methods of tracking real-time gene expression under ex vivo entrainment conditions described in this dissertation are currently limited for entrainment with discrete light pulses and thus extending the applicability to complete light cycle entrainment will be of great interest to the field. This technical limitation arises because optogenetic stimulation mimicking light input interrupts bioluminescence recording of clock gene rhythms. Also, prolonged light illumination in a repeated manner is potentially cytotoxic[134–136], causing at least a confounding effect on SCN rhythms. One potential way to address this limitation is to express a step function opsin in SCN neurons instead of a conventional opsin. In contrast to conventional opsins being active at a millisecond scale, step function opsins (SFOs) show a sustained activity on the order of minutes after lights are off[177,178]. This might allow to activate SCN neurons continuously with discrete light pulses at intervals and mimic exposure to complete light cycles. Some SFOs such as step function opsin with ultra-high light sensitivity (SOUL)[179] show deactivation time constant of ~30 minutes, although photocurrent of SFOs decreases over time following light termination. Given that SFOs are bi-stable opsins that can be activated by blue light and deactivated by orange light[177], it might be technically possible to make SFO photocurrent roughly constant continuously

if SFOs are for example given blue and orange light pulses every 20 minutes. Continuous activation of SFOs in SCN neurons for the duration of mimicked daylight might mimic subthreshold membrane depolarization in daytime[180,181]. Thus, SFOs might greatly serve to mimic complete light cycles in ex vivo SCN while enabling recording SCN rhythms almost seamlessly.

REFERENCES

1. Nikhil, K. L. & Sharma, V. K. On the Origin and Implications of Circadian Timekeeping: An Evolutionary Perspective. *Biol. Timekeep. Clocks, Rhythm. Behav.* 81–129 (2017).
2. Pittendrigh, C. S. & Daan, S. A functional analysis of circadian pacemakers in nocturnal rodents - I. The stability and lability of spontaneous frequency. *J. Comp. Physiol.* **106**, 223–252 (1976).
3. Pittendrigh, C. S. Circadian rhythms and the circadian organization of living systems. *Cold Spring Harb. Symp. Quant. Biol.* **25**, 159–184 (1960).
4. Acosta-Rodríguez, V. A., de Groot, M. H. M., Rijo-Ferreira, F., Green, C. B. & Takahashi, J. S. Mice under Caloric Restriction Self-Impose a Temporal Restriction of Food Intake as Revealed by an Automated Feeder System. *Cell Metab.* **26**, 267-277.e2 (2017).
5. Roberts, S. K. D. F. Circadian Activity Rhythms in Cockroaches II. Entrainment and phase shifting. *J. Cell. Comp. Physiol.* **59**, 175–186 (1962).
6. Underwood, H. Circadian pacemakers in lizards: phase-response curves and effects of pinealectomy. *Am. J. Physiol.* **244**, (1983).
7. Binkley, S. & Mosher, K. Photoperiod modifies circadian resetting responses in sparrows. *Am. J. Physiol.* **251**, (1986).
8. Covington, M. F. *et al.* ELF3 Modulates Resetting of the Circadian Clock in Arabidopsis. *Plant Cell* **13**, 1305–1316 (2001).
9. Engelmann, W., Karlsson, H. G. & Johnsson, A. Phase shifts in the Kalanchoe petal rhythm, caused by light pulses of different duration. *Int. J. Chronobiol.* **1**, 147–156 (1973).

10. Pittendrigh, C. S. Circadian Systems: Entrainment. *Biol. Rhythm.* 95–124 (1981).

11. ASCHOFF, J. Exogenous and Endogenous Components in Circadian Rhythms. *Cold Spring Harb. Symp. Quant. Biol.* **25**, 11–28 (1960).

12. Pittendrigh, C. S. & Daan, S. A functional analysis of circadian pacemakers in nocturnal rodents - IV. Entrainment: Pacemaker as clock. *J. Comp. Physiol.* **106**, 291–331 (1976).

13. Pittendrigh, C. S. & Minis, D. H. The Entrainment of Circadian Oscillations by Light and Their Role as Photoperiodic Clocks. *The American Naturalist* vol. 98 261–294 https://www.jstor.org/stable/2459454?seq=1 (1964).

14. Stephan, F. K. & Zucker, I. Circadian rhythms in drinking behavior and locomotor activity of rats are eliminated by hypothalamic lesions. *Proc. Natl. Acad. Sci. U. S. A.* **69**, 1583–1586 (1972).

15. Moore, R. Y. & Eichler, V. B. Loss of a circadian adrenal corticosterone rhythm following suprachiasmatic lesions in the rat. *Brain Res.* **42**, 201–206 (1972).

16. Ralph, M. R., Foster, R. G., Davis, F. C. & Menaker, M. Transplanted Suprachiasmatic Nucleus Determines Circadian Period. *Science (80-.).* **247**, 975–978 (1990).

17. Sawaki, Y., Nihonmatsu, I. & Kawamura, H. Transplantation of the neonatal suprachiasmatic nuclei into rats with complete bilateral suprachiasmatic lesions. *Neurosci. Res.* **1**, 67–72 (1984).

18. Drucker-Colín, R., Aguilar-Roblero, R., García-Hernández, F., Fernández-Cancino, F. & Rattoni, F. B. Fetal suprachiasmatic nucleus transplants: diurnal rhythm recovery of lesioned rats. *Brain Res.* **311**, 353–357 (1984).

19. Rusak, B. & Morin, L. P. Testicular Responses to Photoperiod Are Blocked by Lesions of the Suprachiasmatic Nuclei in Golden Hamsters1. *Biol. Reprod.* **15**, 366–374 (1976).

20. Stetson, M. H. & Watson-Whitmyre, M. Nucleus Suprachiasmaticus: The Biological Clock in the Hamster? *Science (80-.).* **191**, 197–199 (1976).

21. Stephan, F. K. & Nunez, A. A. Elimination of circadian rhythms in drinking, activity, sleep, and temperature by isolation of the suprachiasmatic nuclei. *Behav. Biol.* **20**, 1–16 (1977).

22. Bhadra, U., Thakkar, N., Das, P. & Pal Bhadra, M. Evolution of circadian rhythms: from bacteria to human. *Sleep Med.* **35**, 49–61 (2017).

23. Takahashi, J. S. Transcriptional architecture of the mammalian circadian clock. *Nature Reviews Genetics* vol. 18 164–179 (2017).

24. Gekakis, N. *et al.* Role of the CLOCK Protein in the Mammalian Circadian Mechanism. *Science* **280**, 1564–1569 (1998).

25. Shearman, L. P. *et al.* Interacting Molecular Loops in the Mammalian Circadian Clock. *Science (80-.).* **288**, 1013–1019 (2000).

26. Kume, K. *et al.* mCRY1 and mCRY2 are essential components of the negative limb of the circadian clock feedback loop. *Cell* **98**, 193–205 (1999).

27. Sato, T. K. *et al.* A functional genomics strategy reveals rora as a component of the mammalian circadian clock. *Neuron* **43**, 527–537 (2004).

28. Preitner, N. *et al.* The orphan nuclear receptor REV-ERBa controls circadian transcription within the positive limb of the mammalian circadian oscillator. *Cell* **110**, 251–260 (2002).

29. Zhang, Y. *et al.* Discrete functions of nuclear receptor Rev-erbα couple metabolism to the clock. *Science* **348**, 1488–1492 (2015).

30. Mitsui, S., Yamaguchi, S., Matsuo, T., Ishida, Y. & Okamura, H. Antagonistic role of E4BP4 and PAR proteins in the circadian oscillatory mechanism. *Genes Dev.* **15**, 995–

1006 (2001).

31. Zhang, R., Lahens, N. F., Ballance, H. I., Hughes, M. E. & Hogenesch, J. B. A circadian gene expression atlas in mammals: Implications for biology and medicine. *Proc. Natl. Acad. Sci. U. S. A.* **111**, 16219–16224 (2014).

32. Bunger, M. K. *et al.* Mop3 is an essential component of the master circadian pacemaker in mammals. *Cell* **103**, 1009–1017 (2000).

33. Kondratov, R. V *et al.* Early aging and age-related pathologies in mice deficient in BMAL1 , the core componentof the circadian clock service Early aging and age-related pathologies in mice deficient in BMAL1 , the core component of the circadian clock. *Genes Dev.* **20**, 1868–1873 (2006).

34. Shi, S. *et al.* Circadian Clock Gene Bmal1 Is Not Essential; Functional Replacement with its Paralog, Bmal2. *Curr. Biol.* **20**, 316–321 (2010).

35. Rey, G. *et al.* Genome-wide and phase-specific DNA-binding rhythms of BMAL1 control circadian output functions in mouse liver. *PLoS Biol.* **9**, (2011).

36. Liu, A. C. *et al.* Redundant function of REV-ERBα and β and non-essential role for Bmal1 cycling in transcriptional regulation of intracellular circadian rhythms. *PLoS Genet.* **4**, (2008).

37. Hattar, S., Kumar, M., Park, A. & Tong, P. Central Projections of Melanopsin- Expressing Retinal Ganglion Cells in the Mouse. *J Comp Neurol* **497**, 326–349 (2006).

38. Fernandez, D. C., Chang, Y.-T., Hattar, S. & Chen, S.-K. Architecture of retinal projections to the central circadian pacemaker. *Proc. Natl. Acad. Sci.* 201523629 (2016) doi:10.1073/pnas.1523629113.

39. Johnson, R. F., Morin, L. P. & Moore, R. Y. Retinohypothalamic projections in the

hamster and rat demonstrated using cholera toxin. *Brain Res.* **462**, 301–312 (1988).

40. Moore, R. Y. & Lenn, N. J. A retinohypothalamic projection in the rat. *J. Comp. Neurol.* **146**, 1–14 (1972).

41. Levine, J. D., Weiss, M. L., Rosenwasser, A. M. & Miselis, R. R. Retinohypothalamic tract in the female albino rat: A study using horseradish peroxidase conjugated to cholera toxin. *J. Comp. Neurol.* **306**, 344–360 (1991).

42. Bunger, M. K. *et al.* Mop3 Is an Essential Component of the Master Circadian Pacemaker in Mammals. *Cell* **103**, 1009–1017 (2000).

43. DeBruyne, J. P. *et al.* A Clock Shock: Mouse CLOCK Is Not Required for Circadian Oscillator Function. *Neuron* **50**, 465–477 (2006).

44. Cermakian, N., Monaco, L., Pando, M. P., Dierich, A. & Sassone-Corsi, P. Altered behavioral rhytms and clock gene expression in mice with targeted mutation in the Period1 gene. *EMBO J.* **20**, 3967–3974 (2001).

45. Zheng, B. *et al.* Nonredundant Roles of the mPer1 and mPer2 Genes in the Mammalian Circadian Clock. *Cell* **105**, 683–694 (2001).

46. Bae, K. *et al.* Differential functions of mPer1, mPer2, and mPer3 in the SCN circadian clock. *Neuron* **30**, 525–536 (2001).

47. Zheng, B. *et al.* The mPer2 gene encodes a functional component of the mammalian circadian clock. *Nat. 1999 4006740* **400**, 169–173 (1999).

48. Shearman, L. P., Jin, X., Lee, C., Reppert, S. M. & Weaver, D. R. Targeted Disruption of the mPer3 Gene: Subtle Effects on Circadian Clock Function . *Mol. Cell. Biol.* **20**, 6269–6275 (2000).

49. van der Horst, G. T. *et al.* Mammalian Cry1 and Cry2 are essential for maintenance of

circadian rhythms. *Nature* **398**, 627–30 (1999).

50. Vitaterna, M. H. *et al.* Differential regulation of mammalian Period genes and circadian rhythmicity by cryptochromes 1 and 2. *Proc. Natl. Acad. Sci.* **96**, 12114–12119 (1999).

51. Thresher, R. J. *et al.* Role of Mouse Cryptochrome Blue-Light Photoreceptor in Circadian Photoresponses. *Science (80-.).* **282**, 1490–1494 (1998).

52. André, E. *et al.* Disruption of retinoid-related orphan receptor β changes circadian behavior, causes retinal degeneration and leads to vacillans phenotype in mice. *EMBO J.* **17**, 3867–3877 (1998).

53. Cho, H. *et al.* Regulation of circadian behaviour and metabolism by REV-ERB-α and REV-ERB-β. *Nat. 2012 4857396* **485**, 123–127 (2012).

54. Lopez-Molina, L., Conquet, F., Dubois-Dauphin, M. & Schibler, U. The DBP gene is expressed according to a circadian rhythm in the suprachiasmatic nucleus and influences circadian behavior. *EMBO J.* **16**, 6762–6771 (1997).

55. Weger, B. D. *et al.* Systematic analysis of differential rhythmic liver gene expression mediated by the circadian clock and feeding rhythms. *Proc. Natl. Acad. Sci. U. S. A.* **118**, (2021).

56. Abrahamson, E. E. & Moore, R. Y. Suprachiasmatic nucleus in the mouse: Retinal innervation, intrinsic organization and efferent projections. *Brain Res.* **916**, 172–191 (2001).

57. Welsh, D. K., Takahashi, J. S. & Kay, S. A. Suprachiasmatic nucleus: cell autonomy and network properties. *Annu. Rev. Physiol.* **72**, 551–77 (2010).

58. Lee, J. E. *et al.* Quantitative peptidomics for discovery of circadian-related peptides from the rat suprachiasmatic nucleus. *J Proteome Res.* **12**, 585–93 (2013).

59. Ono, D., Honma, K. I. & Honma, S. Roles of Neuropeptides, VIP and AVP, in the Mammalian Central Circadian Clock. *Front. Neurosci.* **15**, 351 (2021).

60. Bedont, J. L. & Blackshaw, S. Constructing the suprachiasmatic nucleus: a watchmaker's perspective on the central clockworks. *Front. Syst. Neurosci.* **9**, 74 (2015).

61. Yan, L. *et al.* Exploring spatiotemporal organization of SCN circuits. *Cold Spring Harb. Symp. Quant. Biol.* **72**, 527–541 (2007).

62. Yan, L. *et al.* Phenotype Matters : Identification of Light- Responsive Cells in the Mouse Suprachiasmatic Nucleus Phenotype Matters : Identification of Light-Responsive Cells in the Mouse Suprachiasmatic Nucleus. *J. Neurosci.* **24**, 68–75 (2004).

63. Enoki, R., Ono, D., Kuroda, S., Honma, S. & Honma, K. Dual origins of the intracellular circadian calcium rhythm in the suprachiasmatic nucleus. *Sci. Rep.* **7**, 41733 (2017).

64. Yan, L. & Silver, R. Differential induction and localization of mPer1 and mPer2 during advancing and delaying phase shifts. *Eur. J. Neurosci.* **16**, 1531–1540 (2002).

65. Pennartz, C. M. *et al.* Membrane properties and morphology of vasopressin neurons in slices of rat suprachiasmatic nucleus. *J Neurophysiol* **80**, 2710–2717 (1998).

66. Drouyer, E., Lesauter, J., Hernandez, A. L. & Silver, R. Specializations of gastrin-releasing peptide cells of the mouse suprachiasmatic nucleus. *J. Comp. Neurol.* **518**, 1249–1263 (2010).

67. Kriegsfeld, L. J., Leak, R. K., Yackulic, C. B., LeSauter, J. & Silver, R. Organization of Suprachiasmatic Nucleus Projections in Syrian Hamsters (Mesocricetus auratus): An Anterograde and Retrograde Analysis. *J. Comp. Neurol.* **468**, 361–379 (2004).

68. Freeman, G. M., Krock, R. M., Aton, S. J., Thaben, P. & Herzog, E. D. GABA networks destabilize genetic oscillations in the circadian pacemaker. *Neuron* **78**, 799–806 (2013).

69. Harmar, A. J. *et al.* The VPAC2 receptor is essential for circadian function in the mouse suprachiasmatic nuclei. *Cell* **109**, 497–508 (2002).

70. Colwell, C. S. *et al.* Disrupted circadian rhythms in VIP- and PHI-deficient mice. *Am. J. Physiol. Regul. Integr. Comp. Physiol.* **285**, R939–R949 (2003).

71. Aton, S. J., Colwell, C. S., Harmar, A. J., Waschek, J. & Herzog, E. D. Vasoactive intestinal polypeptide mediates circadian rhythmicity and synchrony in mammalian clock neurons. *Nat. Neurosci.* **8**, 476–483 (2005).

72. Maywood, E. S., Chesham, J. E., O'Brien, J. a & Hastings, M. H. A diversity of paracrine signals sustains molecular circadian cycling in suprachiasmatic nucleus circuits. *Proc. Natl. Acad. Sci. U. S. A.* **108**, 14306–14311 (2011).

73. Yamaguchi, S. *et al.* Synchronization of Cellular Clocks in the Suprachiasmatic Nucleus. *Science (80-.).* **302**, 1408–1412 (2003).

74. Evans, J. A., Leise, T. L., Castanon-Cervantes, O. & Davidson, A. J. Dynamic Interactions Mediated by Nonredundant Signaling Mechanisms Couple Circadian Clock Neurons. *Neuron* **80**, 973–983 (2013).

75. Azzi, A. *et al.* Network Dynamics Mediate Circadian Clock Plasticity. *Neuron* **93**, 441–450 (2017).

76. Brancaccio, M., Maywood, E. S., Chesham, J. E., Loudon, A. S. I. & Hastings, M. H. A Gq-Ca2+ Axis controls circuit-level encoding of circadian time in the suprachiasmatic nucleus. *Neuron* **78**, 714–728 (2013).

77. Foley, N. C. *et al.* Characterization of orderly spatiotemporal patterns of clock gene activation in mammalian suprachiasmatic nucleus. *Eur. J. Neurosci.* **33**, 1851–1865 (2011).

78. Farajnia, S., Van Westering, T. L. E., Meijer, J. H. & Michel, S. Seasonal induction of GABAergic excitation in the central mammalian clock. *Proc. Natl. Acad. Sci. U. S. A.* **111**, 9627–9632 (2014).

79. DeWoskin, D. *et al.* Distinct roles for GABA across multiple timescales in mammalian circadian timekeeping. *Proc. Natl. Acad. Sci. U. S. A.* **112**, E3911–E3919 (2015).

80. Myung, J. *et al.* GABA-mediated repulsive coupling between circadian clock neurons in the SCN encodes seasonal time. *Proc. Natl. Acad. Sci. U. S. A.* **112**, E3920–E3929 (2015).

81. Rohr, K. E. *et al.* Seasonal plasticity in GABAA signaling is necessary for restoring phase synchrony in the master circadian clock network. *Elife* **8**, (2019).

82. Söhl, G., Maxeiner, S. & Willecke, K. Expression and functions of neuronal gap junctions. *Nat. Rev. Neurosci.* **6**, 191–200 (2005).

83. Long, M. A., Jutras, M. J., Connors, B. W. & Burwell, R. D. Electrical synapses coordinate activity in the suprachiasmatic nucleus. *Nat. Neurosci.* **8**, 61–6 (2005).

84. Panda, S. *et al.* Melanopsin is required for non-image-forming photic responses in blind mice. *Science* **301**, 525–527 (2003).

85. Hattar, S. *et al.* Melanopsin and rod-cone photoreceptive systems account for all major accessory visual functions in mice. *Nature* **424**, 76–81 (2003).

86. Ebling, F. J. The role of glutamate in the photic regulation of the suprachiasmatic nucleus. *Prog Neurobiol* **50**, 109–132 (1996).

87. Colwell, C. S. & Menaker, M. NMDA as well as non-NMDA receptor antagonists can prevent the phase-shifting effects of light on the circadian system of the golden hamster. *J. Biol. Rhythms* **7**, 125–36 (1992).

88. Vindlacheruvu, R. R., Ebling, F. J. P., Maywood, E. S. & Hastings, M. H. Blockade of

Glutamatergic Neurotransmission in the Suprachiasmatic Nucleus Prevents Cellular and Behavioural Responses of the Circadian System to Light. *Eur. J. Neurosci.* **4**, 673–679 (1992).

89. Kim, D. Y. *et al.* Voltage-gated calcium channels play crucial roles in the glutamate-induced phase shifts of the rat suprachiasmatic circadian clock. *Eur. J. Neurosci.* **21**, 1215–1222 (2005).

90. Vaudry, D. *et al.* Pituitary Adenylate Cyclase-Activating Polypeptide and Its Receptors : 20 Years after the Discovery. *Pept. Res.* **61**, 283–357 (2009).

91. Ajpru, S., McArthur, A. J., Piggins, H. D. & Sugden, D. Identification of PAC1 receptor isoform mRNAs by real-time PCR in rat suprachiasmatic nucleus. *Mol. Brain Res.* **105**, 29–37 (2002).

92. Cutler, D. J. & Piggins, H. D. The roles of vasoactive intestinal polypeptide in the mammalian circadian clock. *J. Endocrinol.* **177**, 7–15 (2003).

93. Kawaguchi, C. *et al.* PACAP-deficient mice exhibit light parameter-dependent abnormalities on nonvisual photoreception and early activity onset. *PLoS One* **5**, 1–9 (2010).

94. Hannibal, J., Brabet, P. & Fahrenkrug, J. Mice lacking the PACAP type I receptor have impaired photic entrainment and negative masking. *Am. J. Physiol. Regul. Integr. Comp. Physiol.* **295**, R2050–R2058 (2008).

95. Ginty, D. D. *et al.* Regulation of CREB Phosphorylation in the Suprachiasmatic Nucleus by Light and a Circadian Clock. *Science (80-.).* **260**, 238–241 (1993).

96. Miyake, S. *et al.* Phase-dependent responses of Per1 and Per2 genes to a light-stimulus in the suprachiasmatic nucleus of the rat. *Neurosci. Lett.* **294**, 41–44 (2000).

97. Ding, J. M., Faiman, L. E., Hurst, W. J., Kuriashkina, L. R. & Gillette, M. U. Resetting the biological clock: mediation of nocturnal CREB phosphorylation via light, glutamate, and nitric oxide. *J. Neurosci.* **17**, 667–675 (1997).

98. Shigeyoshi, Y. *et al.* Light-induced resetting of a mammalian circadian clock is associated with rapid induction of the mPer1 transcript. *Cell* **91**, 1043–1053 (1997).

99. Tischkau, S. A., Mitchell, J. W., Tyan, S. H., Buchanan, G. F. & Gillette, M. U. Ca2+/cAMP response element-binding protein (CREB)-dependent activation of Per1 is required for light-induced signaling in the suprachiasmatic nucleus circadian clock. *J. Biol. Chem.* **278**, 718–723 (2003).

100. Brenna, A. *et al.* PER2 mediates CREB-dependent light induction of the clock gene Per1. *Sci. Reports 2021 111* **11**, 1–19 (2021).

101. Butcher, G. Q., Lee, B. & Obrietan, K. Temporal regulation of light-induced extracellular signal-regulated kinase activation in the suprachiasmatic nucleus. *J Neurophysiol* **90**, 3854–3863 (2003).

102. Cao, R. *et al.* Light-regulated translational control of circadian behavior by eIF4E phosphorylation. *Nat. Neurosci.* **18**, 855–62 (2015).

103. Hay, N. & Sonenberg, N. Upstream and downstream of mTOR. *Genes Dev.* **18**, 1926–1945 (2004).

104. Cao, R., Li, A., Cho, H. Y., Lee, B. & Obrietan, K. Mammalian Target of Rapamycin Signaling Modulates Photic Entrainment of the Suprachiasmatic Circadian Clock. *J. Neurosci.* **30**, 6302–6314 (2010).

105. Cao, R. *et al.* Translational Control of Entrainment and Synchrony of the Suprachiasmatic Circadian Clock by mTOR/4E-BP1 Signaling. *Neuron* **79**, 712–724 (2013).

106. Azzi, A. *et al.* Circadian behavior is light-reprogrammed by plastic DNA methylation. *Nat. Neurosci.* **17**, 377–382 (2014).

107. Sharma, V. K. & Daan, S. Circadian phase and period responses to light stimuli in two nocturnal rodents. *Chronobiol. Int.* **19**, 659–670 (2002).

108. Sharma, V. K. Period Responses to Zeitgeber Signals Stabilize Circadian Clocks During Entrainment. *Chronobiol. Int.* **20**, 389–404 (2003).

109. Olde Engberink, A. H. O., Huisman, J., Michel, S. & Meijer, J. H. Brief light exposure at dawn and dusk can encode day-length in the neuronal network of the mammalian circadian pacemaker. *FASEB J.* **34**, 13685–13695 (2020).

110. Miller, C. A. *et al.* Cortical DNA methylation maintains remote memory. *Nat. Neurosci. 2010 136* **13**, 664–666 (2010).

111. Day, J. J. *et al.* DNA methylation regulates associative reward learning. *Nat. Neurosci. 2013 1610* **16**, 1445–1452 (2013).

112. Weaver, I. C. G. *et al.* Epigenetic programming by maternal behavior. *Nat. Neurosci. 2004 78* **7**, 847–854 (2004).

113. Siegfried, Z. *et al.* DNA methylation represses transcription in vivo. *Nat. Genet. 1999 222* **22**, 203–206 (1999).

114. Boyes, J. & Bird, A. DNA methylation inhibits transcription indirectly via a methyl-CpG binding protein. *Cell* **64**, 1123–1134 (1991).

115. Neri, F. *et al.* Intragenic DNA methylation prevents spurious transcription initiation. *Nat. 2017 5437643* **543**, 72–77 (2017).

116. Suetake, I., Shinozaki, F., Miyagawa, J., Takeshima, H. & Tajima, S. DNMT3L Stimulates the DNA Methylation Activity of Dnmt3a and Dnmt3b through a Direct

Interaction *. *J. Biol. Chem.* **279**, 27816–27823 (2004).

117. Li, E., Bestor, T. H. & Jaenisch, R. Targeted mutation of the DNA methyltransferase gene results in embryonic lethality. *Cell* **69**, 915–926 (1992).

118. Okano, M., Bell, D. W., Haber, D. A. & Li, E. DNA Methyltransferases Dnmt3a and Dnmt3b Are Essential for De Novo Methylation and Mammalian Development. *Cell* **99**, 247–257 (1999).

119. Jones, P. A. & Liang, G. Rethinking how DNA methylation patterns are maintained. *Nat. Rev. Genet. 2009 1011* **10**, 805–811 (2009).

120. Chen, T., Ueda, Y., Dodge, J. E., Wang, Z. & Li, E. Establishment and Maintenance of Genomic Methylation Patterns in Mouse Embryonic Stem Cells by Dnmt3a and Dnmt3b. *Mol. Cell. Biol.* **23**, 5594–5605 (2003).

121. Aton, S. J., Block, G. D., Tei, H., Yamazaki, S. & Herzog, E. D. Plasticity of circadian behavior and the suprachiasmatic nucleus following exposure to non-24-hour light cycles. *J. Biol. Rhythms* **19**, 198–207 (2004).

122. Molyneux, P. C., Dahlgren, M. K. & Harrington, M. E. Circadian entrainment aftereffects in suprachiasmatic nuclei and peripheral tissues in vitro. *Brain Res.* **1228**, 127–134 (2008).

123. Kuramoto, Y. Chemical Oscillations, Waves, and Turbulence. **19**, (1984).

124. Beersma, D. G. M., Van Bunnik, B. A. D., Hut, R. A. & Daan, S. Emergence of circadian and photoperiodic system level properties from interactions among pacemaker cells. *J. Biol. Rhythms* **23**, 362–373 (2008).

125. Beersma, D. G. M., Gargar, K. A. & Daan, S. Plasticity in the Period of the Circadian Pacemaker Induced by Phase Dispersion of Its Constituent Cellular Clocks. *J. Biol.*

Rhythms **32**, 237–245 (2017).

126. Myung, J. *et al.* Period Coding of Bmal1 Oscillators in the Suprachiasmatic Nucleus. *J. Neurosci.* **32**, 8900–8918 (2012).

127. Messager, S., Hazlerigg, D. G., Mercer, J. G. & Morgan, P. J. Photoperiod differentially regulates the expression of Per1 and ICER in the pars tuberalis and the suprachiasmatic nucleus of the Siberian hamster. *Eur. J. Neurosci.* **12**, 2865–2870 (2000).

128. Schwartz, W. J., Tavakoli-Nezhad, M., Lambert, C. M., Weaver, D. R. & De La Iglesia, H. O. Distinct patterns of Period gene expression in the suprachiasmatic nucleus underlie circadian clock photoentrainment by advances or delays. *Proc. Natl. Acad. Sci. U. S. A.* **108**, 17219–17224 (2011).

129. Kuhlman, S. J., Quintero, J. E. & McMahon, D. G. GFP fluorescence reports Period1 circadian gene regulation in the mammalian biological clock. *Neuroreport* **11**, 1479–1482 (2000).

130. Yoo, S. H. *et al.* PERIOD2::LUCIFERASE real-time reporting of circadian dynamics reveals persistent circadian oscillations in mouse peripheral tissues. *Proc. Natl. Acad. Sci. U. S. A.* **101**, 5339–5346 (2004).

131. Pendergast, J. S., Friday, R. C. & Yamazaki, S. Endogenous rhythms in period1 mutant suprachiasmatic nuclei in vitro do not represent circadian behavior. *J. Neurosci.* **29**, 14681–14686 (2009).

132. Jones, J. R., Tackenberg, M. C. & McMahon, D. G. Manipulating circadian clock neuron firing rate resets molecular circadian rhythms and behavior. *Nat. Neurosci.* **18**, 1–5 (2015).

133. Mazuski, C. *et al.* Entrainment of Circadian Rhythms Depends on Firing Rates and

Neuropeptide Release of VIP SCN Neurons. *Neuron* **99**, 555-563.e5 (2018).

134. Stockley, J. H. *et al.* Surpassing light-induced cell damage in vitro with novel cell culture media. *Sci. Rep.* **7**, 1–11 (2017).

135. Ohara, M., Kawashima, Y., Katoh, O. & Watanabe, H. Blue light inhibits the growth of B16 melanoma cells. *Japanese J. Cancer Res.* **93**, 551–558 (2002).

136. Robertson, J. B., Davis, C. R. & Johnson, C. H. Visible light alters yeast metabolic rhythms by inhibiting respiration. *Proc. Natl. Acad. Sci. U. S. A.* **110**, 21130–21135 (2013).

137. Waldchen, S., Lehmann, J., Klein, T., Van De Linde, S. & Sauer, M. Light-induced cell damage in live-cell super-resolution microscopy. *Sci. Rep.* **5**, 1–12 (2015).

138. De Magalhaes Filho, C. D. *et al.* Visible light reduces C. elegans longevity. *Nat. Commun. 2018 91* **9**, 1–13 (2018).

139. Lin, J. Y., Knutsen, P. M., Muller, A., Kleinfeld, D. & Tsien, R. Y. ReaChR: A red-shifted variant of channelrhodopsin enables deep transcranial optogenetic excitation. *Nat. Neurosci.* **16**, 1499–1508 (2013).

140. Klapoetke, N. C. *et al.* Independent optical excitation of distinct neural populations. *Nat. Methods* **11**, 338–346 (2014).

141. Tackenberg, M. C., Hughey, J. J. & McMahon, D. G. Optogenetic stimulation of VIPergic SCN neurons induces photoperiodic-like changes in the mammalian circadian clock. *Eur. J. Neurosci.* ejn.15442 (2021) doi:10.1111/EJN.15442.

142. Meijer, J. H., Watanabe, K., Schaap, J., Albus, H. & Détári, L. Light responsiveness of the suprachiasmatic nucleus: Long-term multiunit and single-unit recordings in freely moving rats. *J. Neurosci.* **18**, 9078–9087 (1998).

143. Tyssowski, K. M. & Gray, J. M. Blue light increases neuronal activity-regulated gene expression in the absence of optogenetic proteins. *eNeuro* **6**, 0085–19.2019 (2019).

144. Chen, S. K., Badea, T. C. & Hattar, S. Photoentrainment and pupillary light reflex are mediated by distinct populations of ipRGCs. *Nature* **476**, 92–96 (2011).

145. Humpel, C. Neuroscience forefront review organotypic brain slice cultures: A review. *Neuroscience* vol. 305 86–98 (2015).

146. Christie, A. & Butler, M. The adaptation of bhk cells to a non-ammoniagenic glutamate-based culture medium. *Biotechnol. Bioeng.* **64**, 298–309 (1999).

147. Imamoto, Y., Tanaka, H., Takahashi, K., Konno, Y. & Suzawa, T. Advantages of AlaGln as an additive to cell culture medium: Use with anti-CD20 chimeric antibody-producing POTELLIGENT^{TM} CHO cell lines. *Cytotechnology* **65**, 135–143 (2013).

148. Daan, S. & Pittendrigh, C. S. A Functional analysis of circadian pacemakers in nocturnal rodents - II. The variability of phase response curves. *J. Comp. Physiol.* **106**, 253–266 (1976).

149. Johnson, C. H. Forty years of PRCs - What have we learned? *Chronobiology International* vol. 16 711–743 (1999).

150. Goldman, B. D. Mammalian Photoperiodic System: Formal Properties and Neuroendocrine Mechanisms of Photoperiodic Time Measurement. *J. Biol. Rhythms* **16**, 283–301 (2001).

151. Stephan, F. K. Circadian rhythms in the rat: Constant darkness, entrainment to T cycles and to skeleton photoperiods. *Physiol. Behav.* **30**, 451–462 (1983).

152. Messager, S., Ross, A. W., Barrett, P. & Morgan, P. J. Decoding photoperiodic time through Per1 and ICER gene amplitude. *Proc. Natl. Acad. Sci. U. S. A.* **96**, 9938–9943

(1999).

153. Schaap, J. *et al.* Heterogeneity of rhythmic suprachiasmatic nucleus neurons: Implications for circadian waveform and photoperiodic encoding. *Proc. Natl. Acad. Sci. U. S. A.* **100**, 15994–15999 (2003).

154. Mieda, M. *et al.* Cellular clocks in AVP neurons of the scn are critical for interneuronal coupling regulating circadian behavior rhythm. *Neuron* **85**, 1103–1116 (2015).

155. VanderLeest, H. T. *et al.* Seasonal Encoding by the Circadian Pacemaker of the SCN. *Curr. Biol.* **17**, 468–473 (2007).

156. Dibner, C., Schibler, U. & Albrecht, U. The Mammalian Circadian Timing System: Organization and Coordination of Central and Peripheral Clocks. *Annu. Rev. Physiol.* **72**, 517–549 (2010).

157. Ciarleglio, C. M., Resuehr, H. E. S., Axley, J. C., Deneris, E. S. & McMahon, D. G. Pet-1 Deficiency Alters the Circadian Clock and Its Temporal Organization of Behavior. *PLoS One* **9**, e97412 (2014).

158. Hamnett, R., Crosby, P., Chesham, J. E. & Hastings, M. H. Vasoactive intestinal peptide controls the suprachiasmatic circadian clock network via ERK1/2 and DUSP4 signalling. *Nat. Commun. 2019 101* **10**, 1–17 (2019).

159. Patton, A. P. *et al.* The VIP-VPAC2 neuropeptidergic axis is a cellular pacemaking hub of the suprachiasmatic nucleus circadian circuit. *Nat. Commun. 2020 111* **11**, 1–17 (2020).

160. Tso, C. F. *et al.* Astrocytes Regulate Daily Rhythms in the Suprachiasmatic Nucleus and Behavior. *Curr. Biol.* **27**, 1055–1061 (2017).

161. Brancaccio, M., Patton, A. P., Chesham, J. E., Maywood, E. S. & Hastings, M. H. Astrocytes Control Circadian Timekeeping in the Suprachiasmatic Nucleus via

Glutamatergic Signaling. *Neuron* **93**, 1420-1435.e5 (2017).

162. Brancaccio, M. *et al.* Cell-autonomous clock of astrocytes drives circadian behavior in mammals. *Science (80-.).* **363**, 187–192 (2019).

163. Mei, L. *et al.* Long-term in vivo recording of circadian rhythms in brains of freely moving mice. *Proc. Natl. Acad. Sci.* **115**, 4276–4281 (2018).

164. Yang, J. *et al.* Coupling optogenetic stimulation with NanoLuc-based luminescence (BRET) Ca++ sensing. *Nat. Commun.* **7**, 13268 (2016).

165. Suzuki, K. *et al.* Five colour variants of bright luminescent protein for real-time multicolour bioimaging. *Nat. Commun.* **7**, 13718 (2016).

166. Ralph, M. R. *et al.* Targeted modification of the Per2 clock gene alters circadian function in mPer2luciferase (mPer2Luc) mice. *PLOS Comput. Biol.* **17**, e1008987 (2021).

167. Kim, S. OptoLumicycle. GitHub. https://github.com/SuilKim/OptoLumicycle. fffae11. (2021).

168. Begemann, K., Neumann, A. M. & Oster, H. Regulation and function of extra-SCN circadian oscillators in the brain. *Acta Physiol.* **229**, e13446 (2020).

169. Kalsbeek, A. *et al.* SCN outputs and the hypothalamic balance of life. *J. Biol. Rhythms* **21**, 458–469 (2006).

170. Kim, S. & McMahon, D. G. Light sets the brain's daily clock by regional quickening and slowing of the molecular clockworks at dawn and dusk. *Elife* **10**, e70137 (2021).

171. Viitaniemi, H. M. *et al.* Seasonal Variation in Genome-Wide DNA Methylation Patterns and the Onset of Seasonal Timing of Reproduction in Great Tits. *Genome Biol. Evol.* **11**, 970 (2019).

172. Stevenson, T. J. & Prendergast, B. J. Reversible DNA methylation regulates seasonal

photoperiodic time measurement. *Proc. Natl. Acad. Sci. U. S. A.* **110**, 16651–16656 (2013).

173. Laplant, Q. *et al.* Dnmt3a regulates emotional behavior and spine plasticity in the nucleus accumbens. *Nat. Neurosci. 2010 139* **13**, 1137–1143 (2010).

174. Ono, D. *et al.* Dissociation of Per1 and Bmal1 circadian rhythms in the suprachiasmatic nucleus in parallel with behavioral outputs. *Proc. Natl. Acad. Sci. U. S. A.* **114**, E3699–E3708 (2017).

175. Enoki, R. *et al.* Synchronous circadian voltage rhythms with asynchronous calcium rhythms in the suprachiasmatic nucleus. *Proc. Natl. Acad. Sci. U. S. A.* **114**, E2476–E2485 (2017).

176. Colwell, C. S. Linking neural activity and molecular oscillations in the SCN. *Nature Reviews Neuroscience* vol. 12 553–569 (2011).

177. Yizhar, O. *et al.* Neocortical excitation/inhibition balance in information processing and social dysfunction. *Nat. 2011 4777363* **477**, 171–178 (2011).

178. Berndt, A., Yizhar, O., Gunaydin, L. A., Hegemann, P. & Deisseroth, K. Bi-stable neural state switches. *Nat. Neurosci. 2008 122* **12**, 229–234 (2008).

179. Gong, X. *et al.* An Ultra-Sensitive Step-Function Opsin for Minimally Invasive Optogenetic Stimulation in Mice and Macaques. *Neuron* **107**, 38-51.e8 (2020).

180. Kuhlman, S. J. & McMahon, D. G. Rhythmic regulation of membrane potential and potassium current persists in SCN neurons in the absence of environmental input. *Eur. J. Neurosci.* **20**, 1113–1117 (2004).

181. Belle, M. D. C., Diekman, C. O., Forger, D. B. & Piggins, H. D. Daily electrical silencing in the mammalian circadian clock. *Science (80-.).* **326**, 281–284 (2009).